Supporting Information

Structural Analysis of Five-Coordinate Aluminum(Salen) Complexes and its Relatonship to their Catalytic Activity

Heather Fish, Sam Hart, Katie J. Lamb, Michael North, Sophie C. Z. Quek, Adrian C. Whitwood, Barnaby Woods and Xiao Wu*

Department of Chemistry, University of York, Heslington, YO10 5DD.

Email: Michael.north@york.ac.uk

Table of Contents

X-ray data

Crystal data and structure refinement for 1.HCl.

Identification code	mn1405
Empirical formula	$C_{72}H_{107.62}Al_2ClN_4O_{6.31}$
Formula weight	1219.61
Temperature/K	110.1(2)
Crystal system	orthorhombic
Space group	$P2_12_12_1$
a/Å	14.4538(4)
b/Å	19.9792(4)
c/Å	28.2756(6)
α/°	90
β/°	90
γ/°	90
Volume/Å^3	8165.3(3)
Z	4
ρ_{calc}g/cm^3	0.992
μ/mm^{-1}	0.113
F(000)	2644.0
Crystal size/mm^3	0.3377 × 0.253 × 0.1485
Radiation	Mo Kα (λ = 0.71073)
2Θ range for data collection/°	5.734 to 64.454
Index ranges	-20 ≤ h ≤ 18, -27 ≤ k ≤ 29, -32 ≤ l ≤ 42
Reflections collected	37091
Independent reflections	22588 [R_{int} = 0.0321, R_{sigma} = 0.0533]
Data/restraints/parameters	22588/0/808
Goodness-of-fit on F^2	1.020
Final R indexes [I>=2σ (I)]	R_1 = 0.0470, wR_2 = 0.1226
Final R indexes [all data]	R_1 = 0.0607, wR_2 = 0.1322
Largest diff. peak/hole / e Å^{-3}	0.77/-0.30
Flack parameter	0.14(3)

Data collected, solved and refined by Sam Hart and Adrian C Whitwood

Fractional Atomic Coordinates (×10^4) and Equivalent Isotropic Displacement Parameters (Å^2×10^3) for 1.HCl. U_{eq} is defined as 1/3 of of the trace of the orthogonalised U_{IJ} tensor.

Atom	*x*	*y*	*z*	U(eq)
Cl1	3518.2(6)	6129.1(4)	3929.8(2)	36.29(16)
Al1	3978.1(5)	4274.8(3)	3106.0(2)	15.61(13)
Al2	4802.6(4)	2558.2(3)	2961.5(2)	14.83(12)
C1	5759.1(15)	4893.0(11)	3192.5(8)	18.4(4)
C2	6591.9(16)	5082.6(12)	2953.3(9)	20.7(4)
C3	7348.5(17)	5242.0(13)	3230.3(10)	25.0(5)
C4	7370.4(17)	5230.6(13)	3732.0(10)	25.8(5)
C5	6558.9(17)	5045.9(13)	3950.2(9)	25.2(5)
C6	5765.7(16)	4876.8(12)	3694.7(9)	21.0(4)
C7	4966.6(16)	4671.0(12)	3964.6(9)	21.5(5)
C8	6643.3(17)	5059.7(13)	2413.1(9)	23.9(5)
C9	5924.4(18)	5520.2(13)	2191.1(9)	25.4(5)
C10	6488(2)	4330.5(14)	2247.6(10)	33.3(6)
C11	7595.0(19)	5273.9(15)	2234.7(10)	31.6(6)
C12	8268.6(18)	5387.2(14)	3997.6(10)	28.9(6)
C13	9037(2)	4927.0(17)	3829.5(14)	44.8(8)
C14	8540(2)	6118.3(16)	3912.0(12)	38.9(7)
C15	8145(2)	5279(2)	4533.7(12)	47.1(9)
C16	3442.0(15)	4242.2(12)	4104.1(8)	18.5(4)
C17	3668.1(19)	4116.8(14)	4623.6(8)	25.8(5)
C18	2793(2)	3907.0(16)	4895.3(9)	32.0(6)
C19	2332.5(19)	3300.6(14)	4666.6(9)	27.4(5)
C20	2105.8(17)	3422.9(13)	4145.3(8)	22.3(5)
C21	2987.2(16)	3621.8(11)	3882.7(8)	18.1(4)
C22	2134.7(15)	3677.2(11)	3147.2(8)	18.9(4)
C23	1967.3(15)	3849.8(11)	2658.9(8)	18.6(4)
C24	1072.9(16)	3716.4(11)	2483.7(9)	19.9(4)
C25	830.3(16)	3865.7(11)	2023.5(9)	20.5(4)
C26	1512.6(16)	4193.9(12)	1748.3(8)	20.8(4)
C27	2394.5(16)	4355.8(11)	1903.8(8)	18.9(4)
C28	2649.3(15)	4148.9(11)	2370.1(8)	17.4(4)
C29	-112.5(16)	3702.1(12)	1808.2(9)	23.1(5)
C30	-812.9(18)	3482.3(14)	2185.2(11)	30.8(6)
C31	10(2)	3137.9(15)	1448.7(12)	36.1(6)
C32	-513.6(18)	4316.1(14)	1556.4(11)	32.0(6)
C33	3057.2(16)	4782.3(12)	1604.8(8)	21.0(4)
C34	2608(2)	5002.1(17)	1135.6(10)	33.3(6)
C35	3296.5(18)	5429.6(12)	1880.8(10)	25.7(5)
C36	3955.9(18)	4405.1(13)	1486.8(9)	26.5(5)
C37	3668.0(16)	1899.4(11)	3651.0(8)	17.1(4)
C38	3631.0(17)	1622.3(12)	4116.2(8)	20.6(4)
C39	2783.1(19)	1398.6(13)	4277.1(8)	25.1(5)
C40	1953.0(18)	1419.8(12)	4017.3(9)	23.6(5)
C41	2008.7(17)	1689.0(12)	3569.5(9)	22.0(5)

Fractional Atomic Coordinates ($\times 10^4$) and Equivalent Isotropic Displacement Parameters ($Å^2 \times 10^3$) for 1.HCl. U_{eq} is defined as 1/3 of of the trace of the orthogonalised U_{IJ} tensor.

Atom	*x*	*y*	*z*	U(eq)
C42	2842.6(16)	1940.4(12)	3385.7(8)	18.9(4)
C43	2837.8(16)	2178.3(11)	2903.3(8)	18.3(4)
C44	4501.6(18)	1578.1(13)	4423.7(8)	23.4(5)
C45	4876(2)	2285.5(14)	4513.7(10)	29.9(6)
C46	5233(2)	1141.3(14)	4181.1(9)	28.6(5)
C47	4309(2)	1262(2)	4907.8(10)	43.1(8)
C48	1059(2)	1156.8(15)	4237.9(10)	31.6(6)
C49	1200(3)	481(2)	4464.8(13)	51.2(9)
C50	721(3)	1681(2)	4604.7(14)	57.6(11)
C51	291(2)	1085.0(16)	3866.8(12)	36.0(6)
C52	3534.9(15)	2571.2(12)	2180.9(7)	17.9(4)
C53	2644.5(16)	2435.0(13)	1905.1(8)	21.1(4)
C54	2811.1(17)	2609.7(14)	1384.7(8)	24.5(5)
C55	3644.2(18)	2236.4(15)	1180.6(8)	28.4(6)
C56	4521.5(17)	2349.4(15)	1472.2(8)	26.4(5)
C57	4333.3(15)	2153.8(12)	1983.9(8)	18.7(4)
C58	5921.1(15)	2015.0(12)	2186.8(8)	18.6(4)
C59	6748.3(15)	2023.4(12)	2462.1(8)	17.1(4)
C60	7538.0(16)	1725.7(12)	2260.4(8)	19.9(4)
C61	8361.6(16)	1691.8(12)	2504.9(9)	20.1(4)
C62	8386.6(15)	2012.1(12)	2950.1(9)	20.4(4)
C63	7643.3(15)	2342.5(11)	3158.4(8)	18.8(4)
C64	6772.4(15)	2314.1(11)	2918.8(8)	16.8(4)
C65	9194.5(16)	1295.5(12)	2319.3(10)	24.6(5)
C66	9151(2)	1217(2)	1782.3(12)	46.8(9)
C67	10114.8(16)	1634.8(13)	2442.2(10)	26.2(5)
C68	9193(2)	596.6(14)	2558.6(16)	46.1(9)
C69	7745.6(17)	2694.9(13)	3634.8(9)	24.5(5)
C70	8754(2)	2759(2)	3788.1(13)	49.0(9)
C71	7199(3)	2314(2)	4011.3(11)	54.0(10)
C72	7375(3)	3416.4(16)	3605.7(14)	48.1(9)
N1	4231.6(13)	4408.3(9)	3793.3(7)	17.2(4)
N2	2892.9(13)	3782.7(9)	3373.3(7)	16.6(4)
N3	3540.8(13)	2429.9(10)	2692.9(6)	16.6(3)
N4	5115.2(13)	2241.8(10)	2319.4(7)	17.5(4)
O1	5015.6(11)	4731.1(8)	2947.6(6)	18.7(3)
O2	3504.8(11)	4232.8(8)	2517.9(5)	17.6(3)
O3	3243.9(11)	5126.5(8)	3171.6(6)	21.1(3)
O4	4687.3(12)	3453.1(8)	3056.0(6)	18.4(3)
O5	4469.6(11)	2106.8(8)	3474.8(6)	19.1(3)
O6	6011.8(10)	2558.4(8)	3111.3(6)	18.7(3)
O7	6789(5)	4629(4)	889(2)	38(2)

Anisotropic Displacement Parameters ($Å^2×10^3$) for 1.HCl. The Anisotropic displacement factor exponent takes the form: $-2π^2[h^2a^{*2}U_{11}+2hka^*b^*U_{12}+…]$.

Atom	U_{11}	U_{22}	U_{33}	U_{23}	U_{13}	U_{12}
Cl1	55.5(4)	28.3(3)	25.0(3)	1.4(3)	-4.3(3)	-3.4(3)
Al1	15.9(3)	15.8(3)	15.1(3)	1.9(3)	2.0(2)	0.7(3)
Al2	14.8(3)	17.3(3)	12.4(3)	0.3(3)	0.1(2)	1.9(3)
C1	16.9(9)	15.7(9)	22.7(10)	3.3(9)	3.2(8)	-0.4(8)
C2	21.7(10)	16.9(9)	23.5(10)	4.5(9)	4.1(9)	1.1(9)
C3	21.7(11)	22.3(11)	31.1(12)	8.2(10)	2.6(9)	-1.4(9)
C4	22.1(11)	23.2(11)	32.0(12)	7.1(11)	-5.6(10)	-2.1(10)
C5	24.6(12)	27.6(12)	23.3(11)	7.1(10)	-1.2(9)	-3.5(10)
C6	18.4(10)	21.3(10)	23.3(10)	3.6(9)	1.1(9)	-0.1(9)
C7	23.0(11)	20.8(10)	20.6(10)	1.0(9)	1.8(8)	3.6(9)
C8	24.3(11)	23.9(11)	23.6(11)	3.1(10)	5.7(9)	-2.3(10)
C9	27.4(12)	26.7(11)	22.1(10)	7.2(10)	-0.4(9)	-4.3(10)
C10	42.4(15)	28.6(13)	28.9(12)	-2.7(12)	11.8(12)	-0.7(12)
C11	25.9(12)	37.0(14)	31.9(13)	5.4(12)	12.1(11)	-0.1(11)
C12	20.8(11)	30.3(13)	35.6(13)	11.0(12)	-8.5(10)	-8.7(10)
C13	22.0(13)	43.6(17)	69(2)	1.4(17)	-10.7(14)	-4.1(13)
C14	31.0(14)	34.5(14)	51.1(17)	14.9(14)	-13.5(13)	-10.3(12)
C15	37.4(16)	62(2)	42.4(17)	17.5(17)	-15.8(14)	-17.8(16)
C16	18.5(10)	19.2(10)	17.8(9)	0.6(9)	5.2(8)	0.2(9)
C17	30.5(12)	31.6(12)	15.3(10)	3.8(10)	4.3(9)	-1.9(11)
C18	38.6(14)	38.5(14)	18.9(11)	-2.0(11)	9.7(10)	-9.1(13)
C19	30.4(13)	30.1(12)	21.7(11)	4.0(11)	8.7(10)	-3.8(11)
C20	23.2(11)	23.8(11)	20.0(10)	2.4(9)	4.8(9)	-1.3(10)
C21	21.8(10)	17.1(9)	15.5(9)	1.7(8)	4.1(8)	2.5(9)
C22	17.9(10)	17.2(9)	21.5(10)	2.4(9)	5.3(8)	-0.8(8)
C23	16.8(10)	16.9(9)	22.1(10)	2.5(9)	2.2(8)	0.9(8)
C24	17.2(10)	17.8(10)	24.6(10)	2.4(9)	1.4(8)	1.7(9)
C25	19.7(10)	16.1(9)	25.6(11)	-0.1(9)	-0.8(9)	3.3(8)
C26	23.4(11)	17.7(10)	21.3(10)	4.3(9)	-2.1(9)	2.6(9)
C27	19.2(10)	17.8(9)	19.7(10)	1.7(9)	1.5(8)	2.9(8)
C28	16.3(9)	16.4(9)	19.3(10)	-1.6(8)	2.1(8)	2.3(8)
C29	20.7(10)	18.8(10)	29.7(12)	4.1(10)	-3.8(9)	-2.6(9)
C30	20.6(11)	30.0(13)	42.0(15)	11.6(12)	-4.6(10)	-3.3(10)
C31	36.3(15)	31.1(13)	40.9(16)	-3.2(13)	-10.5(12)	-4.1(12)
C32	20.5(11)	31.9(13)	43.8(15)	11.6(13)	-5.6(11)	0.6(11)
C33	20.3(10)	23.0(11)	19.6(10)	6.3(9)	-1.2(8)	1.0(9)
C34	29.7(13)	44.4(16)	25.9(12)	17.8(13)	-0.8(10)	-7.6(12)
C35	26.8(11)	20.5(11)	29.7(12)	4.1(10)	4.8(10)	-2.0(10)
C36	24.6(11)	30.2(12)	24.7(11)	2.6(10)	4.8(10)	0.2(11)
C37	20.1(10)	14.1(9)	17.0(9)	-2.9(8)	1.6(8)	-1.1(8)
C38	26.0(11)	19.9(10)	15.9(9)	-3.8(9)	1.0(9)	2.6(9)
C39	37.2(13)	21.6(11)	16.4(10)	-1.9(9)	7.5(9)	-3.6(11)
C40	29.4(12)	18.9(10)	22.4(11)	-5.7(9)	8.6(9)	-2.5(10)

C41	21.4(11)	22.4(11)	22.2(11)	-7.2(9)	2.6(9)	1.0(9)
C42	20.5(10)	18.2(10)	17.9(10)	-3.6(9)	0.2(8)	0.9(9)
C43	17.2(9)	18.0(9)	19.8(10)	-0.1(9)	-1.0(8)	1.5(8)
C44	27.9(12)	26.2(11)	16.1(10)	1.2(9)	1.8(9)	4.6(10)
C45	33.7(13)	29.7(12)	26.4(12)	-8.8(11)	-7.7(11)	5.1(11)
C46	37.3(14)	26.5(12)	22.1(11)	2.2(10)	-1.7(10)	8.9(11)
C47	44.6(17)	64(2)	21.0(12)	13.2(15)	0.4(12)	6.5(17)
C48	31.8(13)	32.4(13)	30.5(13)	-5.7(12)	10.6(11)	-6.2(12)
C49	54(2)	59(2)	40.3(17)	19.9(17)	-8.5(15)	-28.6(18)
C50	52(2)	68(2)	53(2)	-26(2)	34.5(17)	-19.4(19)
C51	25.4(13)	35.9(14)	46.8(16)	-0.8(14)	8.3(12)	-3.9(12)
C52	19.1(9)	21.2(10)	13.3(8)	-1.1(8)	-1.6(7)	3.0(9)
C53	20.2(10)	24.3(11)	18.8(9)	1.4(9)	-3.8(8)	1.5(9)
C54	24.0(11)	30.6(12)	19.0(10)	0.1(10)	-6.1(9)	5.1(10)
C55	27.9(12)	41.9(15)	15.3(10)	-4.0(11)	-4.1(9)	10.4(12)
C56	25.1(11)	39.6(14)	14.7(10)	-1.1(10)	-1.2(8)	8.0(11)
C57	18.6(10)	22.2(10)	15.4(9)	-1.0(9)	-3.2(8)	3.1(9)
C58	19.4(10)	20.2(10)	16.2(9)	-3.0(8)	0.7(8)	1.9(9)
C59	15.2(9)	18.4(9)	17.6(9)	-1.5(9)	0.3(8)	1.1(8)
C60	20.3(10)	20.0(10)	19.6(10)	-1.3(9)	0.7(8)	1.5(9)
C61	16.8(10)	18.9(10)	24.6(11)	-1.7(9)	2.3(8)	2.6(9)
C62	15.7(9)	21.0(10)	24.5(10)	-0.1(9)	-2.8(8)	-0.6(9)
C63	17.6(9)	17.9(9)	20.8(10)	-1.8(9)	-1.4(8)	0.9(8)
C64	17.4(9)	16.1(9)	16.8(9)	2.0(8)	-0.7(8)	2.0(8)
C65	15.5(10)	21.6(11)	36.6(13)	-3.7(11)	4.0(9)	2.7(9)
C66	24.3(13)	71(2)	45.6(17)	-27.8(18)	3.4(12)	12.3(15)
C67	13.4(10)	28.4(12)	36.8(13)	0.5(11)	2.9(9)	1.1(9)
C68	29.0(14)	21.7(12)	88(3)	7.1(16)	12.2(16)	6.7(11)
C69	24.8(11)	26.3(12)	22.3(10)	-8.1(10)	-6.3(9)	5.8(10)
C70	33.2(15)	61(2)	53.0(19)	-35.7(18)	-19.1(14)	13.0(15)
C71	62(2)	79(3)	20.8(13)	0.4(16)	-6.7(14)	-16(2)
C72	55(2)	32.2(15)	57(2)	-24.2(16)	-27.5(17)	14.5(15)
N1	17.9(8)	15.3(8)	18.4(8)	0.8(7)	3.6(7)	2.3(7)
N2	18.7(8)	13.6(8)	17.7(8)	2.8(7)	3.9(7)	2.4(7)
N3	17.7(8)	19.6(8)	12.5(7)	1.0(7)	-0.3(6)	3.9(7)
N4	16.7(8)	20.1(8)	15.7(8)	-1.0(7)	-1.6(7)	1.6(7)
O1	19.5(7)	19.1(7)	17.5(7)	3.0(6)	0.9(6)	-2.8(6)
O2	15.6(7)	20.6(7)	16.5(7)	4.1(6)	0.2(6)	1.4(6)
O3	22.9(8)	18.6(7)	21.8(7)	0.6(7)	-1.3(7)	5.3(7)
O4	15.2(8)	18.2(7)	21.8(8)	2.3(6)	1.4(6)	2.9(6)
O5	19.6(7)	22.4(8)	15.4(7)	3.3(7)	-0.8(6)	-1.0(7)
O6	16.9(7)	21.2(7)	18.0(7)	-2.5(7)	0.7(6)	4.3(6)
O7	46(4)	52(4)	15(3)	17(3)	-13(2)	-44(3)

Bond Lengths for 1.HCl.

Atom	Atom	Length/Å	Atom	Atom	Length/Å
Al1	N1	1.996(2)	C29	C31	1.528(4)
Al1	N2	2.000(2)	C29	C32	1.532(4)
Al1	O1	1.8112(17)	C33	C34	1.541(3)
Al1	O2	1.8000(17)	C33	C35	1.549(4)
Al1	O3	2.0139(18)	C33	C36	1.538(3)
Al1	O4	1.9407(18)	C37	C38	1.428(3)
Al2	N3	1.992(2)	C37	C42	1.412(3)
Al2	N4	1.975(2)	C37	O5	1.327(3)
Al2	O4	1.8154(18)	C38	C39	1.382(4)
Al2	O5	1.7754(17)	C38	C44	1.532(3)
Al2	O6	1.7983(17)	C39	C40	1.408(4)
C1	C2	1.432(3)	C40	C41	1.378(4)
C1	C6	1.420(3)	C40	C48	1.528(4)
C1	O1	1.319(3)	C41	C42	1.405(3)
C2	C3	1.382(3)	C42	C43	1.444(3)
C2	C8	1.530(3)	C43	N3	1.280(3)
C3	C4	1.419(4)	C44	C45	1.535(4)
C4	C5	1.376(3)	C44	C46	1.533(4)
C4	C12	1.532(3)	C44	C47	1.533(4)
C5	C6	1.397(3)	C48	C49	1.509(5)
C6	C7	1.444(3)	C48	C50	1.553(4)
C7	N1	1.280(3)	C48	C51	1.534(4)
C8	C9	1.523(4)	C52	C53	1.529(3)
C8	C10	1.547(4)	C52	C57	1.529(3)
C8	C11	1.526(3)	C52	N3	1.475(3)
C12	C13	1.519(4)	C53	C54	1.531(3)
C12	C14	1.532(4)	C54	C55	1.530(3)
C12	C15	1.542(4)	C55	C56	1.529(3)
C16	C17	1.526(3)	C56	C57	1.523(3)
C16	C21	1.536(3)	C57	N4	1.486(3)
C16	N1	1.478(3)	C58	C59	1.427(3)
C17	C18	1.538(4)	C58	N4	1.305(3)
C18	C19	1.526(4)	C59	C60	1.408(3)
C19	C20	1.530(3)	C59	C64	1.416(3)
C20	C21	1.527(3)	C60	C61	1.378(3)
C21	N2	1.482(3)	C61	C62	1.413(3)
C22	C23	1.444(3)	C61	C65	1.533(3)
C22	N2	1.286(3)	C62	C63	1.392(3)
C23	C24	1.410(3)	C63	C64	1.431(3)
C23	C28	1.413(3)	C63	C69	1.527(3)
C24	C25	1.380(3)	C64	O6	1.320(3)
C25	C26	1.417(3)	C65	C66	1.528(4)
C25	C29	1.528(3)	C65	C67	1.533(3)
C26	C27	1.387(3)	C65	C68	1.552(4)

Bond Lengths for 1.HCl.

Atom	Atom	Length/Å	Atom	Atom	Length/Å
C27	C28	1.430(3)	C69	C70	1.526(4)
C27	C33	1.536(3)	C69	C71	1.529(4)
C28	O2	1.316(3)	C69	C72	1.540(4)
C29	C30	1.534(4)			

Bond Angles for 1.HCl

Atom	Atom	Atom	Angle/˚	Atom	Atom	Atom	Angle/˚
N1	Al1	N2	80.88(8)	C27	C33	C36	112.0(2)
N1	Al1	O3	83.92(7)	C34	C33	C35	106.9(2)
N2	Al1	O3	88.12(8)	C36	C33	C34	108.0(2)
O1	Al1	N1	91.24(8)	C36	C33	C35	109.2(2)
O1	Al1	N2	172.07(9)	C42	C37	C38	118.7(2)
O1	Al1	O3	91.94(8)	O5	C37	C38	120.0(2)
O1	Al1	O4	88.31(8)	O5	C37	C42	121.33(19)
O2	Al1	N1	167.33(8)	C37	C38	C44	121.0(2)
O2	Al1	N2	91.62(8)	C39	C38	C37	117.5(2)
O2	Al1	O1	96.30(8)	C39	C38	C44	121.5(2)
O2	Al1	O3	85.65(8)	C38	C39	C40	125.1(2)
O2	Al1	O4	95.40(8)	C39	C40	C48	119.8(2)
O4	Al1	N1	94.99(8)	C41	C40	C39	116.2(2)
O4	Al1	N2	91.48(8)	C41	C40	C48	124.0(2)
O4	Al1	O3	178.89(8)	C40	C41	C42	122.0(2)
N4	Al2	N3	79.50(8)	C37	C42	C43	121.7(2)
O4	Al2	N3	95.67(8)	C41	C42	C37	120.5(2)
O4	Al2	N4	118.14(8)	C41	C42	C43	117.6(2)
O5	Al2	N3	89.89(8)	N3	C43	C42	124.3(2)
O5	Al2	N4	130.62(9)	C38	C44	C45	109.3(2)
O5	Al2	O4	110.80(8)	C38	C44	C46	110.2(2)
O5	Al2	O6	94.08(8)	C38	C44	C47	112.4(2)
O6	Al2	N3	168.39(8)	C46	C44	C45	110.8(2)
O6	Al2	N4	89.67(8)	C47	C44	C45	107.2(2)
O6	Al2	O4	93.12(8)	C47	C44	C46	106.9(2)
C6	C1	C2	118.2(2)	C40	C48	C50	107.9(2)
O1	C1	C2	120.1(2)	C40	C48	C51	111.4(2)
O1	C1	C6	121.7(2)	C49	C48	C40	111.6(3)
C1	C2	C8	120.3(2)	C49	C48	C50	111.2(3)
C3	C2	C1	117.3(2)	C49	C48	C51	107.7(2)
C3	C2	C8	122.3(2)	C51	C48	C50	107.0(3)
C2	C3	C4	125.5(2)	C57	C52	C53	110.63(18)
C3	C4	C12	120.4(2)	N3	C52	C53	118.12(19)
C5	C4	C3	115.7(2)	N3	C52	C57	104.41(17)
C5	C4	C12	123.9(2)	C52	C53	C54	108.50(19)
C4	C5	C6	122.2(2)	C55	C54	C53	112.0(2)
C1	C6	C7	122.0(2)	C56	C55	C54	112.2(2)
C5	C6	C1	121.1(2)	C57	C56	C55	109.0(2)
C5	C6	C7	116.9(2)	C56	C57	C52	109.93(19)
N1	C7	C6	125.5(2)	N4	C57	C52	106.09(17)
C2	C8	C10	108.9(2)	N4	C57	C56	116.12(19)
C9	C8	C2	111.1(2)	N4	C58	C59	126.0(2)
C9	C8	C10	110.2(2)	C60	C59	C58	116.96(19)
C9	C8	C11	108.0(2)	C60	C59	C64	121.5(2)

Bond Angles for 1.HCl

Atom	Atom	Atom	Angle/˚	Atom	Atom	Atom	Angle/˚
C11	C8	C2	111.4(2)	C64	C59	C58	121.53(19)
C11	C8	C10	107.2(2)	C61	C60	C59	121.2(2)
C4	C12	C15	110.8(2)	C60	C61	C62	116.5(2)
C13	C12	C4	110.1(2)	C60	C61	C65	122.1(2)
C13	C12	C14	109.9(2)	C62	C61	C65	121.2(2)
C13	C12	C15	107.9(3)	C63	C62	C61	124.9(2)
C14	C12	C4	109.5(2)	C62	C63	C64	117.4(2)
C14	C12	C15	108.6(3)	C62	C63	C69	121.1(2)
C17	C16	C21	110.58(19)	C64	C63	C69	121.41(19)
N1	C16	C17	116.35(19)	C59	C64	C63	118.01(19)
N1	C16	C21	105.63(17)	O6	C64	C59	120.46(19)
C16	C17	C18	110.5(2)	O6	C64	C63	121.53(19)
C19	C18	C17	111.3(2)	C61	C65	C68	108.3(2)
C18	C19	C20	112.0(2)	C66	C65	C61	111.1(2)
C21	C20	C19	109.4(2)	C66	C65	C67	107.9(2)
C20	C21	C16	111.65(18)	C66	C65	C68	109.9(3)
N2	C21	C16	105.09(18)	C67	C65	C61	112.0(2)
N2	C21	C20	116.89(19)	C67	C65	C68	107.5(2)
N2	C22	C23	125.4(2)	C63	C69	C71	109.6(2)
C24	C23	C22	116.4(2)	C63	C69	C72	110.5(2)
C24	C23	C28	121.1(2)	C70	C69	C63	112.5(2)
C28	C23	C22	122.5(2)	C70	C69	C71	109.8(3)
C25	C24	C23	121.6(2)	C70	C69	C72	105.6(3)
C24	C25	C26	116.2(2)	C71	C69	C72	108.8(3)
C24	C25	C29	123.8(2)	C7	N1	Al1	125.14(16)
C26	C25	C29	120.1(2)	C7	N1	C16	120.52(19)
C27	C26	C25	125.0(2)	C16	N1	Al1	114.03(14)
C26	C27	C28	117.5(2)	C21	N2	Al1	113.70(14)
C26	C27	C33	121.9(2)	C22	N2	Al1	124.12(15)
C28	C27	C33	120.5(2)	C22	N2	C21	121.73(19)
C23	C28	C27	118.4(2)	C43	N3	Al2	126.87(15)
O2	C28	C23	121.7(2)	C43	N3	C52	121.78(19)
O2	C28	C27	119.9(2)	C52	N3	Al2	110.78(14)
C25	C29	C30	111.9(2)	C57	N4	Al2	116.79(14)
C25	C29	C31	108.6(2)	C58	N4	Al2	125.41(15)
C25	C29	C32	110.6(2)	C58	N4	C57	117.04(18)
C31	C29	C30	109.1(2)	C1	O1	Al1	131.93(15)
C31	C29	C32	109.0(2)	C28	O2	Al1	131.02(14)
C32	C29	C30	107.6(2)	Al2	O4	Al1	153.17(11)
C27	C33	C34	111.7(2)	C37	O5	Al2	134.59(14)
C27	C33	C35	108.97(19)	C64	O6	Al2	135.41(14)

Torsion Angles for 1.HCl.

A	B	C	D	Angle/˚	A	B	C	D	Angle/˚
C1	C2	C3	C4	0.3(4)	C41	C40	C48	C50	-104.5(3)
C1	C2	C8	C9	60.2(3)	C41	C40	C48	C51	12.6(4)
C1	C2	C8	C10	-61.3(3)	C41	C42	C43	N3	178.8(2)
C1	C2	C8	C11	-179.3(2)	C42	C37	C38	C39	1.0(3)
C1	C6	C7	N1	9.2(4)	C42	C37	C38	C44	-178.8(2)
C2	C1	C6	C5	0.5(4)	C42	C37	O5	Al2	9.5(3)
C2	C1	C6	C7	-178.0(2)	C42	C43	N3	Al2	0.2(3)
C2	C1	O1	Al1	161.63(16)	C42	C43	N3	C52	170.7(2)
C2	C3	C4	C5	-0.3(4)	C44	C38	C39	C40	-179.8(2)
C2	C3	C4	C12	177.1(2)	C48	C40	C41	C42	178.4(2)
C3	C2	C8	C9	-124.1(2)	C52	C53	C54	C55	55.1(3)
C3	C2	C8	C10	114.4(3)	C52	C57	N4	Al2	19.8(2)
C3	C2	C8	C11	-3.5(3)	C52	C57	N4	C58	-169.6(2)
C3	C4	C5	C6	0.3(4)	C53	C52	C57	C56	62.3(3)
C3	C4	C12	C13	-55.4(3)	C53	C52	C57	N4	-171.38(18)
C3	C4	C12	C14	65.6(3)	C53	C52	N3	Al2	174.32(16)
C3	C4	C12	C15	-174.7(3)	C53	C52	N3	C43	2.4(3)
C4	C5	C6	C1	-0.5(4)	C53	C54	C55	C56	-54.7(3)
C4	C5	C6	C7	178.1(2)	C54	C55	C56	C57	55.4(3)
C5	C4	C12	C13	121.8(3)	C55	C56	C57	C52	-58.8(3)
C5	C4	C12	C14	-117.3(3)	C55	C56	C57	N4	-179.2(2)
C5	C4	C12	C15	2.5(4)	C56	C57	N4	Al2	142.23(18)
C5	C6	C7	N1	-169.3(2)	C56	C57	N4	C58	-47.2(3)
C6	C1	C2	C3	-0.4(3)	C57	C52	C53	C54	-59.1(3)
C6	C1	C2	C8	175.6(2)	C57	C52	N3	Al2	50.97(19)
C6	C1	O1	Al1	-17.5(3)	C57	C52	N3	C43	-120.9(2)
C6	C7	N1	Al1	-4.3(3)	C58	C59	C60	C61	-178.1(2)
C6	C7	N1	C16	-177.6(2)	C58	C59	C64	C63	-175.8(2)
C8	C2	C3	C4	-175.6(2)	C58	C59	C64	O6	3.2(3)
C12	C4	C5	C6	-176.9(2)	C59	C58	N4	Al2	-7.5(3)
C16	C17	C18	C19	55.2(3)	C59	C58	N4	C57	-177.2(2)
C16	C21	N2	Al1	39.4(2)	C59	C60	C61	C62	-4.4(3)
C16	C21	N2	C22	-133.2(2)	C59	C60	C61	C65	172.3(2)
C17	C16	C21	C20	57.9(3)	C59	C64	O6	Al2	7.7(3)
C17	C16	C21	N2	-174.40(18)	C60	C59	C64	C63	4.6(3)
C17	C16	N1	Al1	161.12(17)	C60	C59	C64	O6	-176.4(2)
C17	C16	N1	C7	-24.9(3)	C60	C61	C62	C63	1.3(4)
C17	C18	C19	C20	-55.8(3)	C60	C61	C65	C66	24.1(4)
C18	C19	C20	C21	56.0(3)	C60	C61	C65	C67	144.8(2)
C19	C20	C21	C16	-57.0(3)	C60	C61	C65	C68	-96.8(3)
C19	C20	C21	N2	-178.0(2)	C61	C62	C63	C64	4.7(4)
C20	C21	N2	Al1	163.83(16)	C61	C62	C63	C69	-177.9(2)
C20	C21	N2	C22	-8.8(3)	C62	C61	C65	C66	-159.4(3)
C21	C16	C17	C18	-55.9(3)	C62	C61	C65	C67	-38.6(3)

Torsion Angles for 1.HCl.

A	B	C	D	Angle/˚	A	B	C	D	Angle/˚
C21	C16	N1	Al1	38.0(2)	C62	C61	C65	C68	79.8(3)
C21	C16	N1	C7	-148.0(2)	C62	C63	C64	C59	-7.4(3)
C22	C23	C24	C25	179.4(2)	C62	C63	C64	O6	173.6(2)
C22	C23	C28	C27	-174.6(2)	C62	C63	C69	C70	11.7(4)
C22	C23	C28	O2	6.2(3)	C62	C63	C69	C71	-110.7(3)
C23	C22	N2	Al1	4.8(3)	C62	C63	C69	C72	129.4(3)
C23	C22	N2	C21	176.6(2)	C63	C64	O6	Al2	-173.29(17)
C23	C24	C25	C26	-3.5(3)	C64	C59	C60	C61	1.6(4)
C23	C24	C25	C29	177.0(2)	C64	C63	C69	C70	-171.1(3)
C23	C28	O2	Al1	-22.1(3)	C64	C63	C69	C71	66.6(3)
C24	C23	C28	C27	4.2(3)	C64	C63	C69	C72	-53.4(3)
C24	C23	C28	O2	-175.1(2)	C65	C61	C62	C63	-175.4(2)
C24	C25	C26	C27	1.7(3)	C69	C63	C64	C59	175.2(2)
C24	C25	C29	C30	11.2(3)	C69	C63	C64	O6	-3.8(3)
C24	C25	C29	C31	-109.3(3)	N1	Al1	O1	C1	17.8(2)
C24	C25	C29	C32	131.1(3)	N1	Al1	O2	C28	-31.1(5)
C25	C26	C27	C28	3.0(3)	N1	C16	C17	C18	-176.4(2)
C25	C26	C27	C33	-172.9(2)	N1	C16	C21	C20	-175.38(18)
C26	C25	C29	C30	-168.3(2)	N1	C16	C21	N2	-47.7(2)
C26	C25	C29	C31	71.2(3)	N2	Al1	O2	C28	22.2(2)
C26	C25	C29	C32	-48.4(3)	N2	C22	C23	C24	-177.4(2)
C26	C27	C28	C23	-5.8(3)	N2	C22	C23	C28	1.4(4)
C26	C27	C28	O2	173.5(2)	N3	Al2	O4	Al1	14.3(2)
C26	C27	C33	C34	1.1(3)	N3	Al2	O5	C37	-12.7(2)
C26	C27	C33	C35	118.9(2)	N3	Al2	O6	C64	7.9(6)
C26	C27	C33	C36	-120.1(2)	N3	C52	C53	C54	-179.2(2)
C27	C28	O2	Al1	158.64(17)	N3	C52	C57	C56	-169.61(19)
C28	C23	C24	C25	0.7(3)	N3	C52	C57	N4	-43.3(2)
C28	C27	C33	C34	-174.7(2)	N4	Al2	O4	Al1	95.4(2)
C28	C27	C33	C35	-56.9(3)	N4	Al2	O5	C37	-88.7(2)
C28	C27	C33	C36	64.1(3)	N4	Al2	O6	C64	-13.1(2)
C29	C25	C26	C27	-178.8(2)	N4	C58	C59	C60	177.3(2)
C33	C27	C28	C23	170.2(2)	N4	C58	C59	C64	-2.3(4)
C33	C27	C28	O2	-10.6(3)	O1	Al1	O2	C28	-157.3(2)
C37	C38	C39	C40	0.3(4)	O1	C1	C2	C3	-179.6(2)
C37	C38	C44	C45	61.4(3)	O1	C1	C2	C8	-3.6(3)
C37	C38	C44	C46	-60.6(3)	O1	C1	C6	C5	179.7(2)
C37	C38	C44	C47	-179.7(2)	O1	C1	C6	C7	1.2(4)
C37	C42	C43	N3	-7.2(4)	O2	Al1	O1	C1	-172.42(19)
C38	C37	C42	C41	-2.5(3)	O3	Al1	O1	C1	101.7(2)
C38	C37	C42	C43	-176.3(2)	O3	Al1	O2	C28	-65.8(2)
C38	C37	O5	Al2	-171.08(17)	O4	Al1	O1	C1	-77.2(2)
C38	C39	C40	C41	-0.2(4)	O4	Al1	O2	C28	113.8(2)
C38	C39	C40	C48	-179.8(2)	O4	Al2	O5	C37	83.3(2)

Torsion Angles for 1.HCl.

A	B	C	D	Angle/˚	A	B	C	D	Angle/˚
C39	C38	C44	C45	-118.4(3)	O4	Al2	O6	C64	-131.3(2)
C39	C38	C44	C46	119.6(3)	O5	Al2	O4	Al1	-77.7(2)
C39	C38	C44	C47	0.5(3)	O5	Al2	O6	C64	117.6(2)
C39	C40	C41	C42	-1.2(3)	O5	C37	C38	C39	-178.4(2)
C39	C40	C48	C49	-47.4(3)	O5	C37	C38	C44	1.8(3)
C39	C40	C48	C50	75.1(3)	O5	C37	C42	C41	176.9(2)
C39	C40	C48	C51	-167.8(2)	O5	C37	C42	C43	3.1(3)
C40	C41	C42	C37	2.6(4)	O6	Al2	O4	Al1	-173.3(2)
C40	C41	C42	C43	176.7(2)	O6	Al2	O5	C37	178.2(2)
C41	C40	C48	C49	133.1(3)					

Hydrogen Atom Coordinates (Å×10⁴) and Isotropic Displacement Parameters (Å²×10³) for 1.HCl.

Atom	*x*	*y*	*z*	U(eq)
H3	7900.1	5369.85	3071.52	30
H5	6537.3	5033	4285.88	30
H7	4988.22	4736.06	4297.27	26
H9A	5307.07	5395.97	2304.34	38
H9B	5947.21	5476.35	1846.06	38
H9C	6056.44	5984.62	2279.92	38
H10A	6970.27	4042.29	2380.98	50
H10B	6513.98	4311.22	1901.58	50
H10C	5879.7	4175.8	2355.51	50
H11A	8069.27	4980.45	2370.26	47
H11B	7715.16	5737.28	2330.37	47
H11C	7611.74	5241.48	1888.99	47
H13A	8882.4	4463.02	3909.29	67
H13B	9618.71	5051.67	3984.54	67
H13C	9107.12	4969.26	3486	67
H14A	8582.06	6201.67	3571.15	58
H14B	9140.91	6207.61	4059.72	58
H14C	8071.01	6413.36	4050.43	58
H15A	7713	5612.56	4658.87	71
H15B	8745.05	5326.28	4691.96	71
H15C	7899.91	4828.91	4591.03	71
H16	2988.66	4619.56	4087.59	22
H17A	3926.7	4529.31	4765.61	31
H17B	4140.32	3759.64	4648.61	31
H18A	2959.96	3797.96	5225.98	38
H18B	2350.89	4285.26	4901.3	38
H19A	1755.13	3194.31	4839.36	33
H19B	2749.9	2909.42	4692.9	33
H20A	1843.64	3011.27	4003.79	27
H20B	1640.03	3784.11	4117.5	27
H21	3434.41	3242.11	3911.33	22
H22	1644.42	3468.37	3315.38	23
H24	626.63	3519.17	2687.22	24
H26	1353.61	4312.13	1433.15	25
H30A	-613.01	3057.22	2324.75	46
H30B	-1422.33	3424.76	2038.86	46
H30C	-850.64	3824.47	2432.77	46
H31A	447.35	3278.96	1203.39	54
H31B	-588.62	3034.1	1303.18	54
H31C	249.06	2738.9	1608.9	54
H32A	-607.36	4677.05	1786.11	48
H32B	-1107.34	4198.16	1411.27	48
H32C	-82.54	4465.85	1310.62	48
H34A	2467.46	4606.15	944.08	50

Hydrogen Atom Coordinates (Å×10⁴) and Isotropic Displacement Parameters (Å²×10³) for 1.HCl.

Atom	*x*	*y*	*z*	U(eq)
H34B	3036.39	5292.83	962.37	50
H34C	2035.3	5246.96	1201.97	50
H35A	2724.72	5667.19	1961.5	39
H35B	3687.21	5717.96	1684.05	39
H35C	3628.85	5312.94	2171.43	39
H36A	4248.82	4252.72	1780.24	40
H36B	4378.84	4704.62	1317.68	40
H36C	3812.58	4017.65	1287.28	40
H39	2758.42	1216.41	4587.2	30
H41	1467.26	1705.12	3379.43	26
H43	2275.7	2145.88	2730.71	22
H45A	4977.34	2512.09	4210.75	45
H45B	5462.15	2256.64	4686.5	45
H45C	4426.67	2539.46	4701.39	45
H46A	4976.32	695.39	4121.02	43
H46B	5776.71	1101.78	4386.5	43
H46C	5414.84	1347.42	3880.55	43
H47A	3846.6	1529.64	5076.45	65
H47B	4882.48	1247.7	5092.26	65
H47C	4074.27	805.73	4863.97	65
H49A	1475.92	173.24	4234.5	77
H49B	602.11	303.37	4569.71	77
H49C	1613.54	526.39	4737.61	77
H50A	1195.48	1740.92	4848.9	86
H50B	146.96	1523.64	4751.5	86
H50C	608.73	2108.67	4445.35	86
H51A	180.94	1519.14	3715.74	54
H51B	-278.03	931.65	4020.65	54
H51C	480.74	758.34	3627.09	54
H52	3696.35	3053.99	2137.13	21
H53A	2133.73	2710.86	2033.21	25
H53B	2470.21	1957.7	1935.12	25
H54A	2252.58	2495	1198.88	29
H54B	2915.14	3097.71	1355.29	29
H55A	3505.24	1751.45	1170.39	34
H55B	3753.04	2389.38	852.2	34
H56A	5033.31	2074.92	1343.65	32
H56B	4706.16	2826	1455.54	32
H57	4143.67	1672.55	1989.87	22
H58	5960.72	1827.24	1878.77	22
H60	7502.66	1545.05	1950.11	24
H62	8953.35	2001.22	3120.1	25
H66A	8628.76	927.09	1698.41	70
H66B	9727.65	1015.49	1668.56	70

Hydrogen Atom Coordinates (Å×10⁴) and Isotropic Displacement Parameters (Å²×10³) for 1.HCl.

Atom	*x*	*y*	*z*	U(eq)
H66C	9067.84	1657.03	1635.62	70
H67A	10143	2074.93	2289.88	39
H67B	10628.42	1357.19	2329.37	39
H67C	10161.45	1689.15	2785.8	39
H68A	9177.59	651.1	2903	69
H68B	9754.09	352.43	2468.31	69
H68C	8647.21	344.87	2455.78	69
H70A	9011.2	2313.02	3846.52	73
H70B	8789.16	3025.69	4078.62	73
H70C	9109.44	2980.57	3537.78	73
H71A	6545.46	2294.38	3919.18	81
H71B	7255.49	2545.57	4315.53	81
H71C	7443.92	1858.9	4040.5	81
H72A	7680.93	3652.4	3345.19	72
H72B	7501.85	3649.35	3903.71	72
H72C	6705.91	3406.72	3549.6	72
H3A	3229.37	5385.26	3426.3	32
H3B	2881.37	5302.86	2951.6	32
H7A	6692.96	4845.79	627.19	57
H7B	6507.39	4244.49	877.57	57
H4	5160(30)	3480(20)	3082(15)	48(12)

Atomic Occupancy for 1.HCl.

Atom	*Occupancy*	Atom	*Occupancy*	Atom	*Occupancy*
O7	0.313(8)	H7A	0.313(8)	H7B	0.313(8)

Solvent masks information for 1.HCl.

Number	X	Y	Z	Volume	Electron count	Content
1	-0.258	0.250	0.000	841.6	142.4	3 CH_2Cl_2
2	-0.812	-0.250	0.500	841.6	142.6	3 CH_2Cl_2

NMR spectra

Compound **1** ^{1}H NMR spectrum

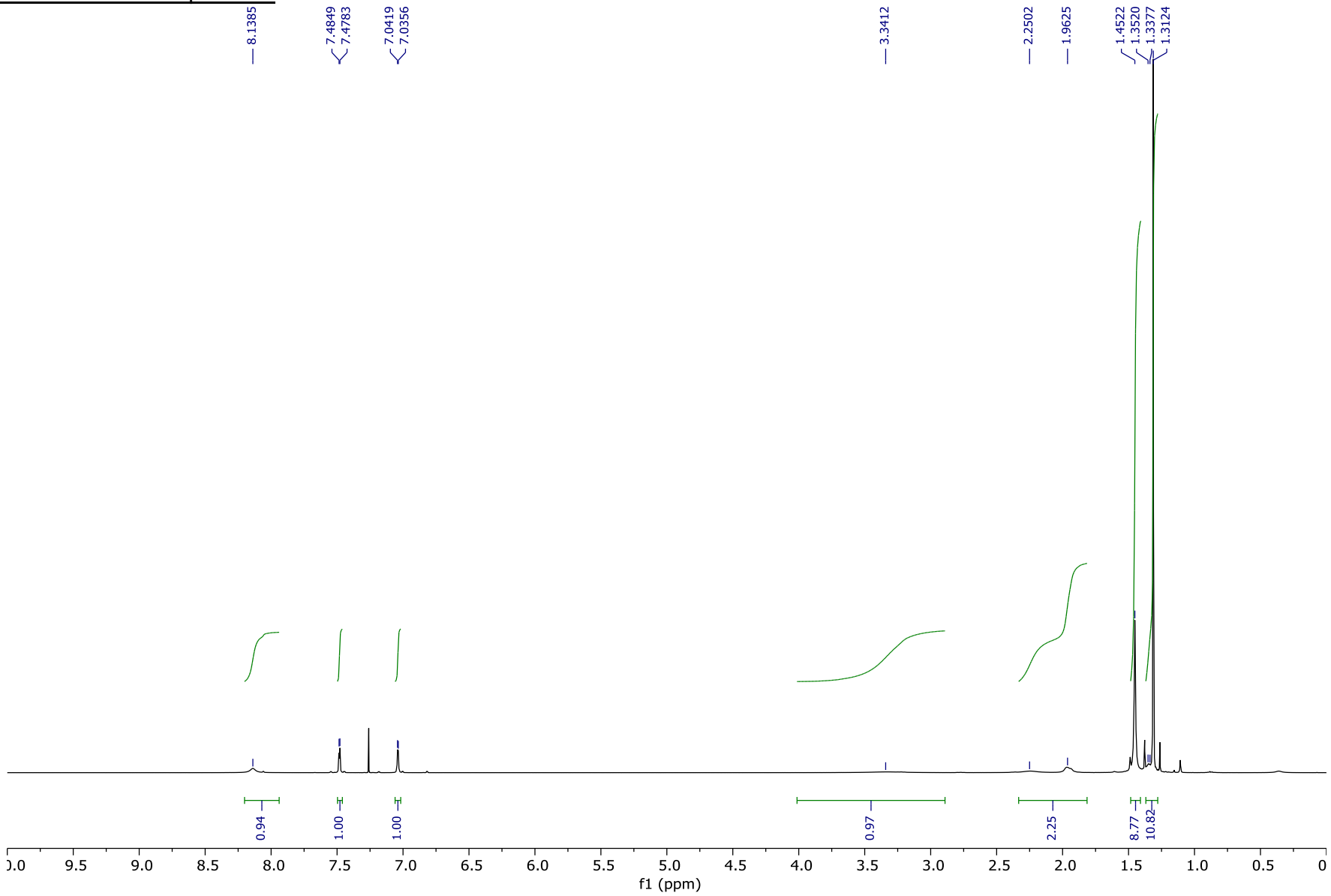

VT NMR spectra (298-328 K) of **1** (7.6–7.4 ppm region)

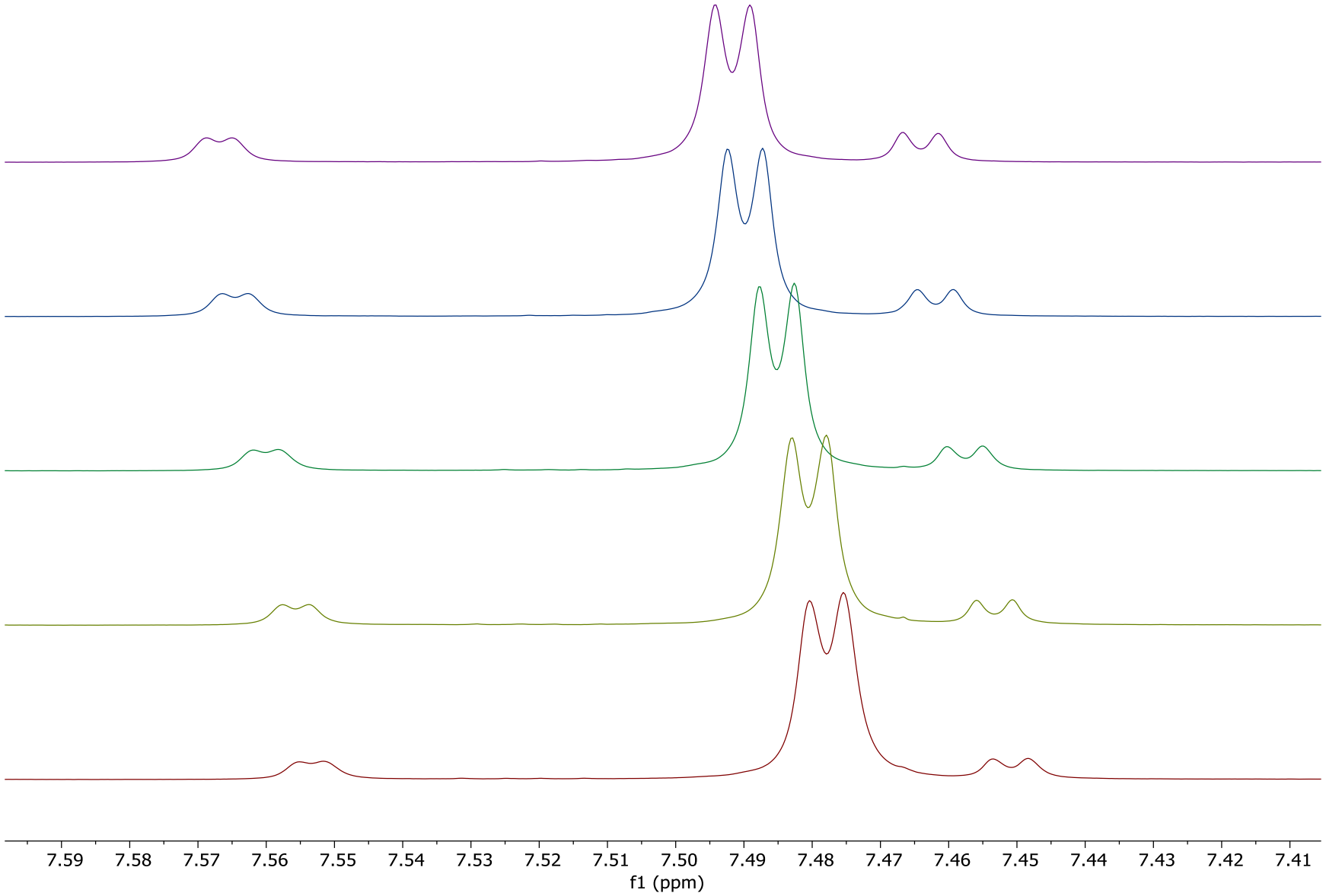

VT NMR spectra (298-328 K) of **1** (7.25–6.81 ppm region)

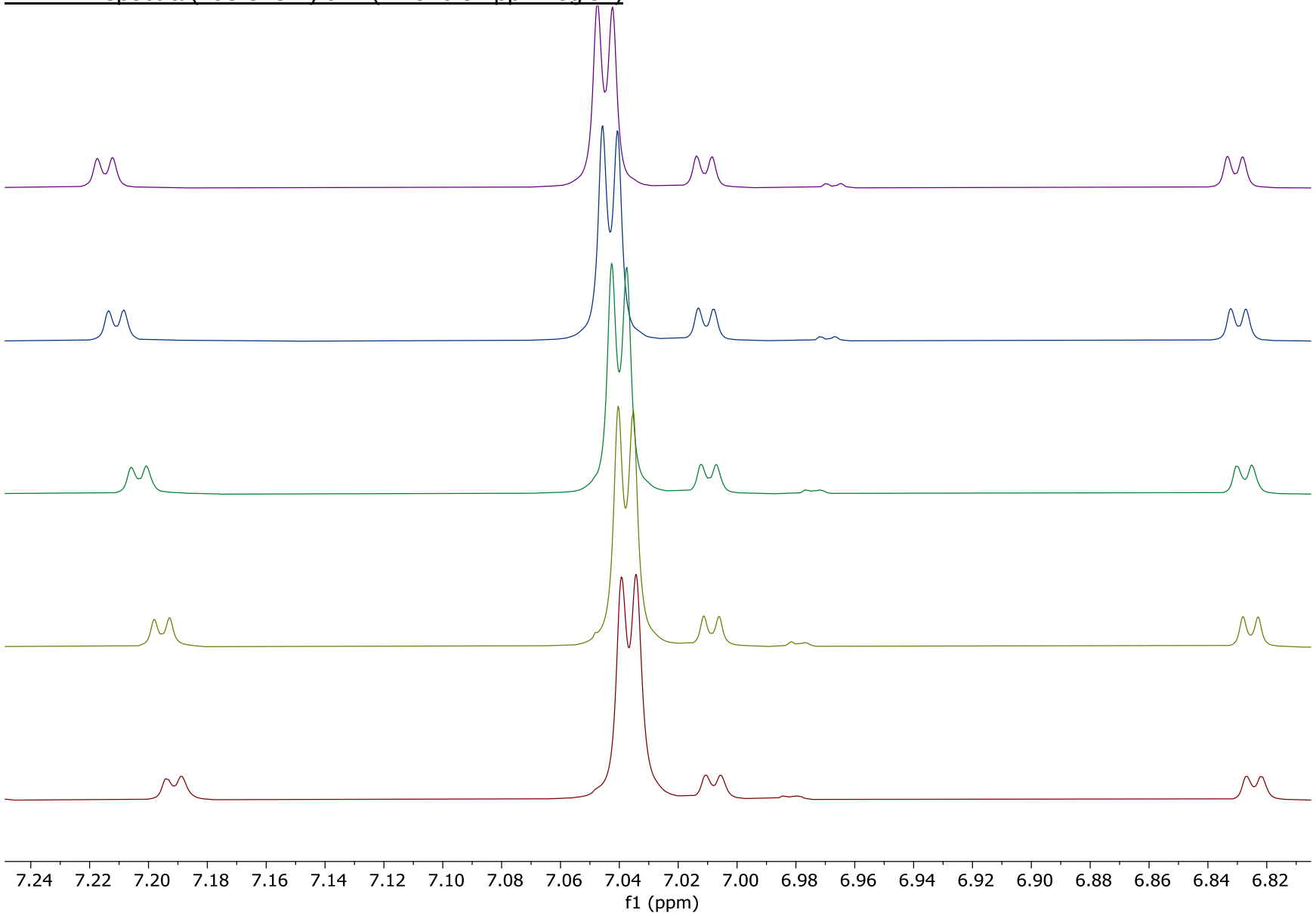

VT NMR spectra (298-328 K) of **1** (1.55–1.05 ppm region)

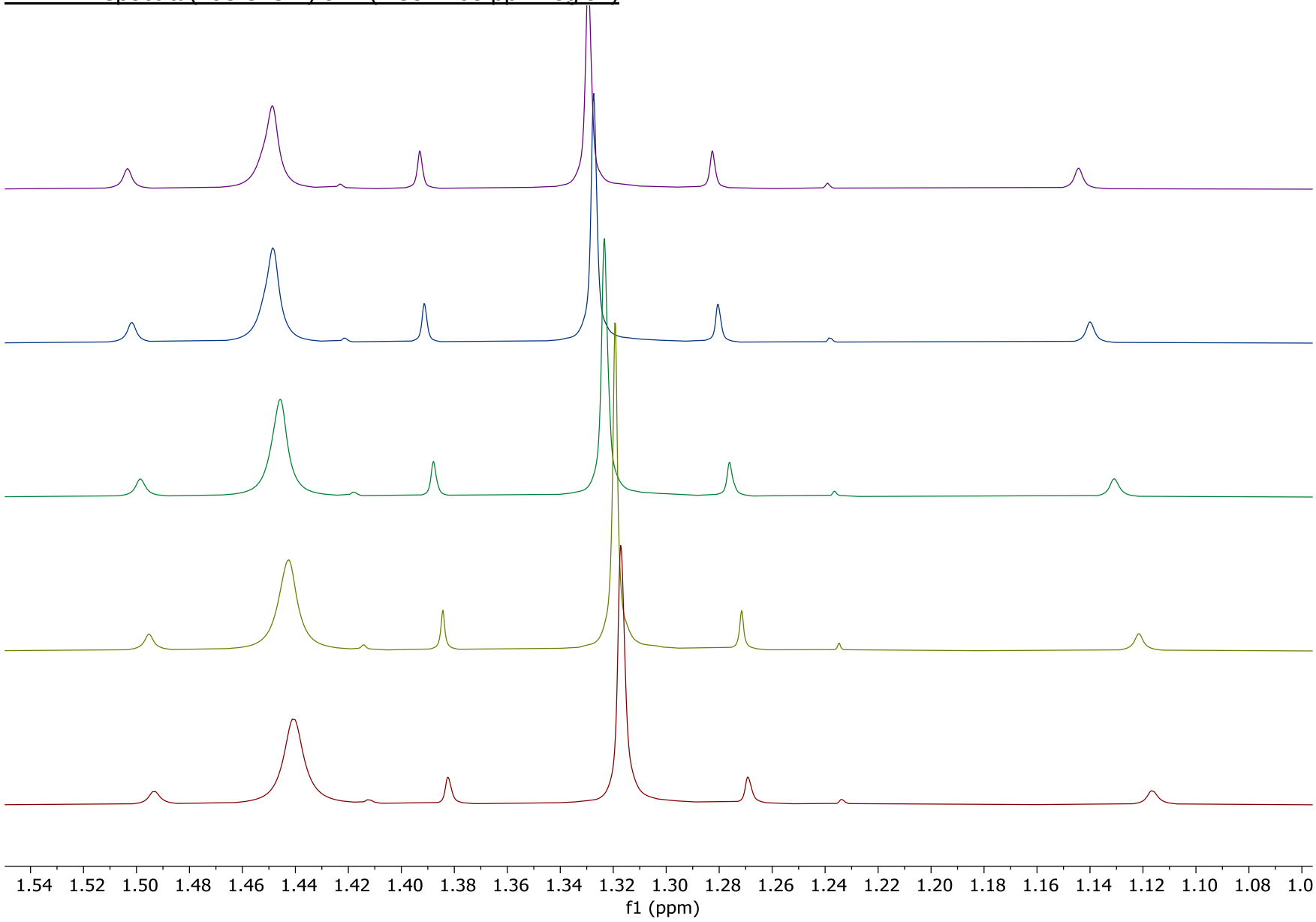

Compound **1** DOSY spectrum

Full spectrum

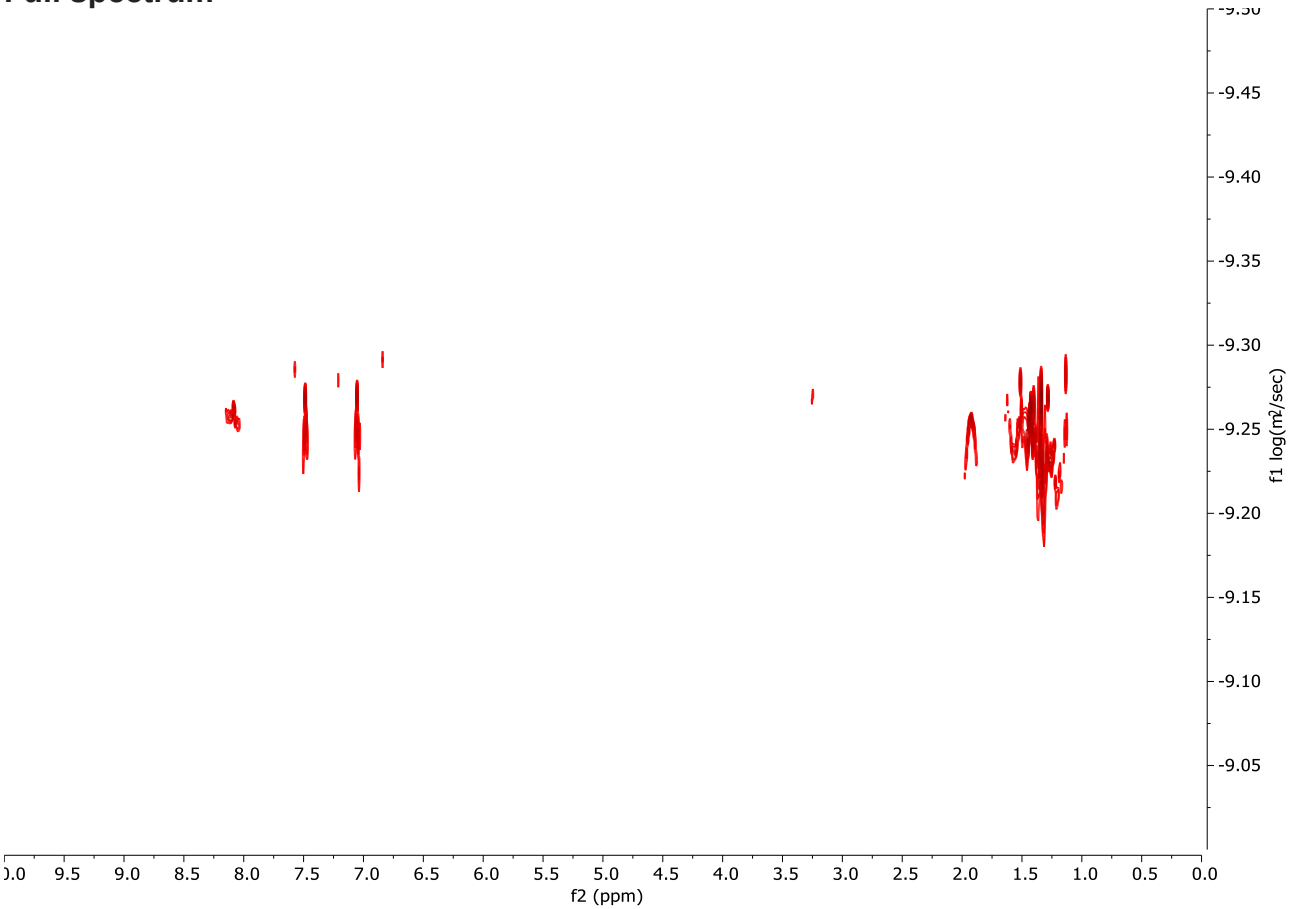

Expansion of aromatic / imine region

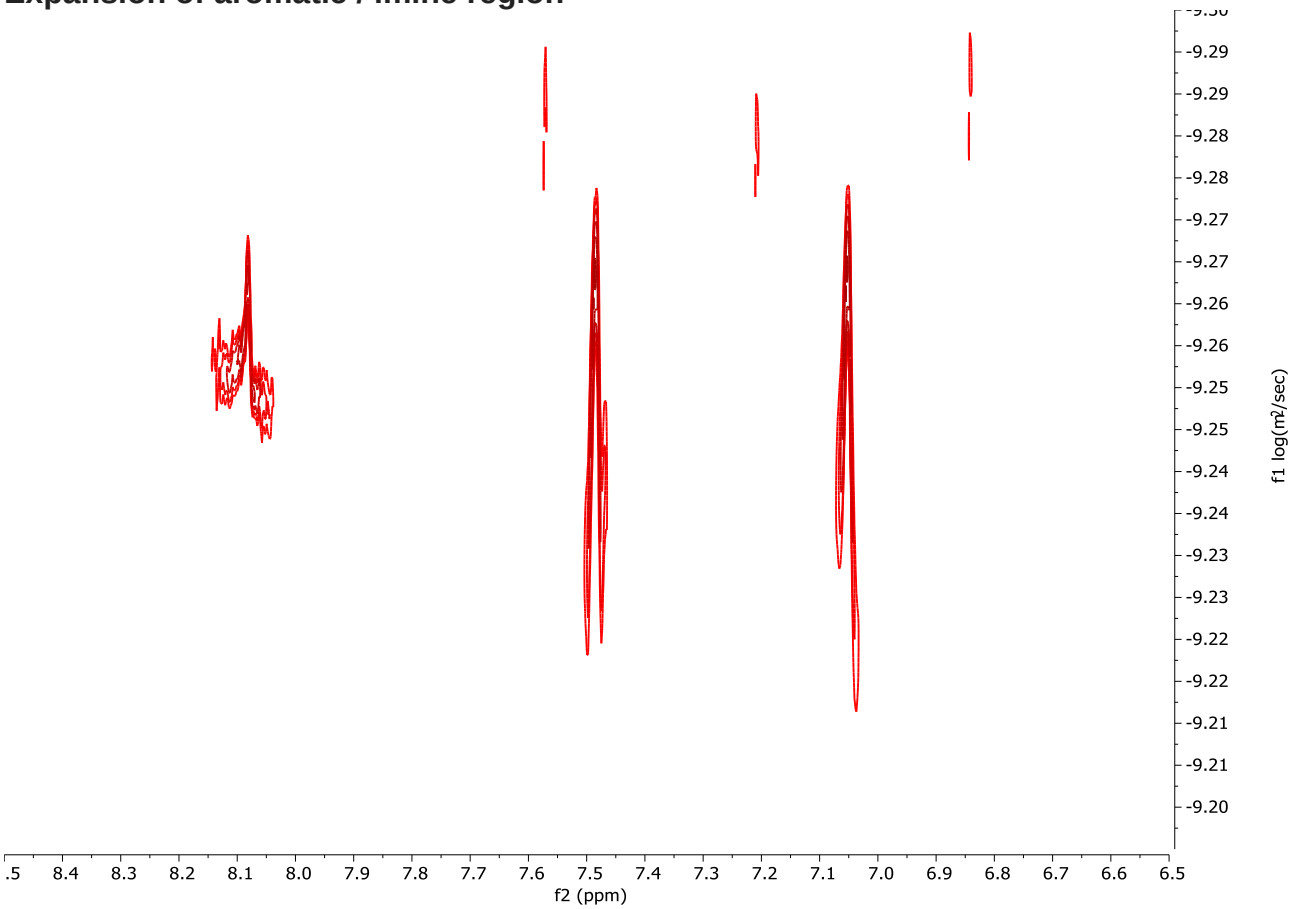

Peak assignment	ppm	Diffusion coefficient (m^2 s^{-1})
Imine (major species)	8.1	5.4×10^{-10}
Imine (minor species)	7.6	5.0×10^{-10}
Aromatic CH (major species)	7.5	5.4×10^{-10}
Chloroform	7.3	2.0×10^{-9}
Aromatic CH (minor species)	7.2	5.1×10^{-10}
Aromatic CH (major species)	7.1	5.4×10^{-10}
Aromatic CH (minor species)	6.8	5.1×10^{-10}

The other signals for the minor species present in Figure 7 are not resolved in the DOSY spectrum due to the lower frequency domain resolution used.

The DOSY experiment was performed on a 600 MHz spectrometer at 298K. The Bruker pulse sequence ledbpgp2s was used, which contains bipolar gradient pulses and an eddy current delay. The diffusion delay was 60 ms, the gradient pulse length was 1 ms, and the delay between scans was 6 s. 16 Subspectra were acquired with linearly spaced gradient strengths, and were processed using MestreNova.

Compound **1**.TFA ^{1}H NMR spectrum

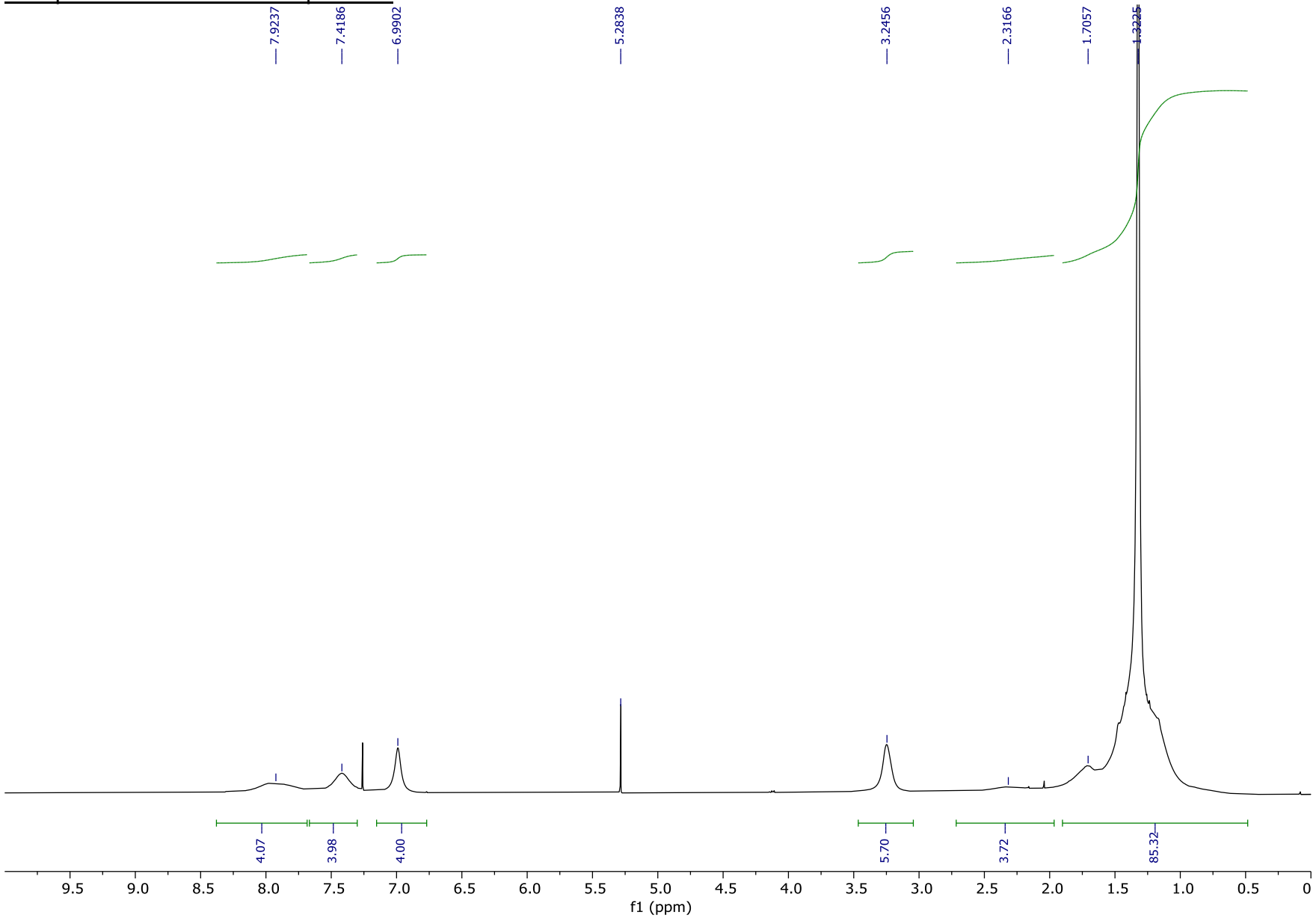

VT NMR spectra (233-328 K) of **1**.TFA (6.7–8.3 ppm region)

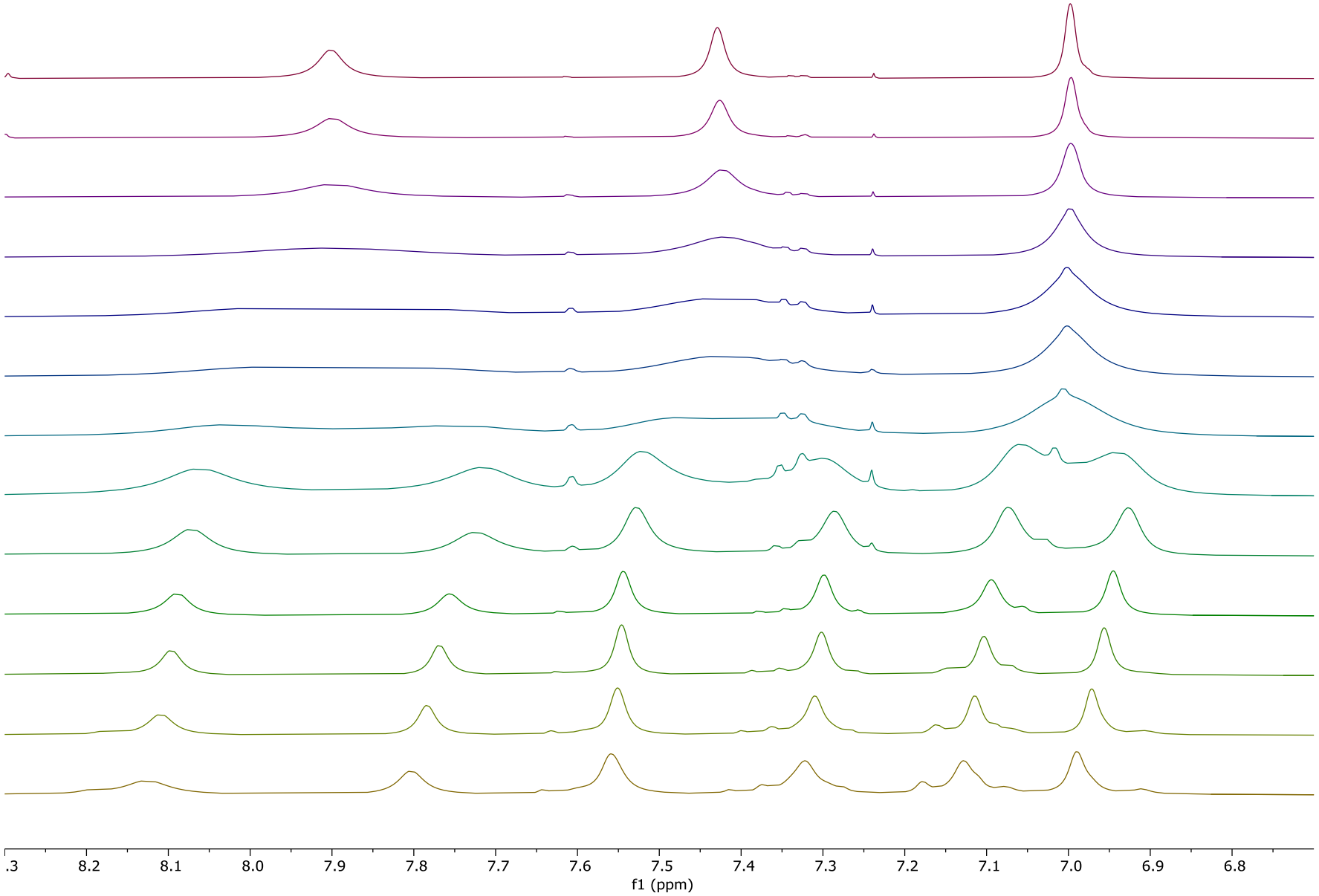

VT NMR spectra (233-328 K) of **1**.TFA (6.0–2.9 ppm region)

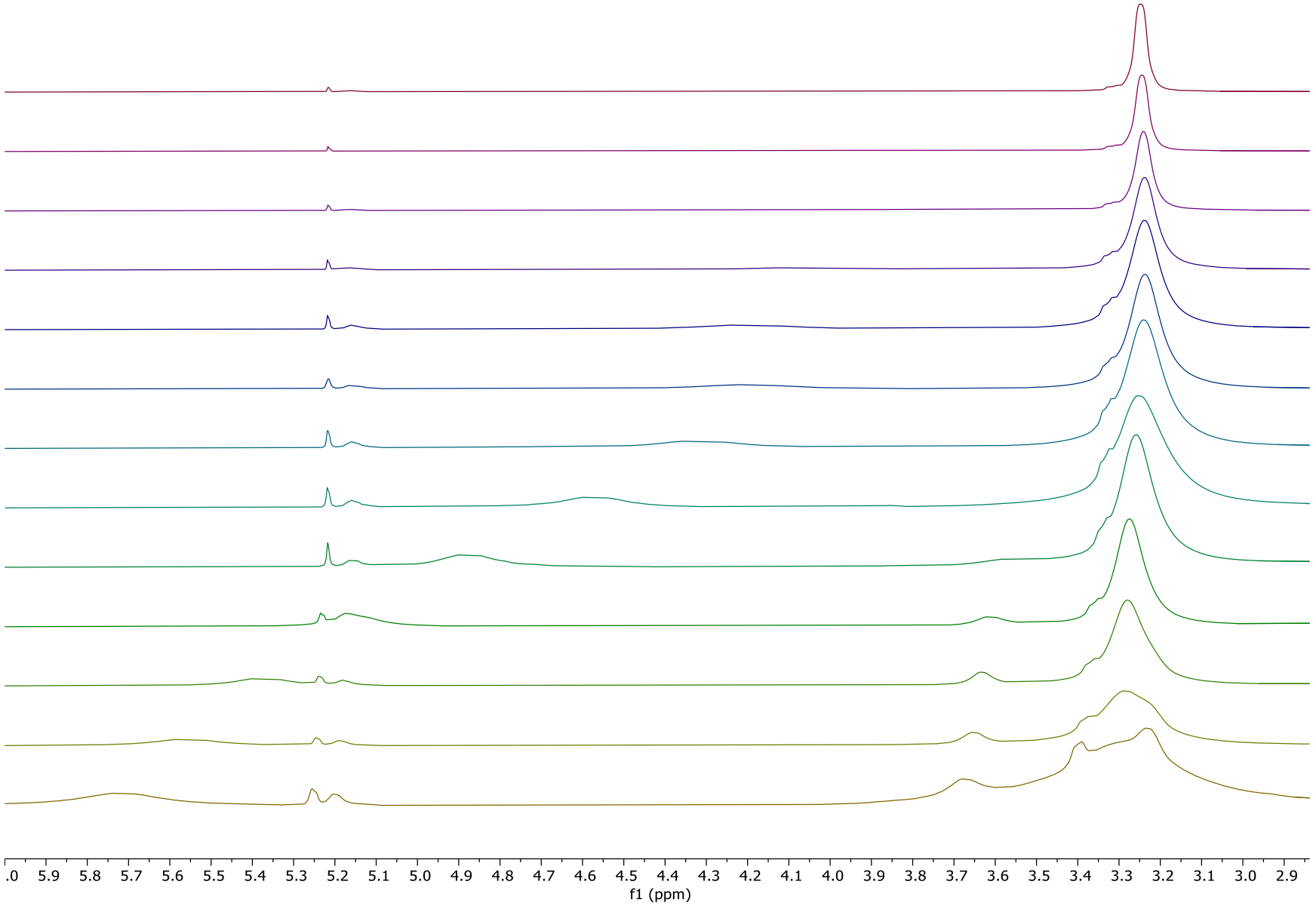

VT NMR spectra (233-328 K) of **1**.TFA (2.9–0.2 ppm region) emphasising the changes in the signals in this region which do not correspond to *tert*-butyl groups

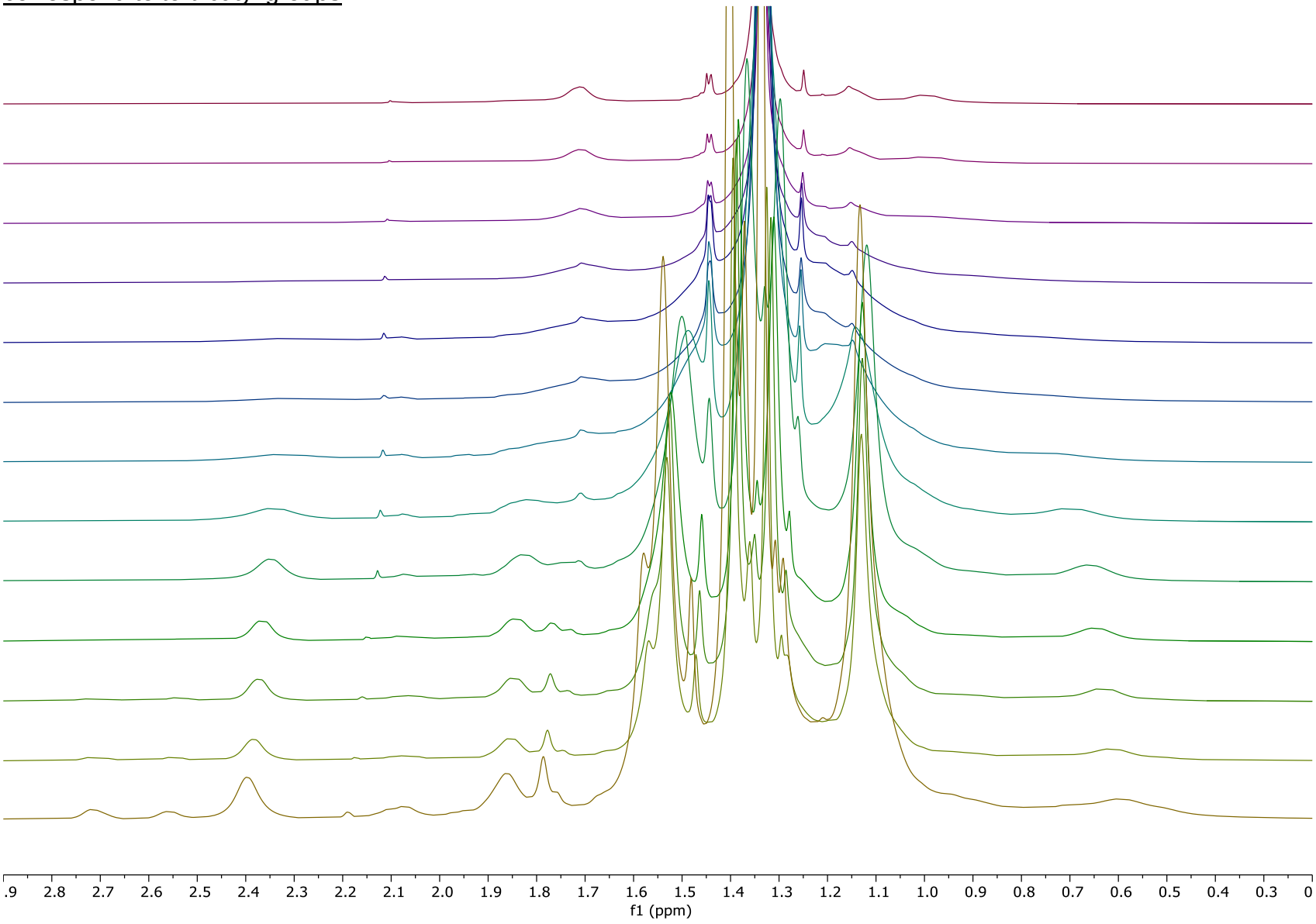

VT NMR spectra (233-328 K) of **1**.TFA (1.7–0.8 ppm region) emphasising the changes in the signals in this region correspond to *tert*-butyl groups

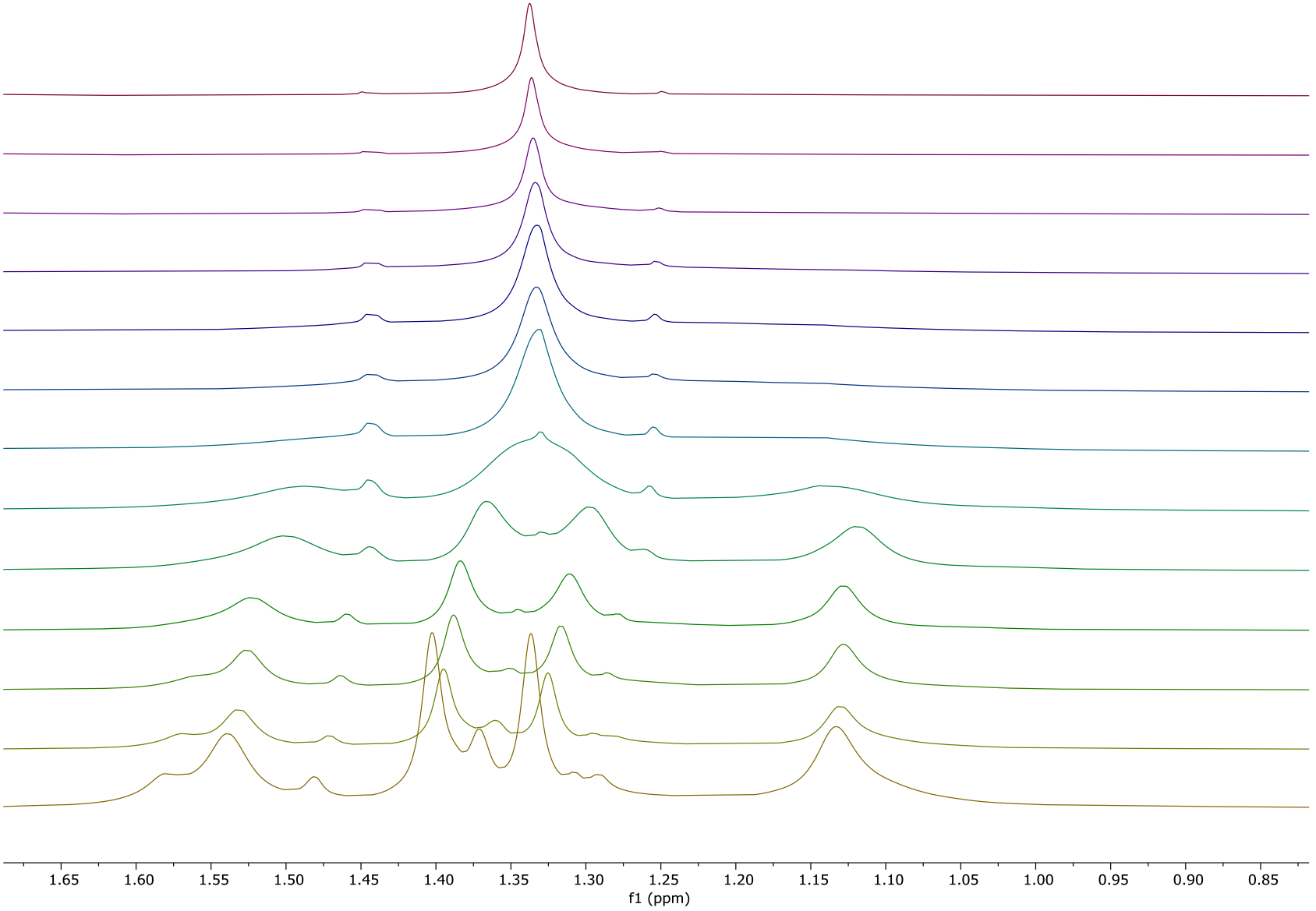

Compound **1**.TFA ^{13}C NMR spectrum

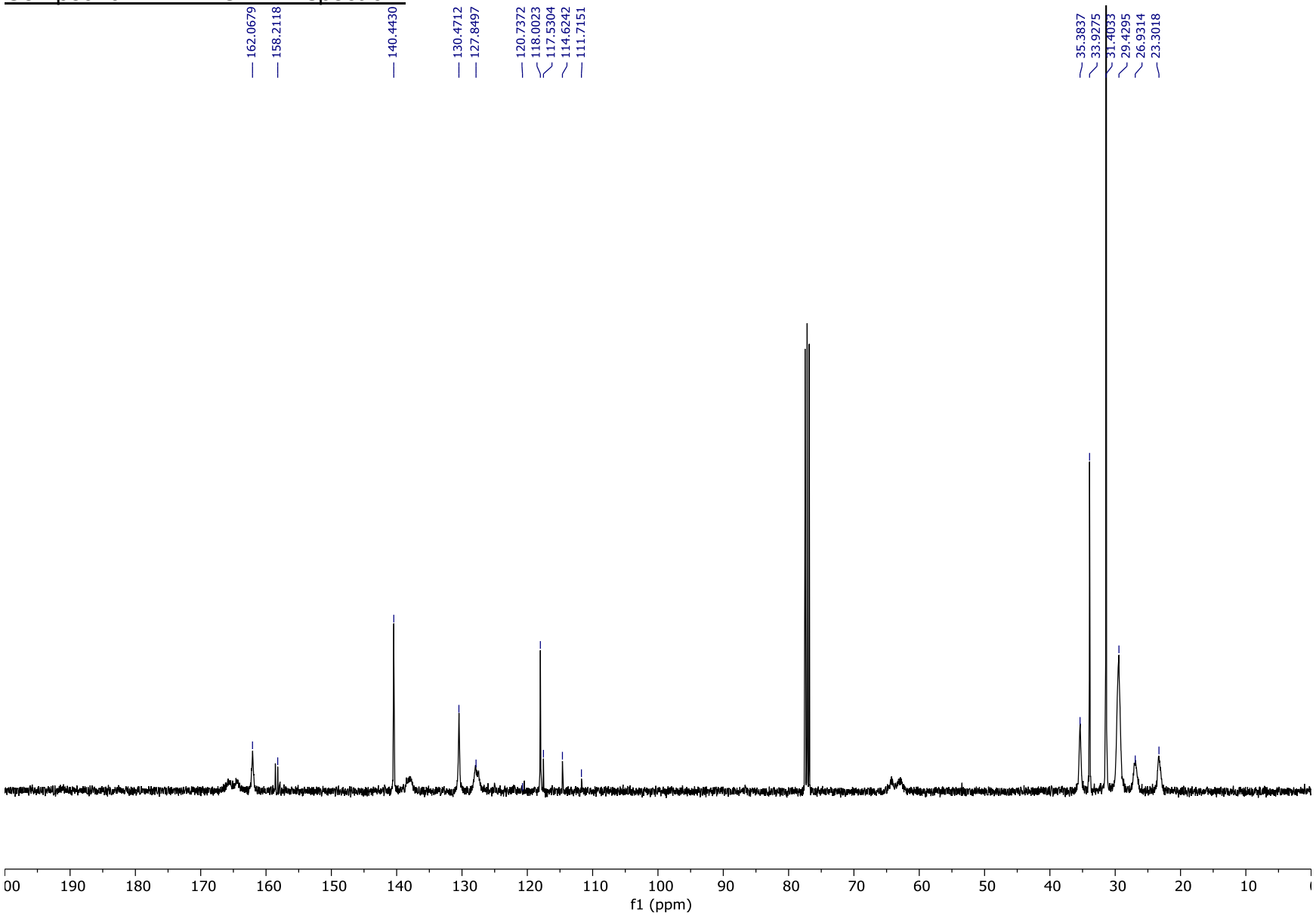

Compound **1**.TFA ^{19}F NMR spectrum

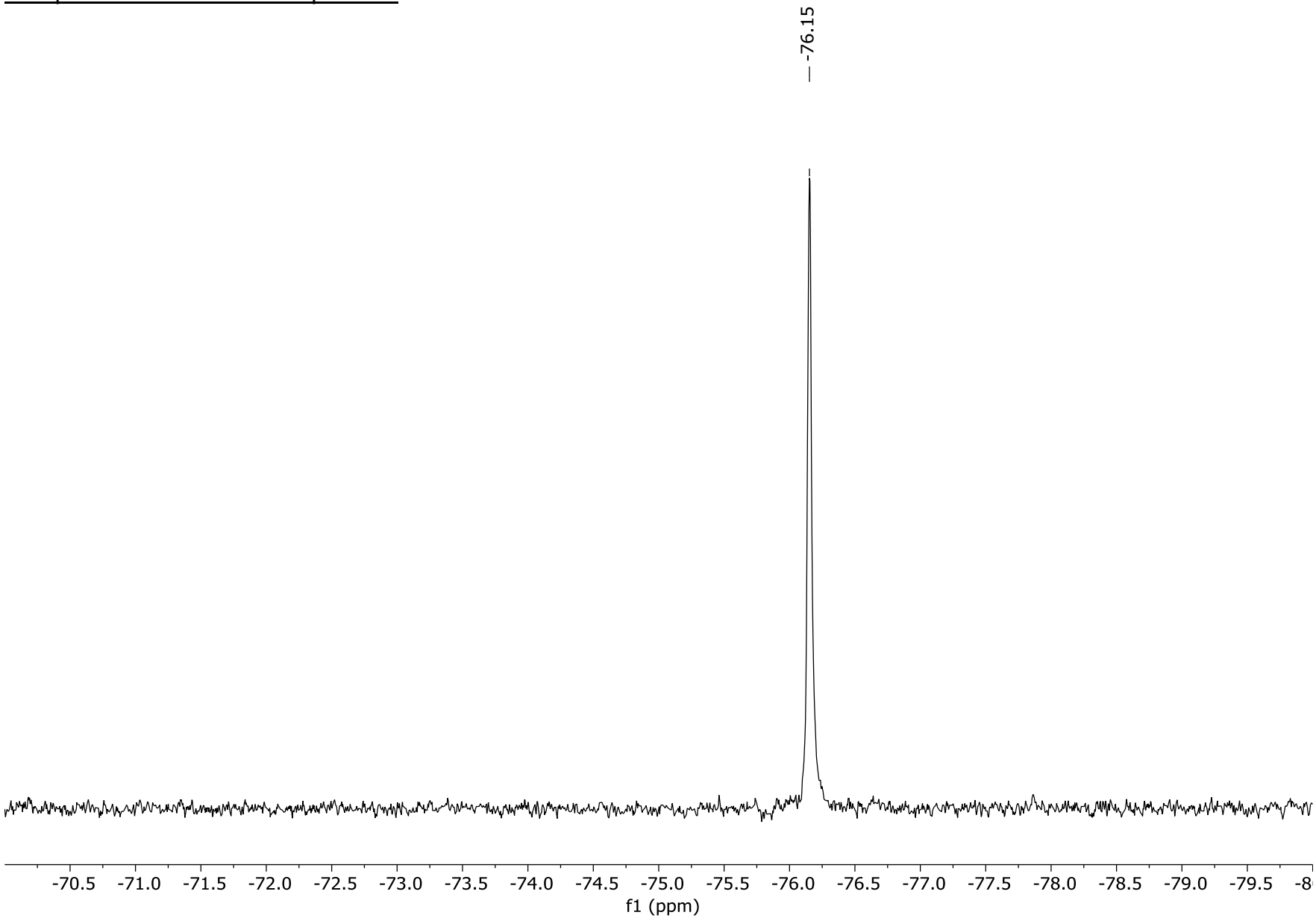

Compound **8** ^{1}H NMR spectrum

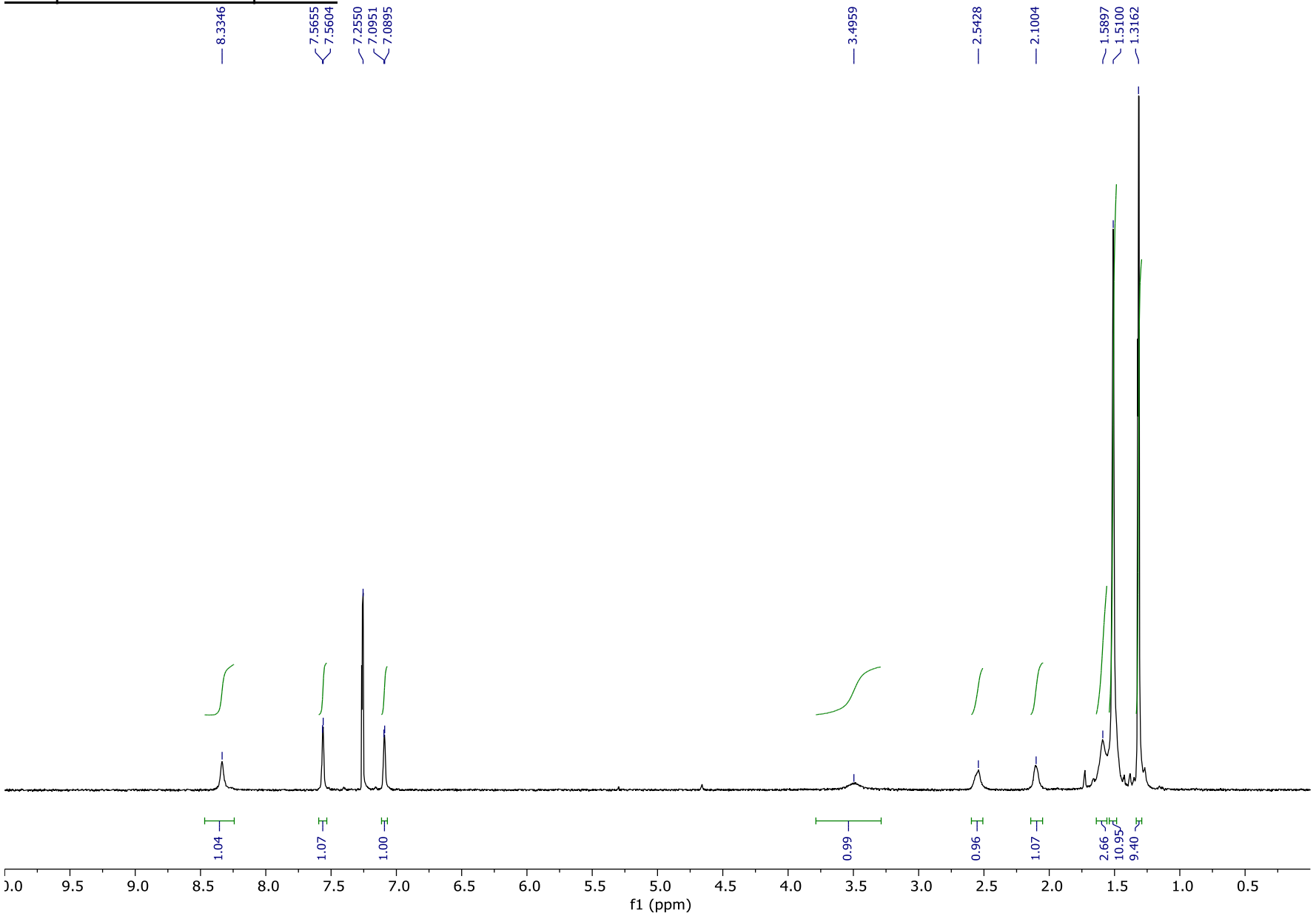

VT NMR spectra (218-298 K) of **8** (6.7–8.3 ppm region)

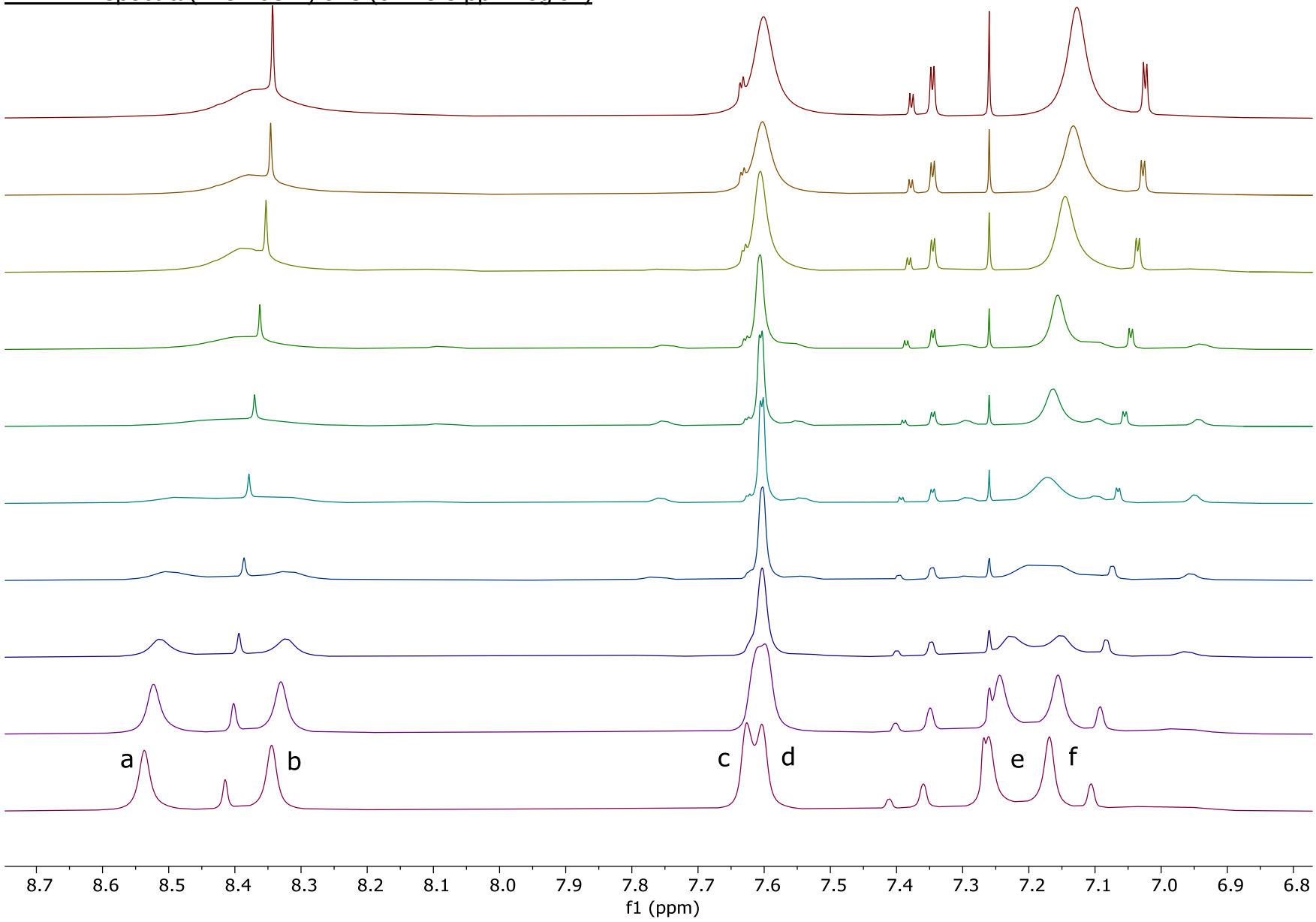

VT NMR spectra (218-298 K) of **8** (4.5–2.0 ppm region)

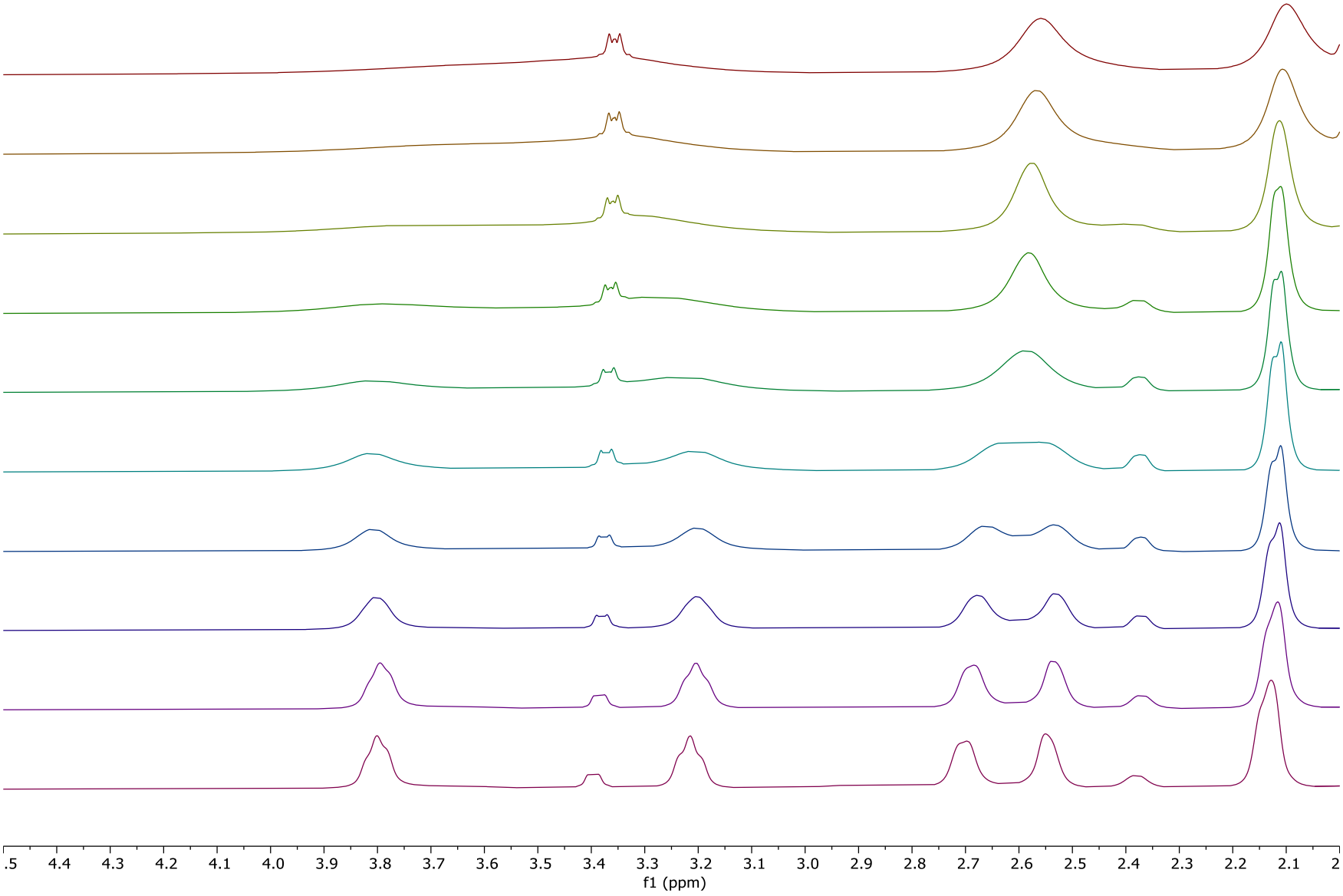

VT NMR spectra (218-298 K) of **8** (3.0–0.5 ppm region) emphasising the changes in the signals in this region which do not correspond to *tert*-butyl groups

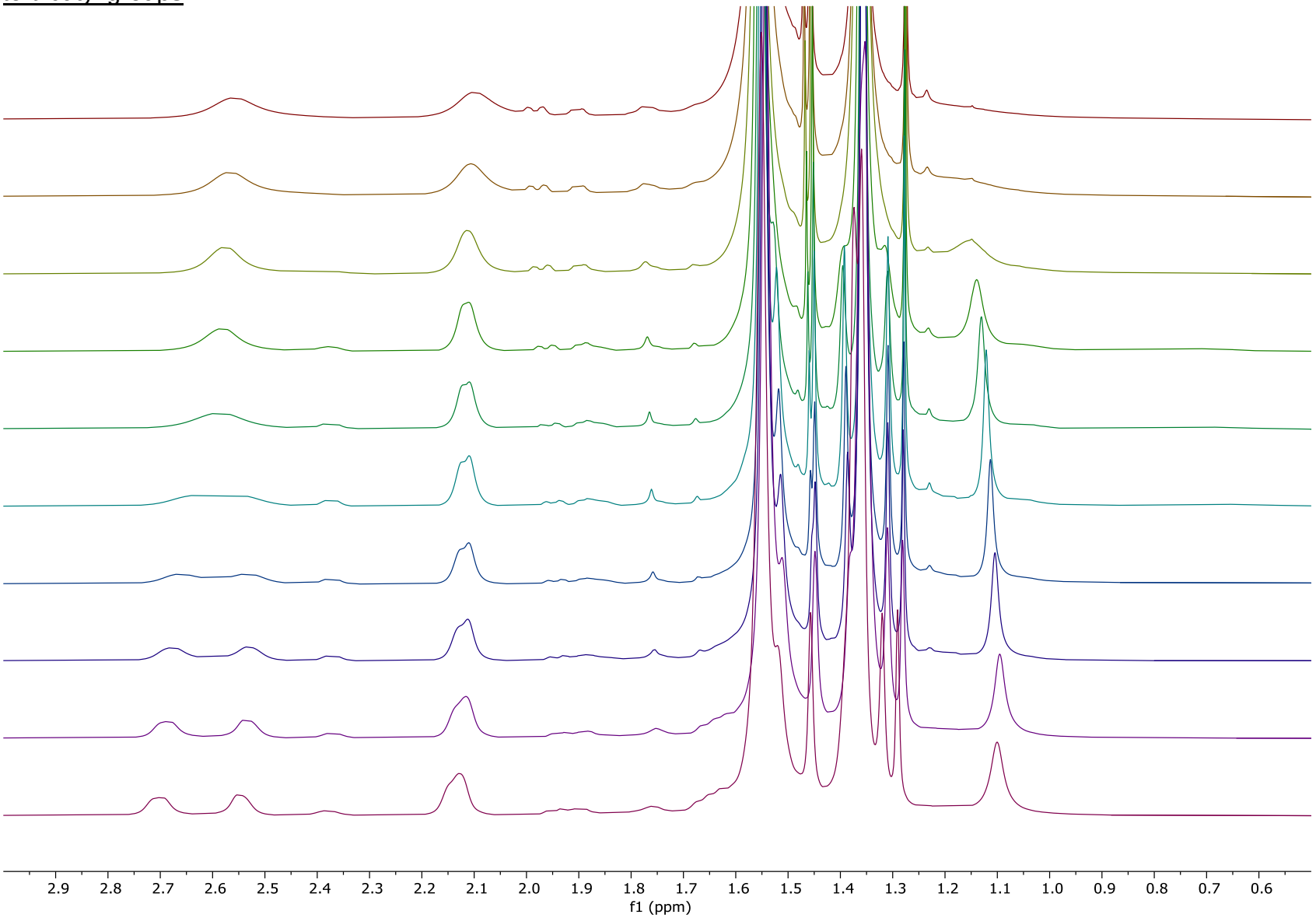

VT NMR spectra (218-298 K) of **8** (3.0–0.5 ppm region) emphasising the changes in the *tert*-butyl signals

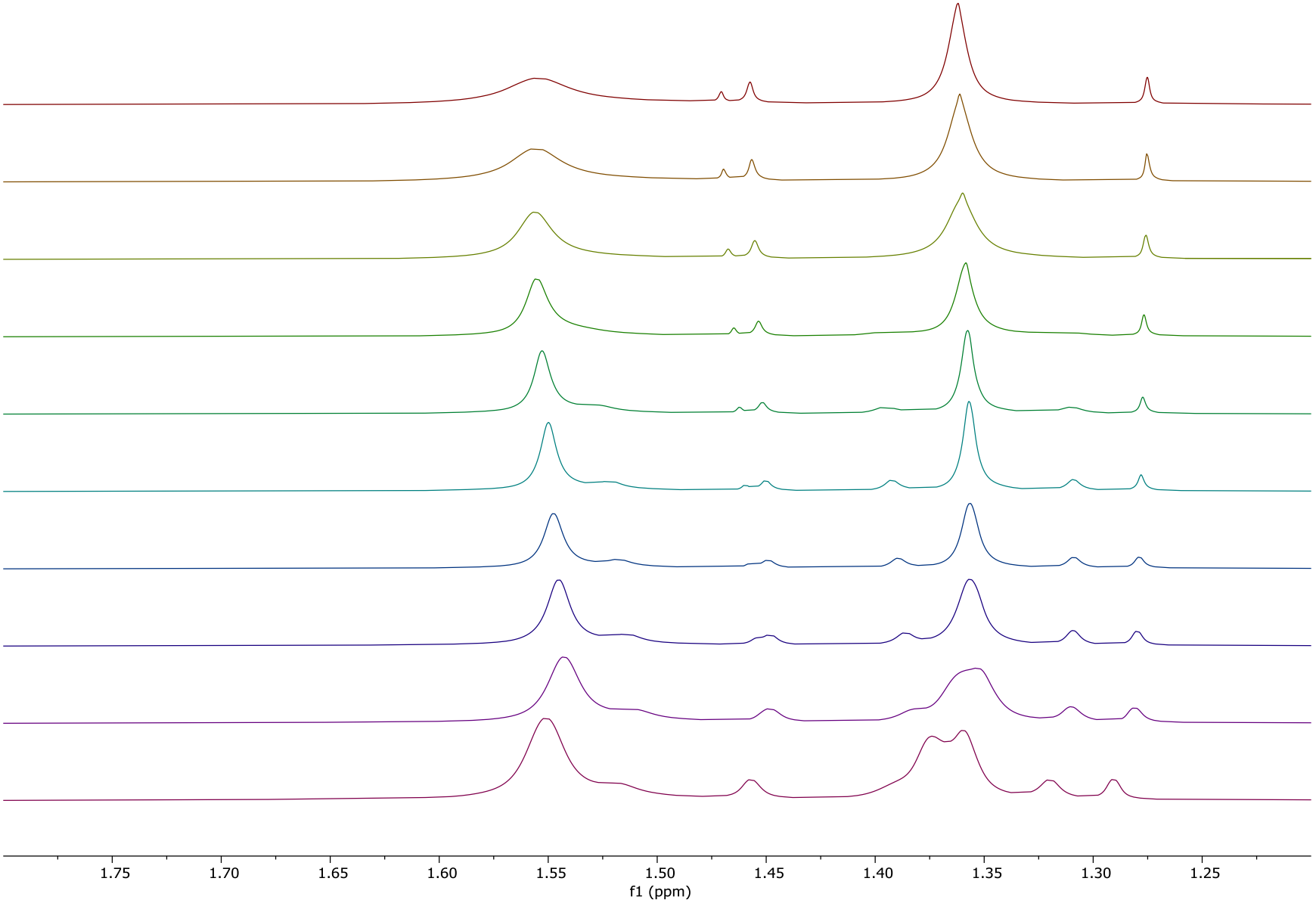

Compound **8** ^{13}C NMR spectrum

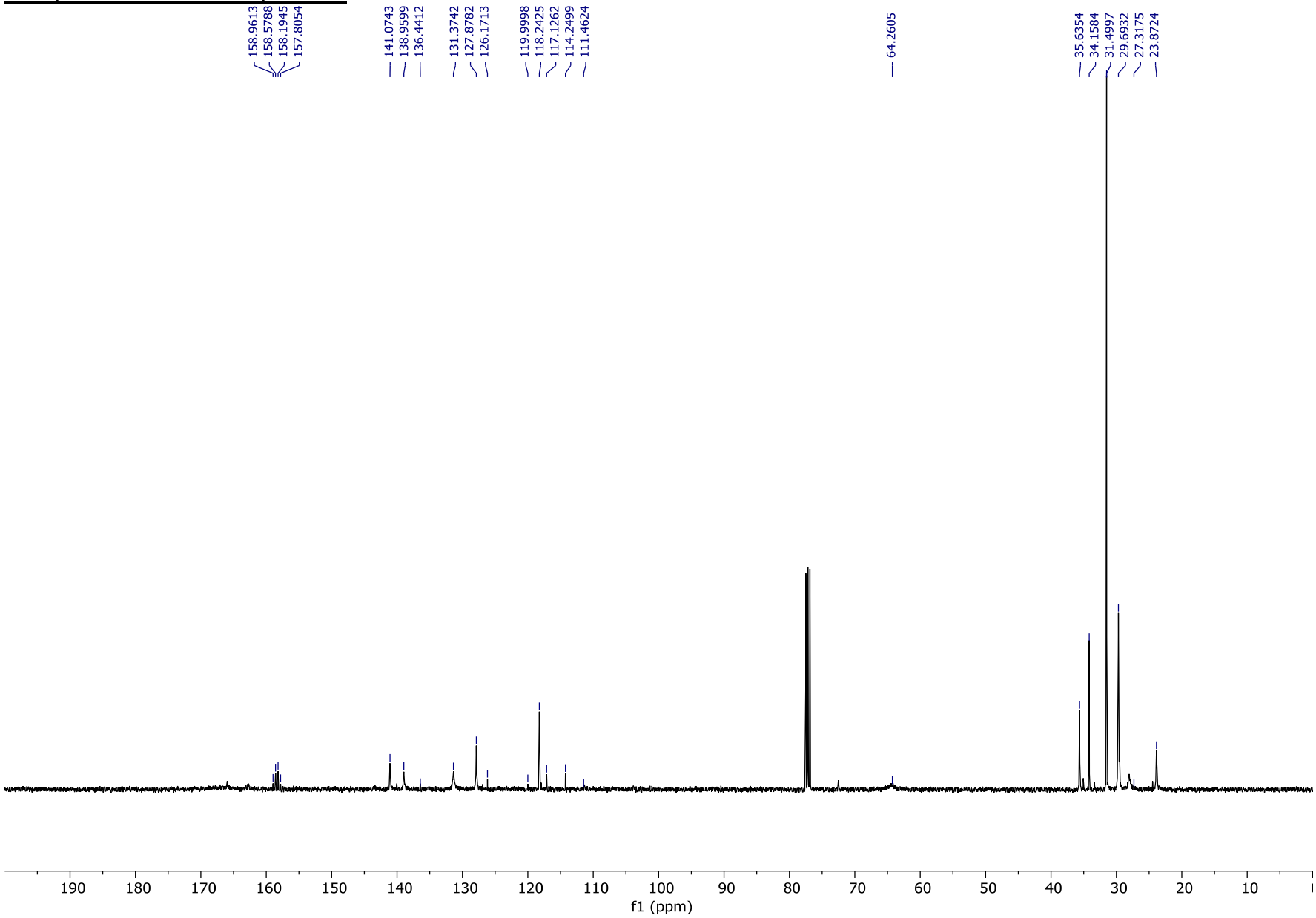

Compound **8** ^{19}F NMR spectrum

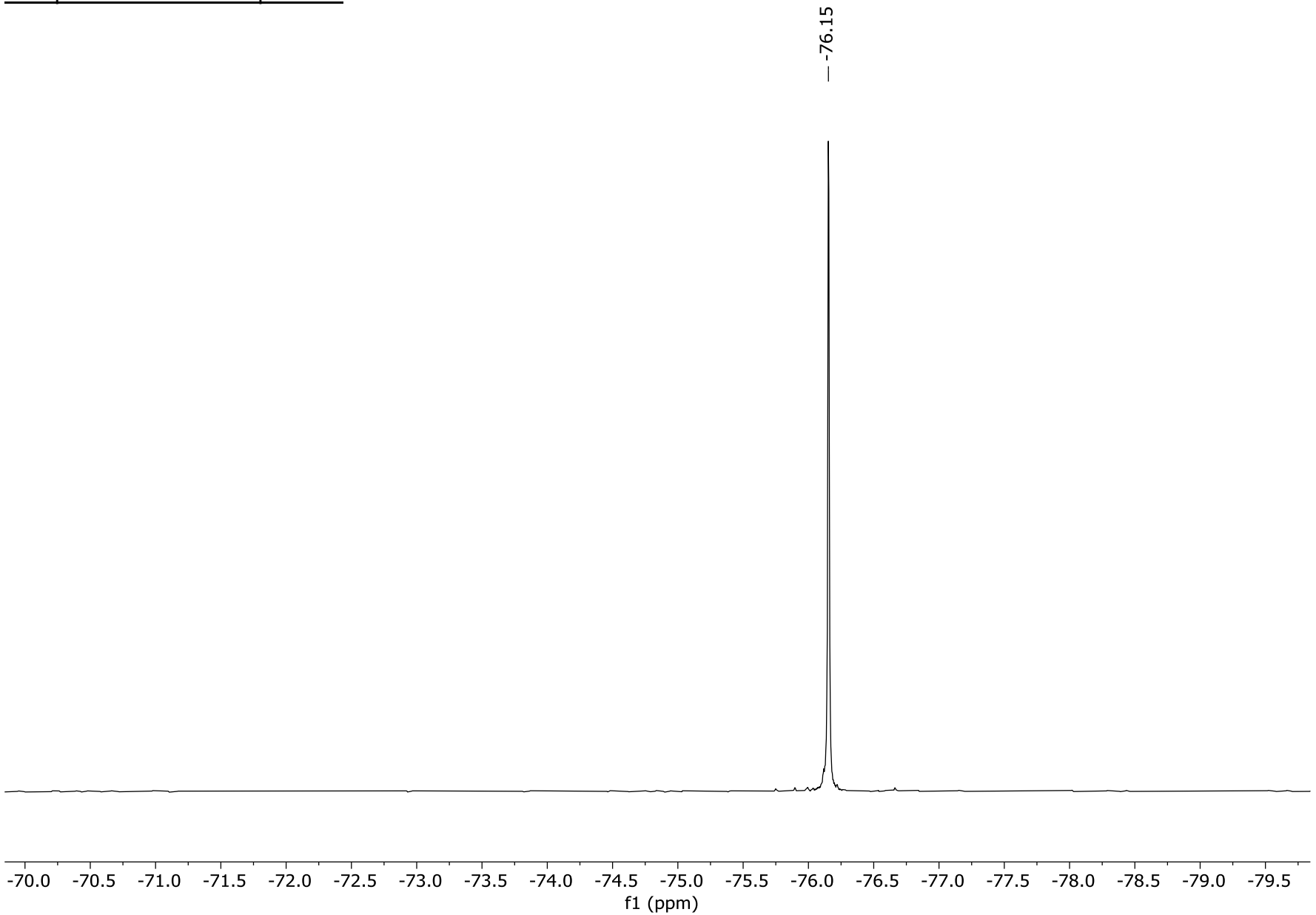

Compound **9** ^{1}H NMR spectrum

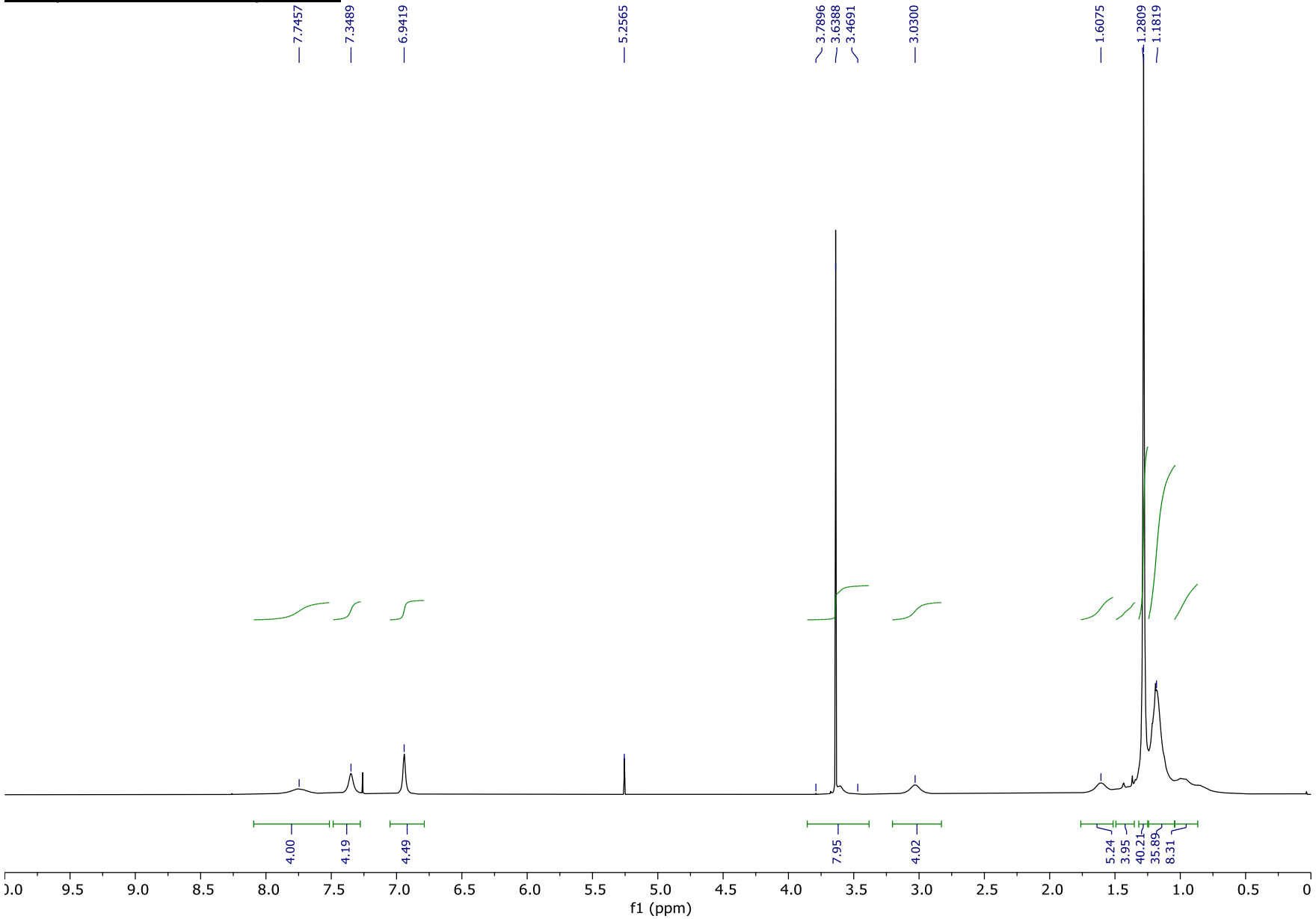

Compound **9** ^{13}C NMR spectrum

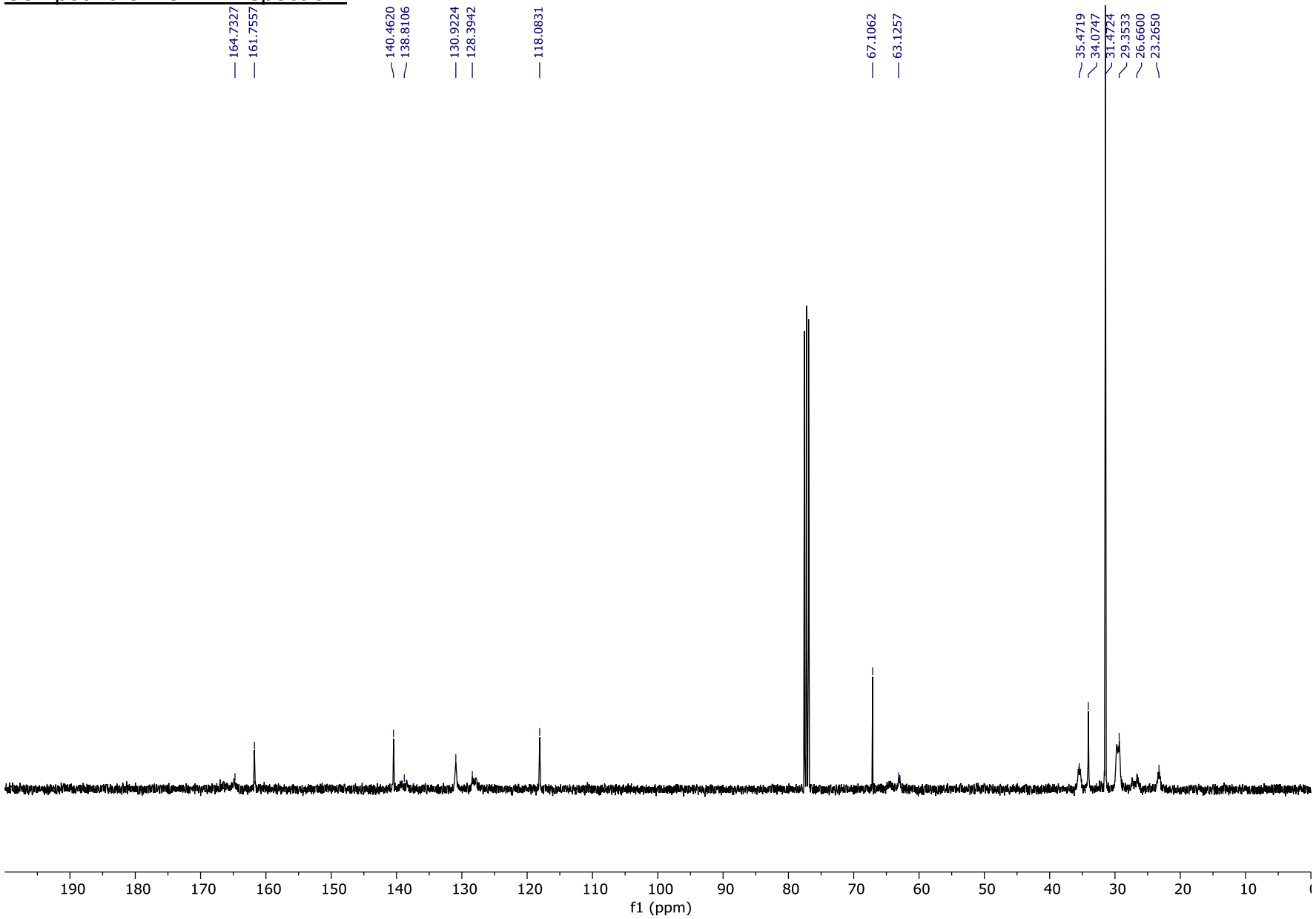

11 From Al(ᵗBu-salen)Cl and dioxane ^{1}H NMR spectrum

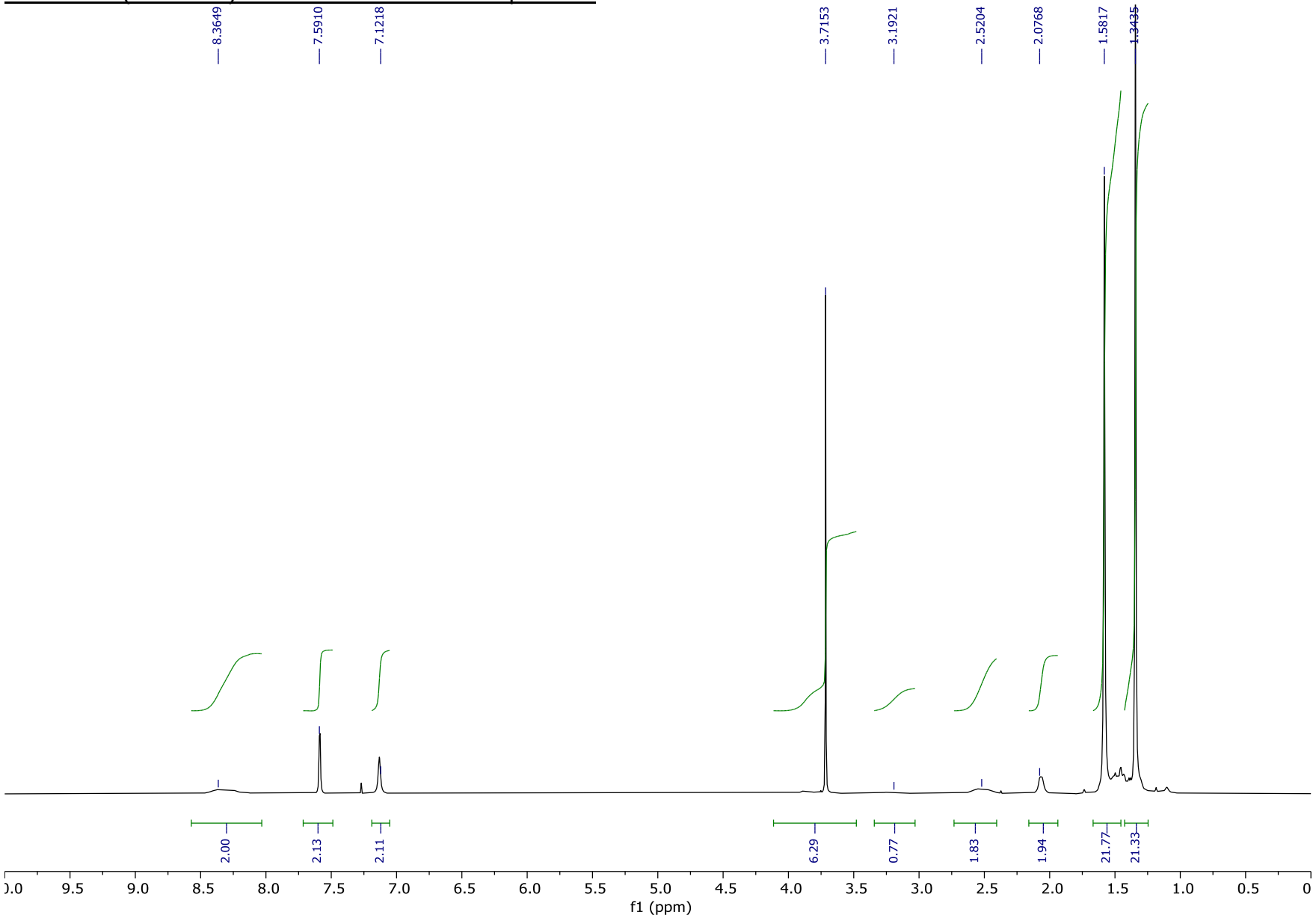

11 From Al(ᵗBu-salen)Cl and dioxane ^{13}C NMR spectrum

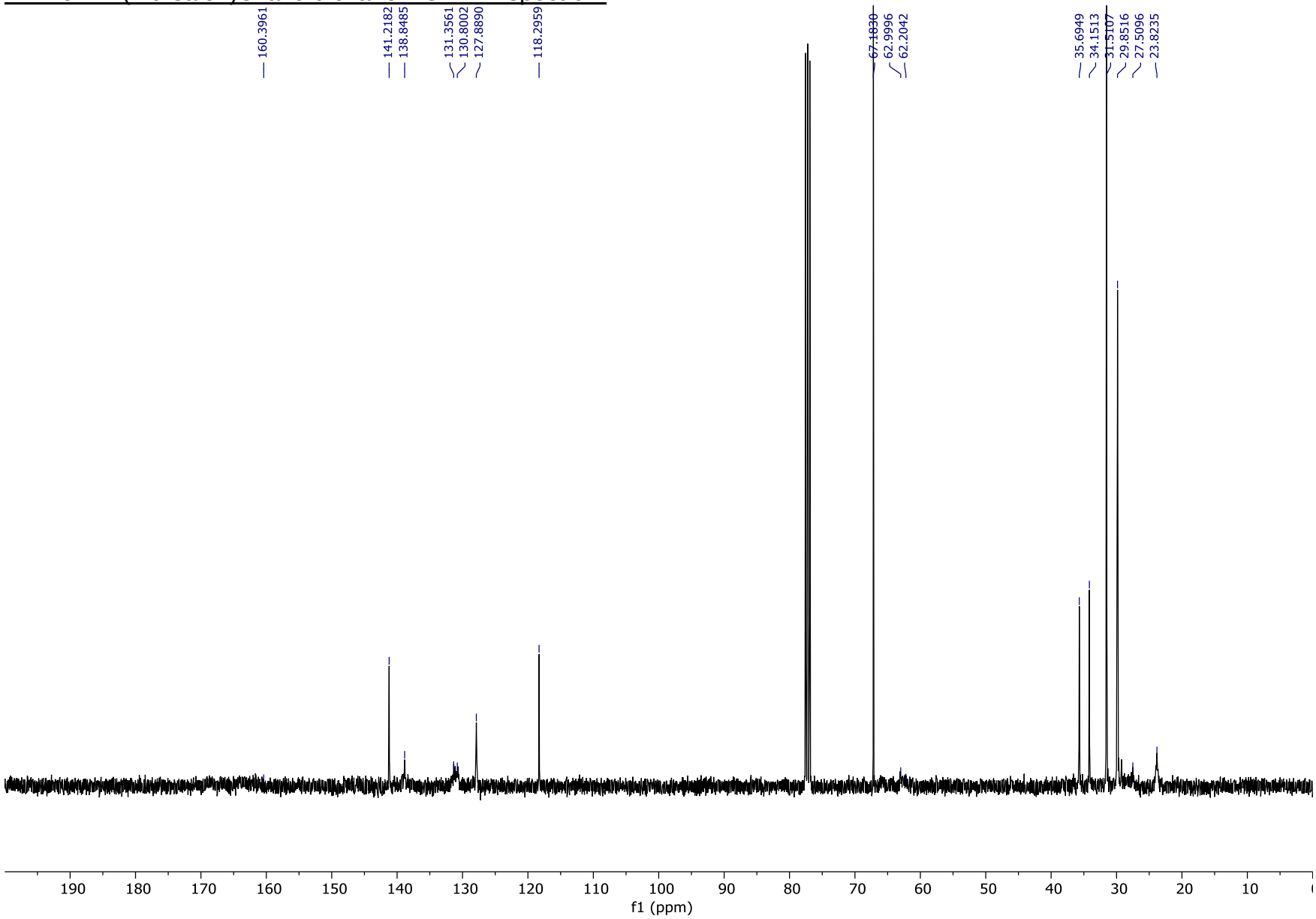

10+**11** From HCl addition to **1** ^{1}H NMR spectrum

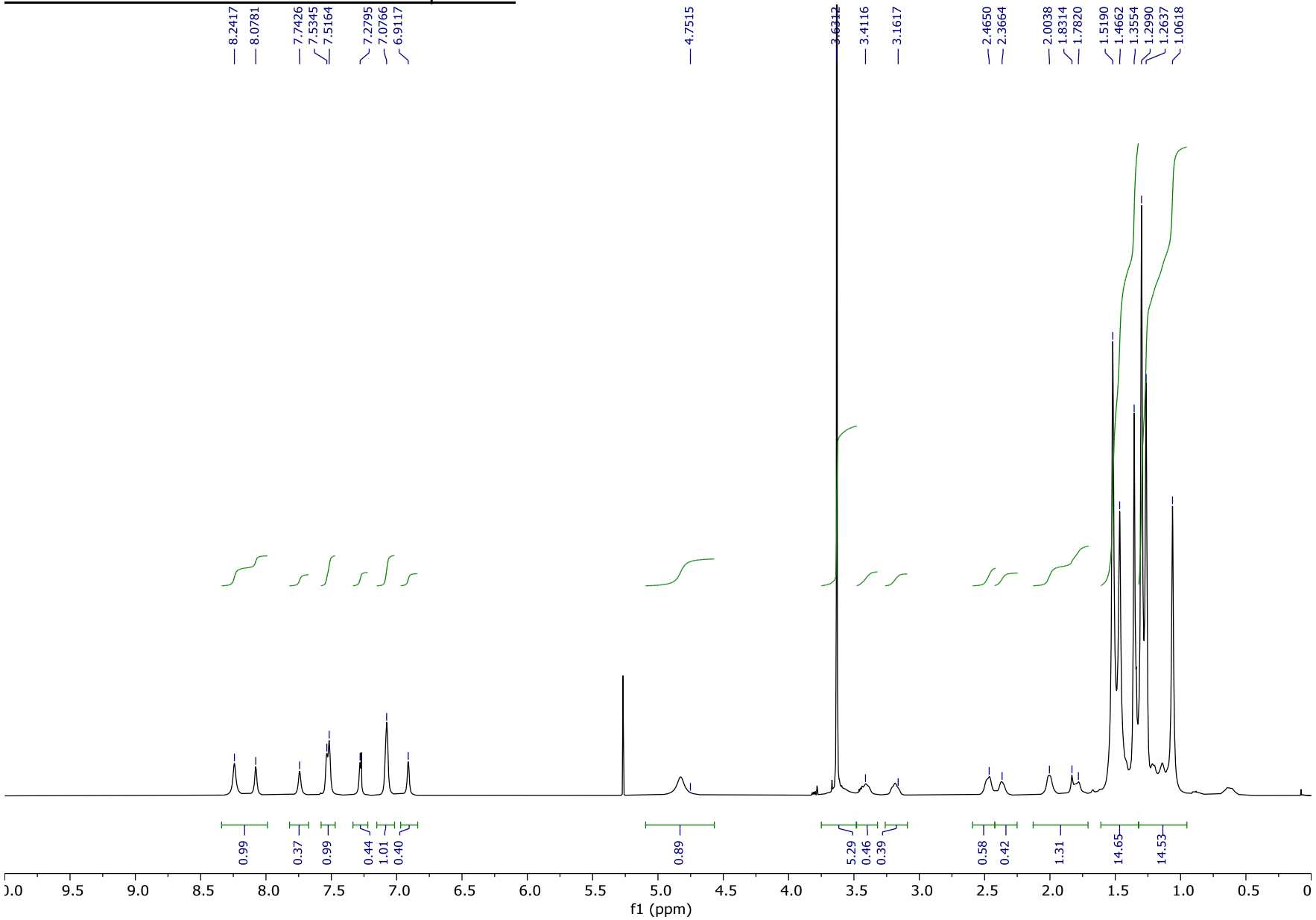

10+**11** From Al(ᵗBu-salen)Cl and dioxane ^{1}H NMR spectrum

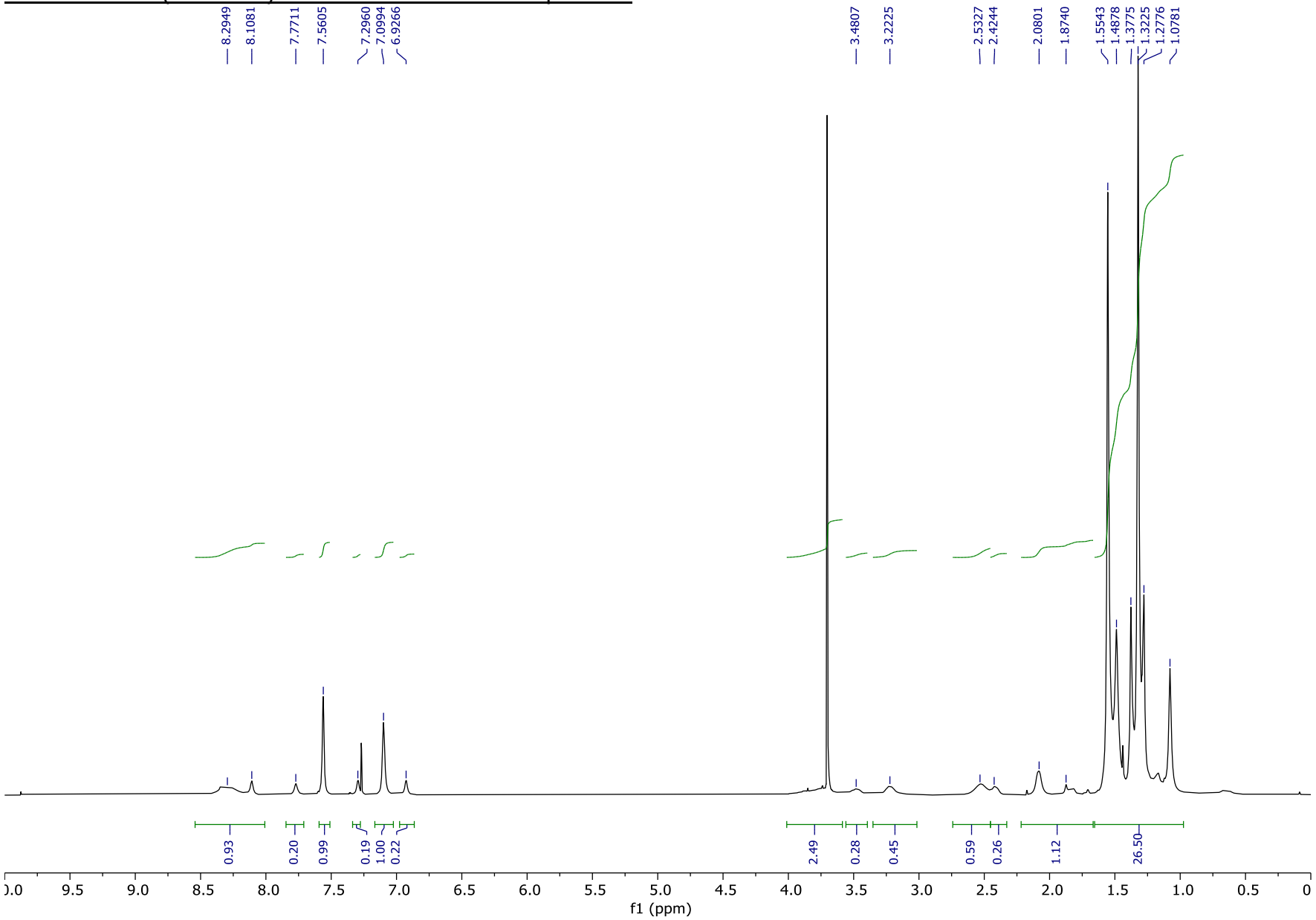

NOESY spectrum of **10**+**11** from Al(ᵗBu-salen)Cl and dioxane (on-diagonal peaks above 3 pm have been assigned to **10** or **11**)

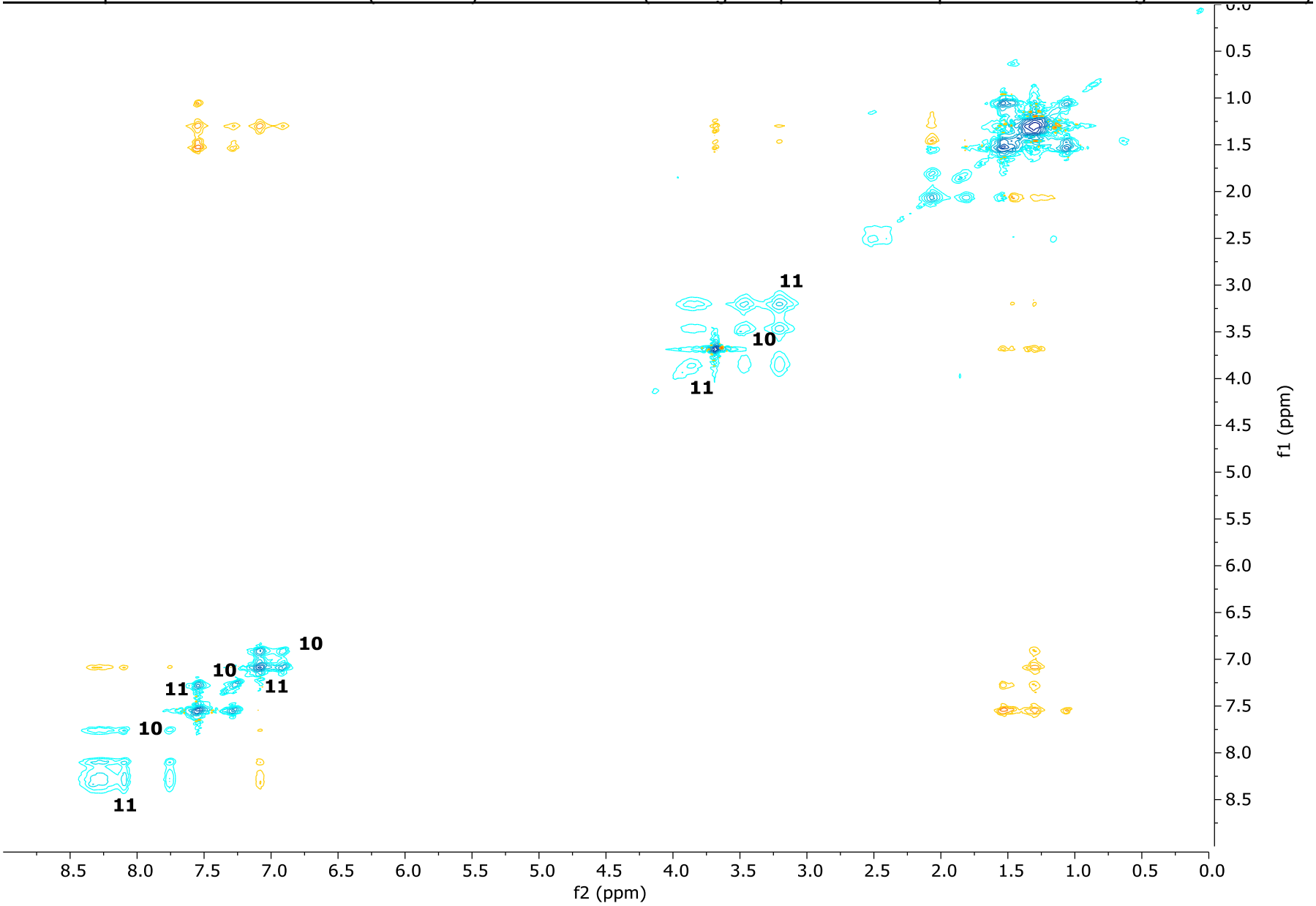

VT NMR spectra (218-328 K) of **10**+**11** from Al(^{t}Bu-salen)Cl and dioxane (6.5-9.5 ppm region)

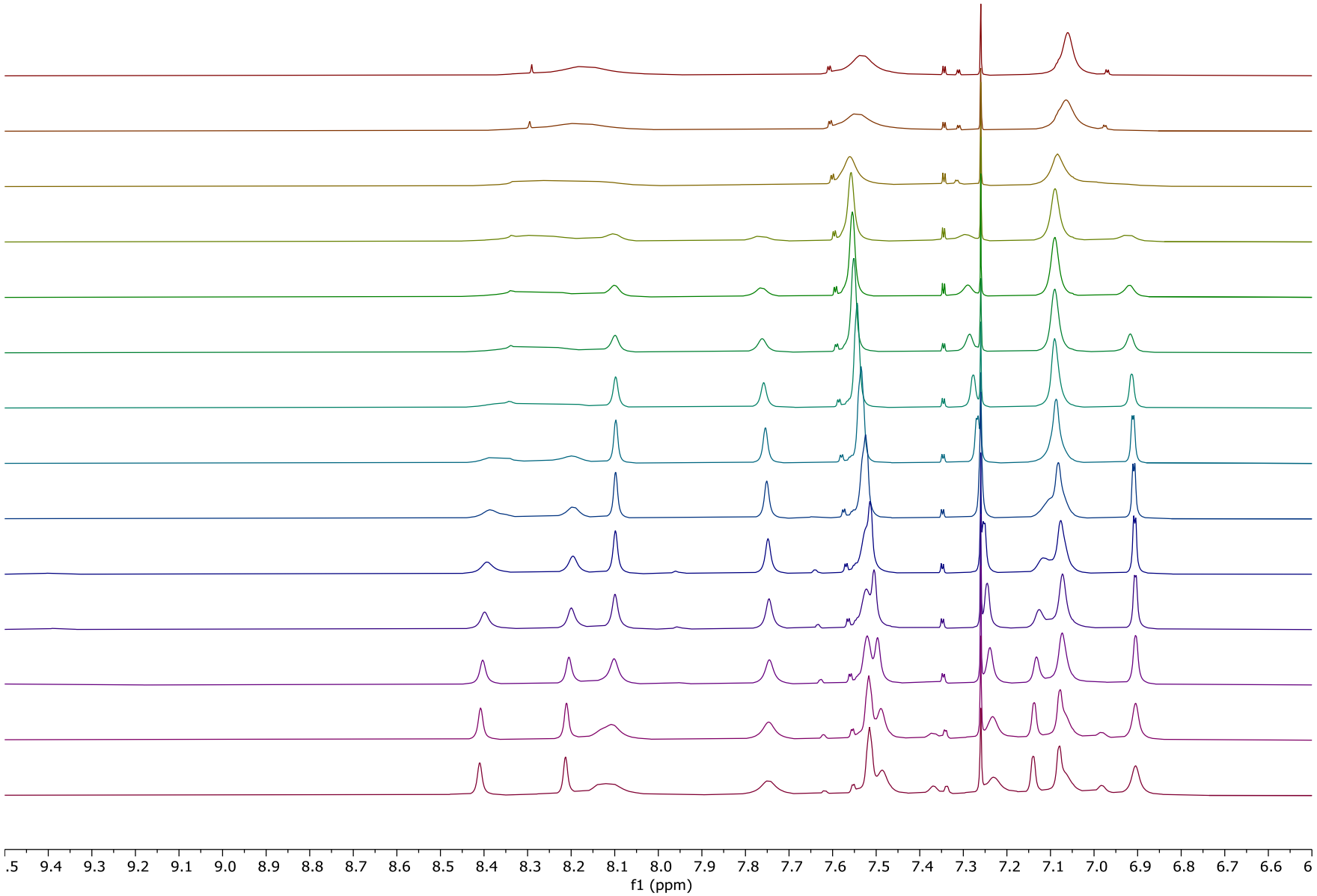

VT NMR spectra (218-328 K) of **10**+**11** from Al(^{t}Bu-salen)Cl and dioxane (6.5-3.0 ppm region)

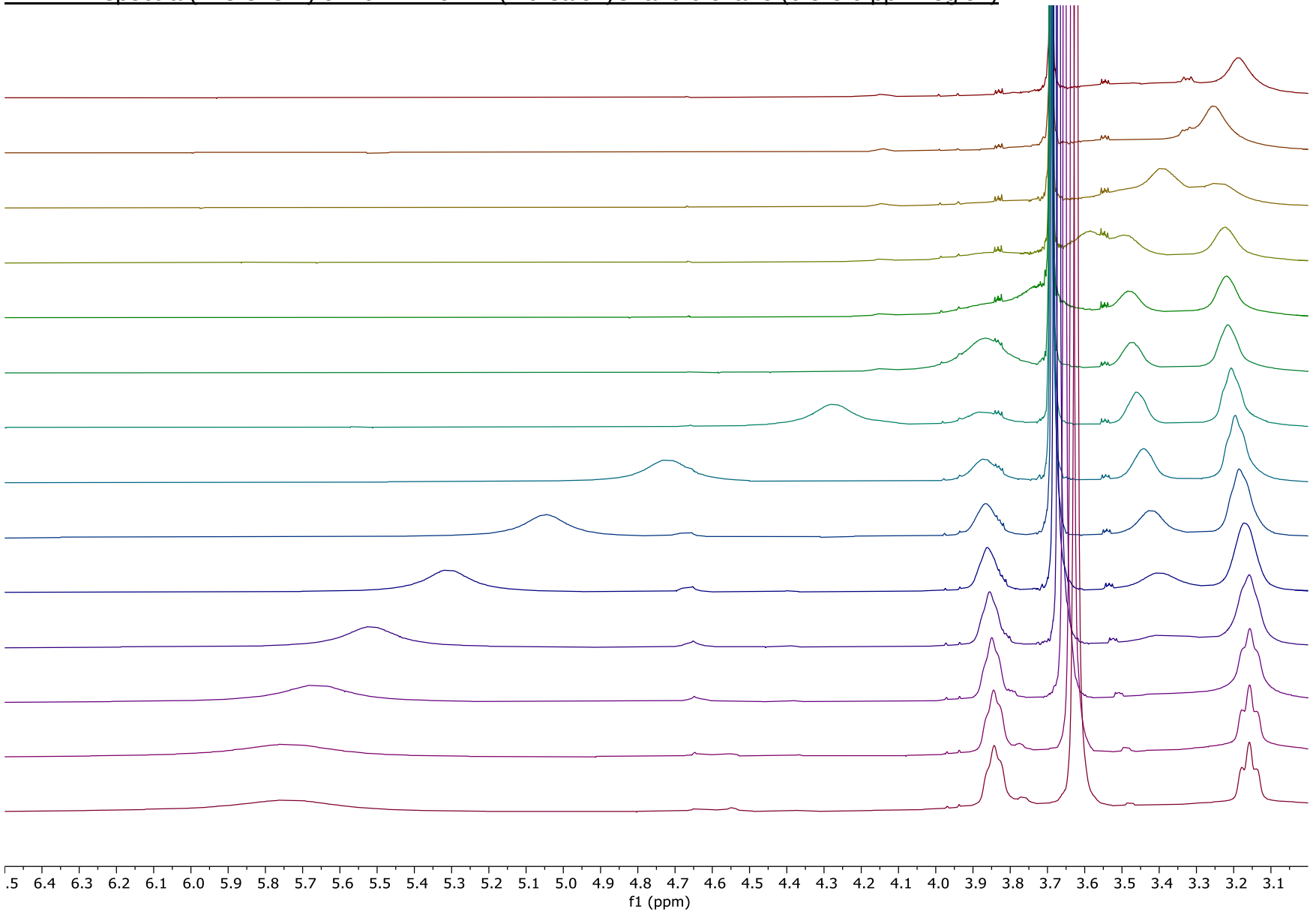

VT NMR spectra (218-328 K) of **10**+**11** from Al(^{t}Bu-salen)Cl and dioxane (3.0-0 ppm region emphasising changes in non-tert-butyl peaks)

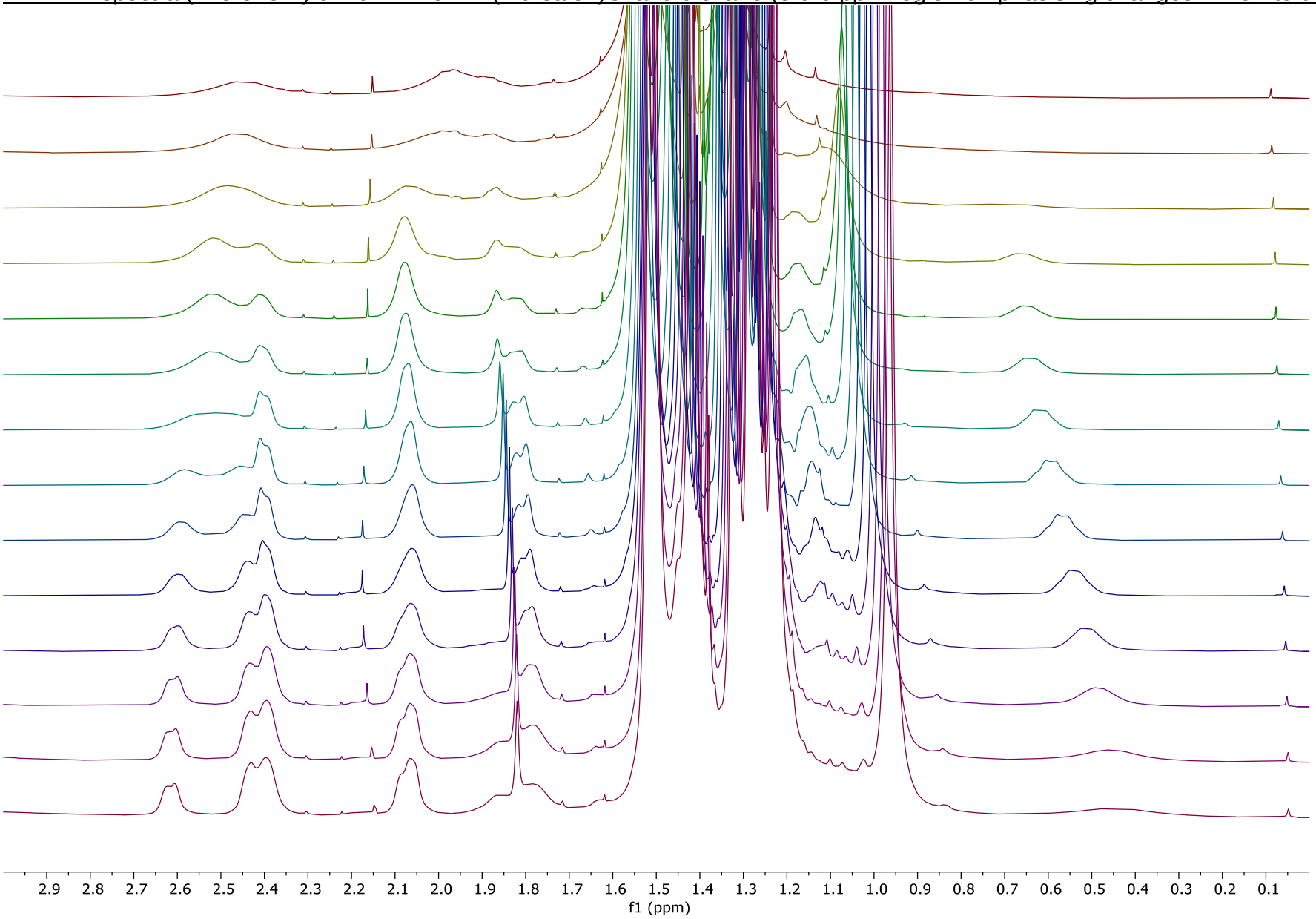

VT NMR spectra (218-328 K) of **10**+**11** from Al(^{t}Bu-salen)Cl and dioxane (3.0-0 ppm region emphasising changes in tert-butyl peaks)

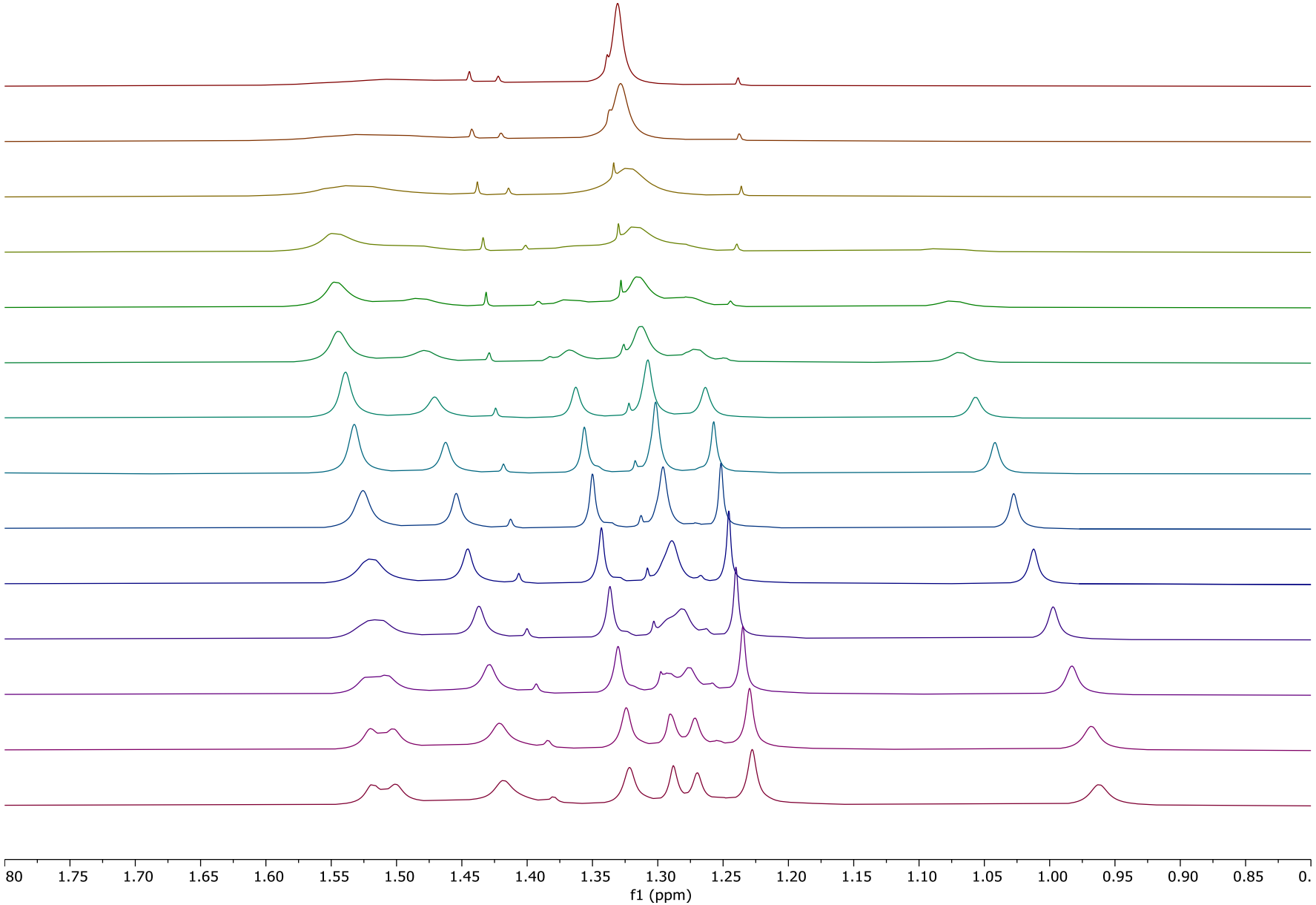

Al(^{t}Bu-salen)Cl ^{1}H NMR spectrum

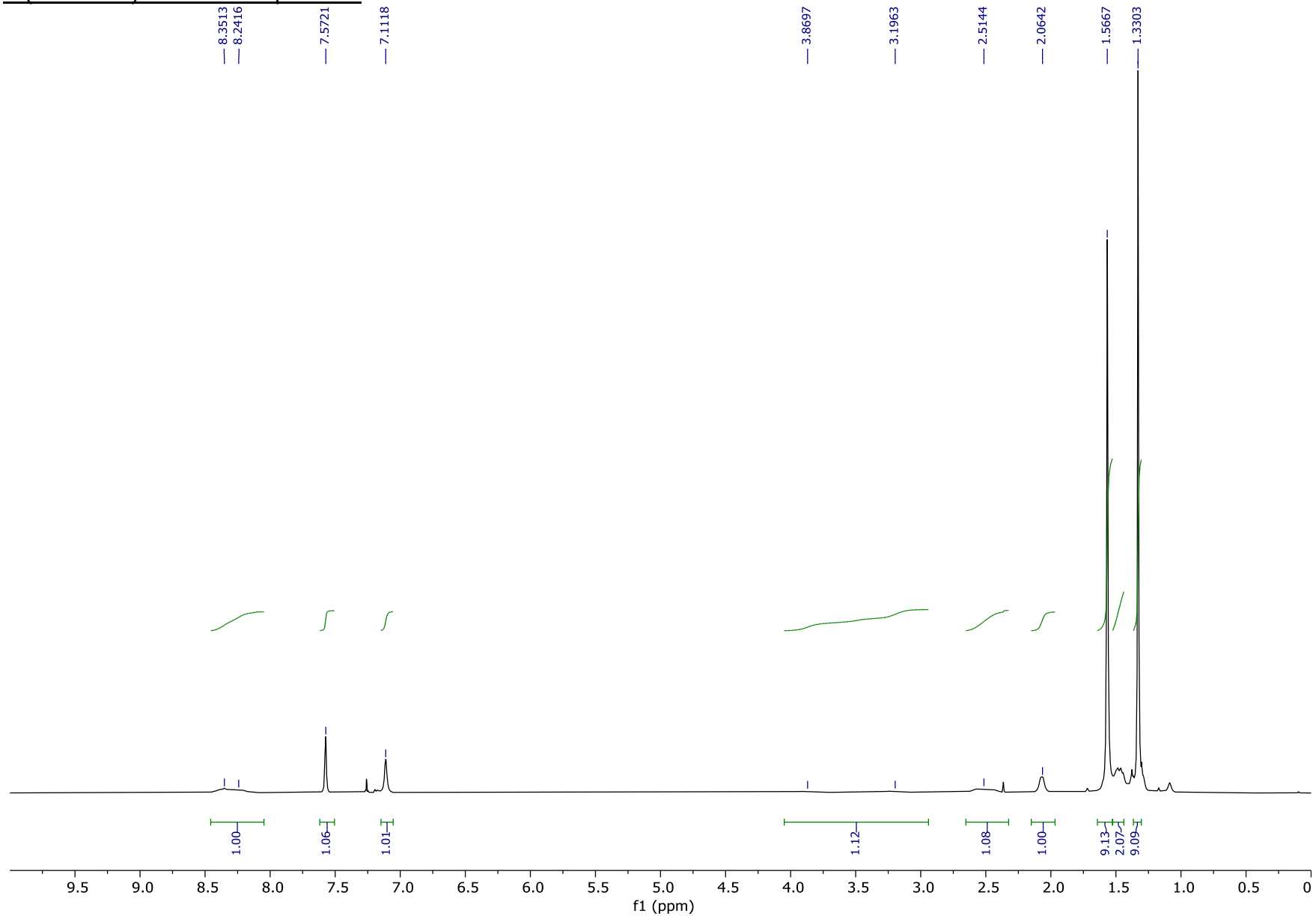

[Al(^{t}Bu-salen)(dioxane)$_2$]$^{+}$Cl^{-} ^{1}H NMR spectrum

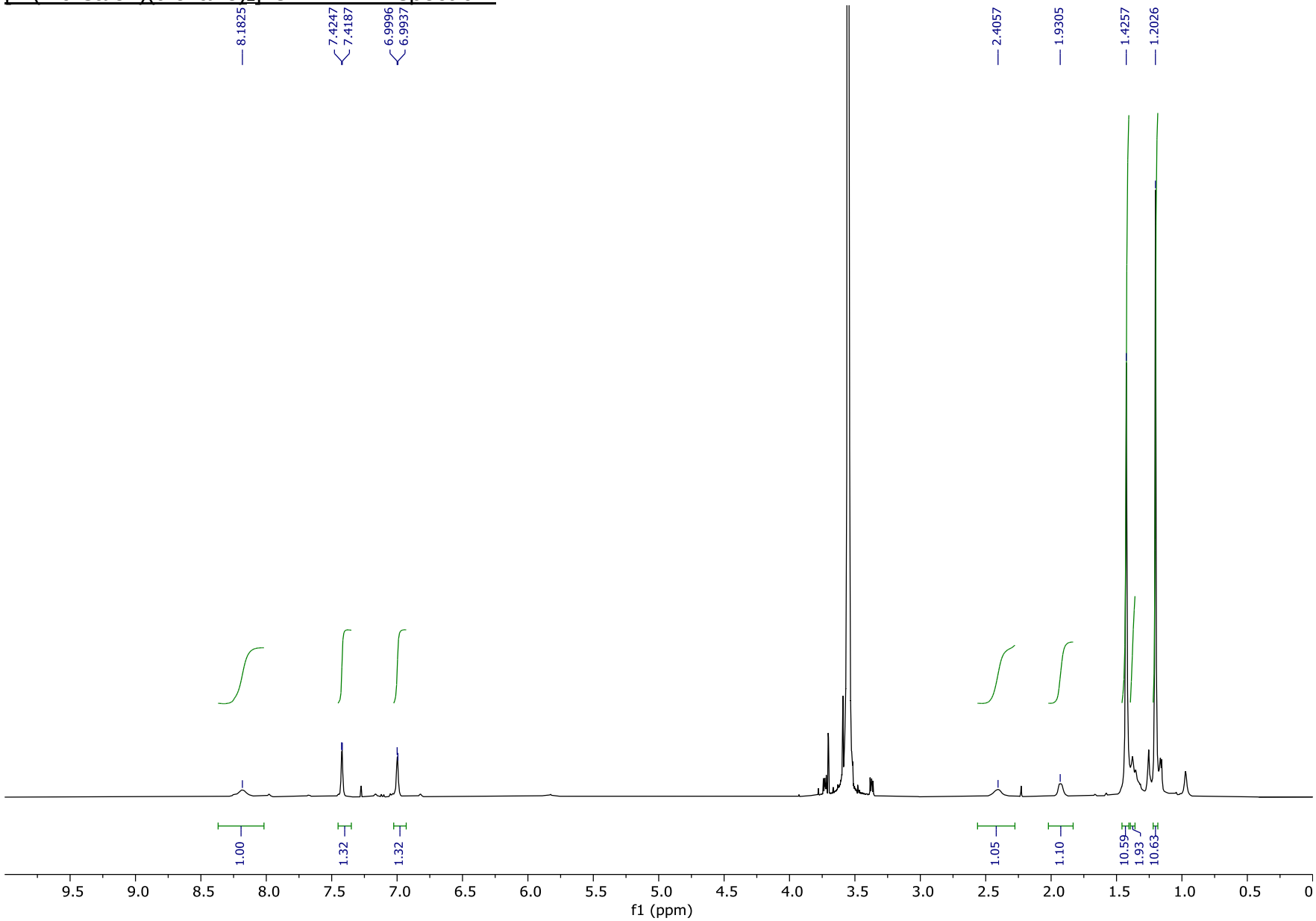

^{1}H NMR spectra of the addition of 1,2-epoxyhexane to complex **1** in $CDCl_3$ (full spectra)

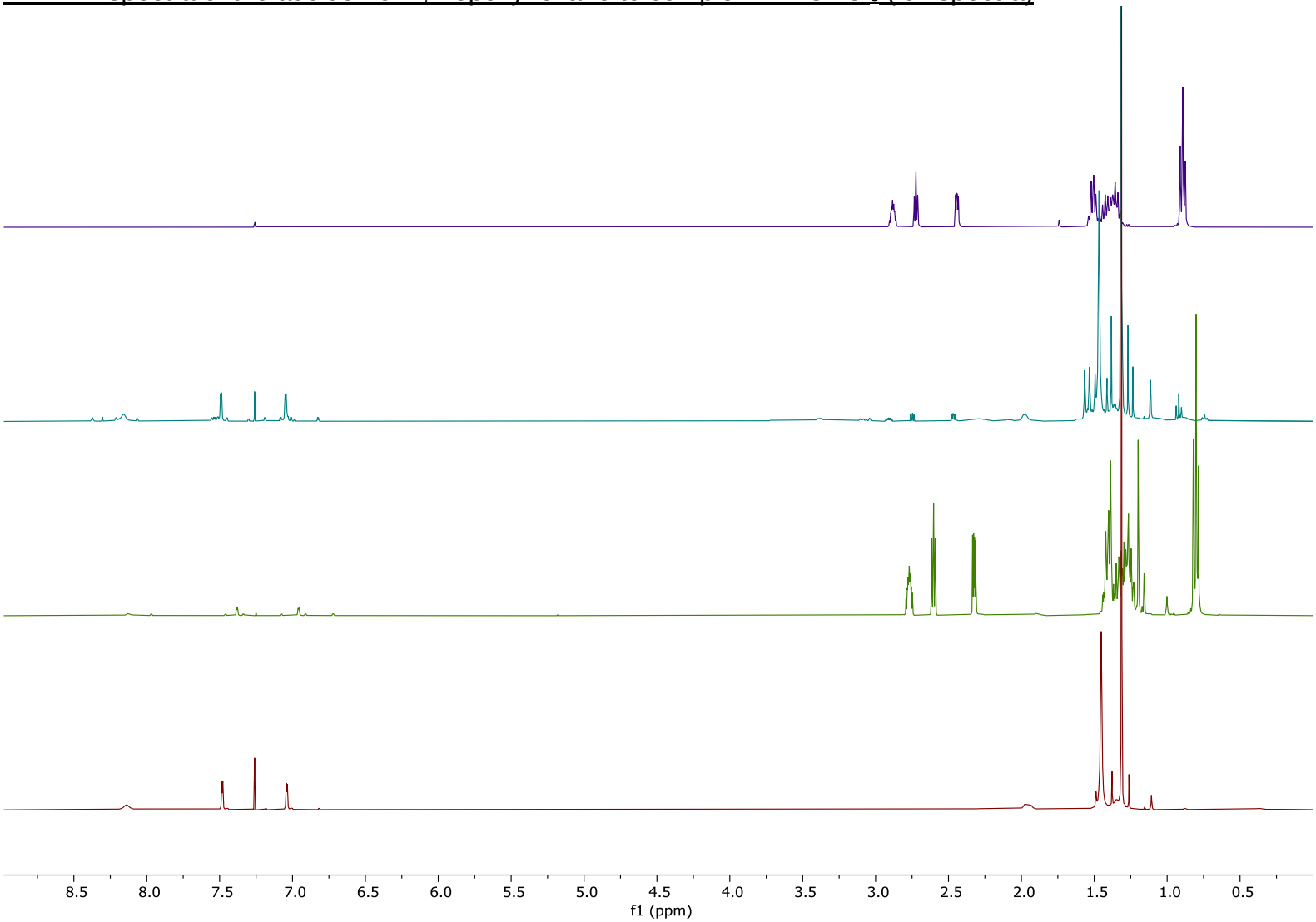

From bottom to top: complex **1**; complex **1** and excess 1,2-epoxyhexane; complex **1** after evaporation of excess 1,2-epoxyhexane; and 1,2-epoxyhexane.

^{1}H NMR spectra of the addition of 1,2-epoxyhexane to complex **1** in $CDCl_3$ (7.7–6.7 ppm)

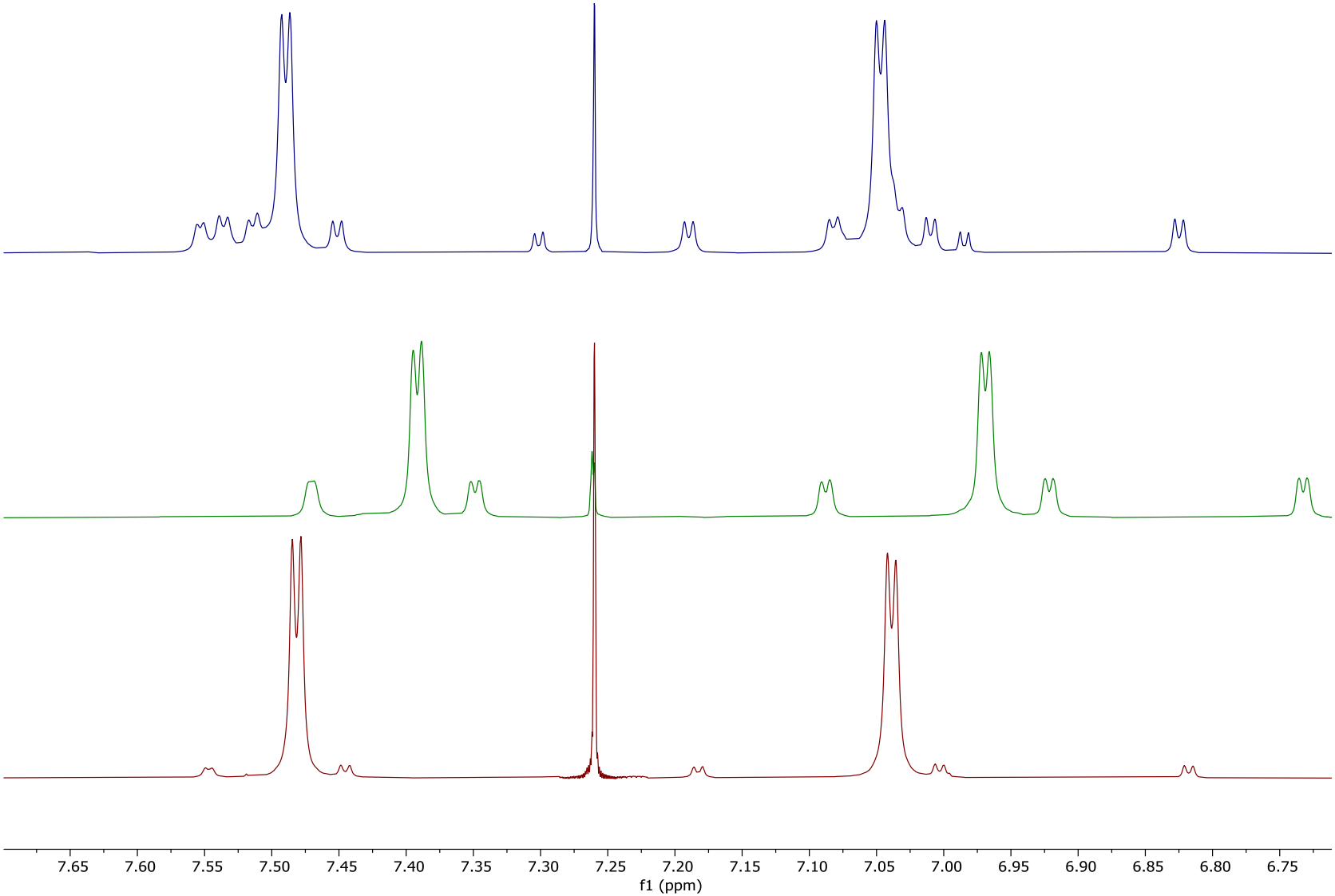

From bottom to top: complex **1**; complex **1** and excess 1,2-epoxyhexane; complex **1** after evaporation of excess 1,2-epoxyhexane.

^{1}H NMR spectra of the addition of 1,2-epoxyhexane to complex **1** in $CDCl_3$ (3.5–2.0 ppm)

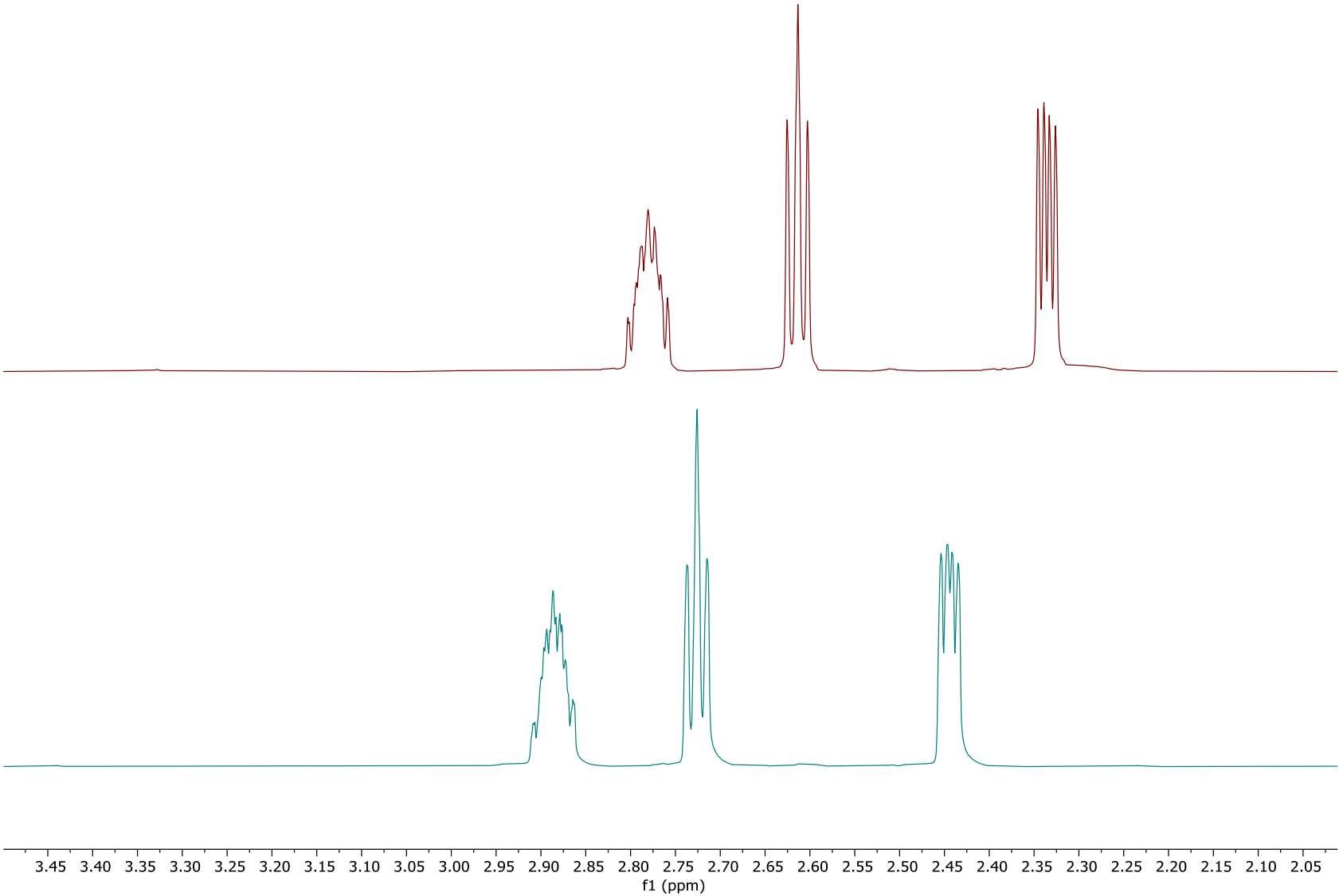

Bottom, 1,2-epoxyhexane; top, complex **1** and excess 1,2-epoxyhexane

^{1}H NMR spectra of the addition of 1,2-epoxyhexane to (^{t}Bu-salen)AlCl in $CDCl_3$ (full spectra)

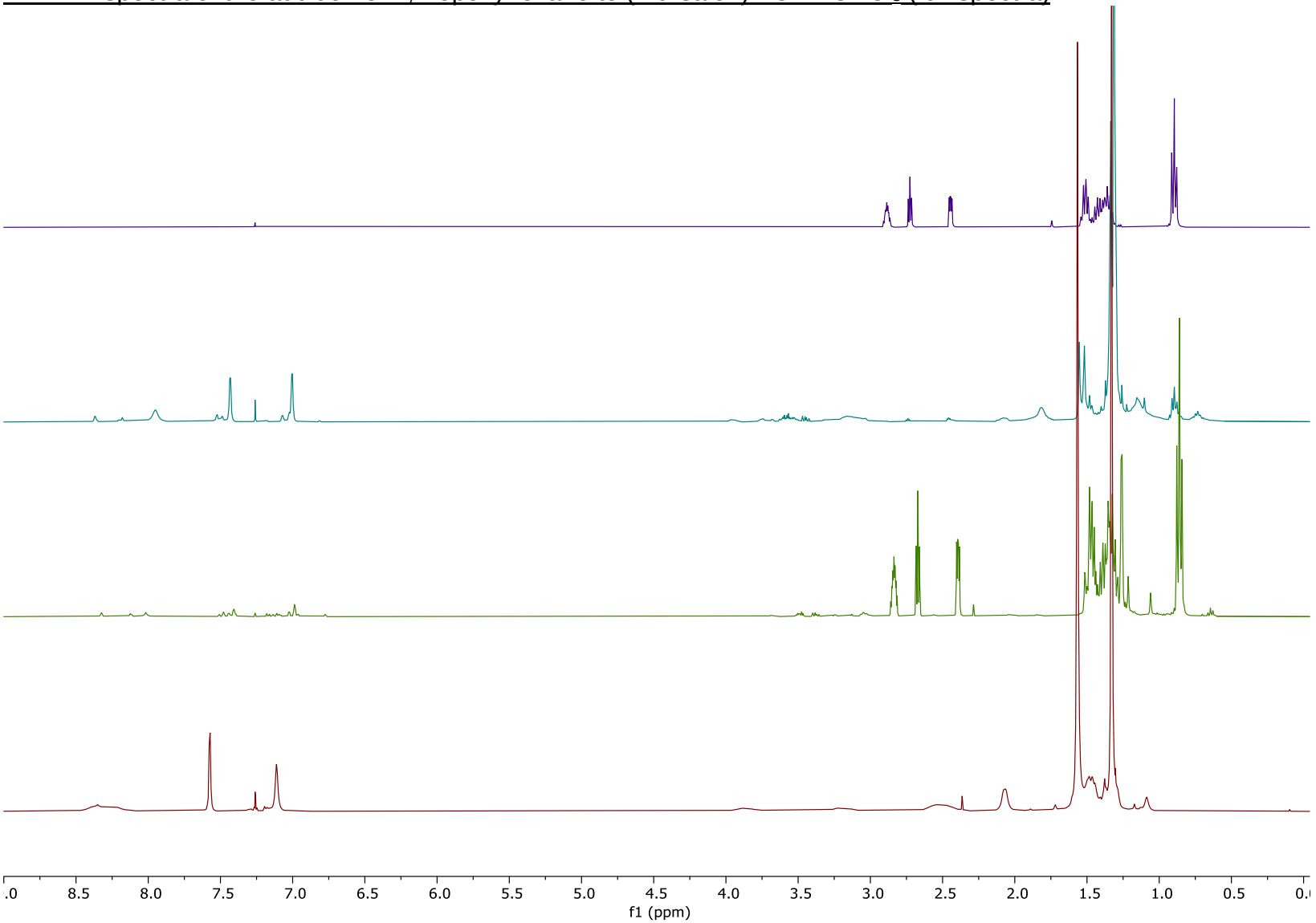

From bottom to top: (^{t}Bu-salen)AlCl; (^{t}Bu-salen)AlCl and excess 1,2-epoxyhexane; (^{t}Bu-salen)AlCl after evaporation of excess 1,2-epoxyhexane; and 1,2-epoxyhexane.

^{1}H NMR spectra of the addition of 1,2-epoxyhexane to (^{t}Bu-salen)AlCl in $CDCl_3$ (9.0–6.5 ppm)

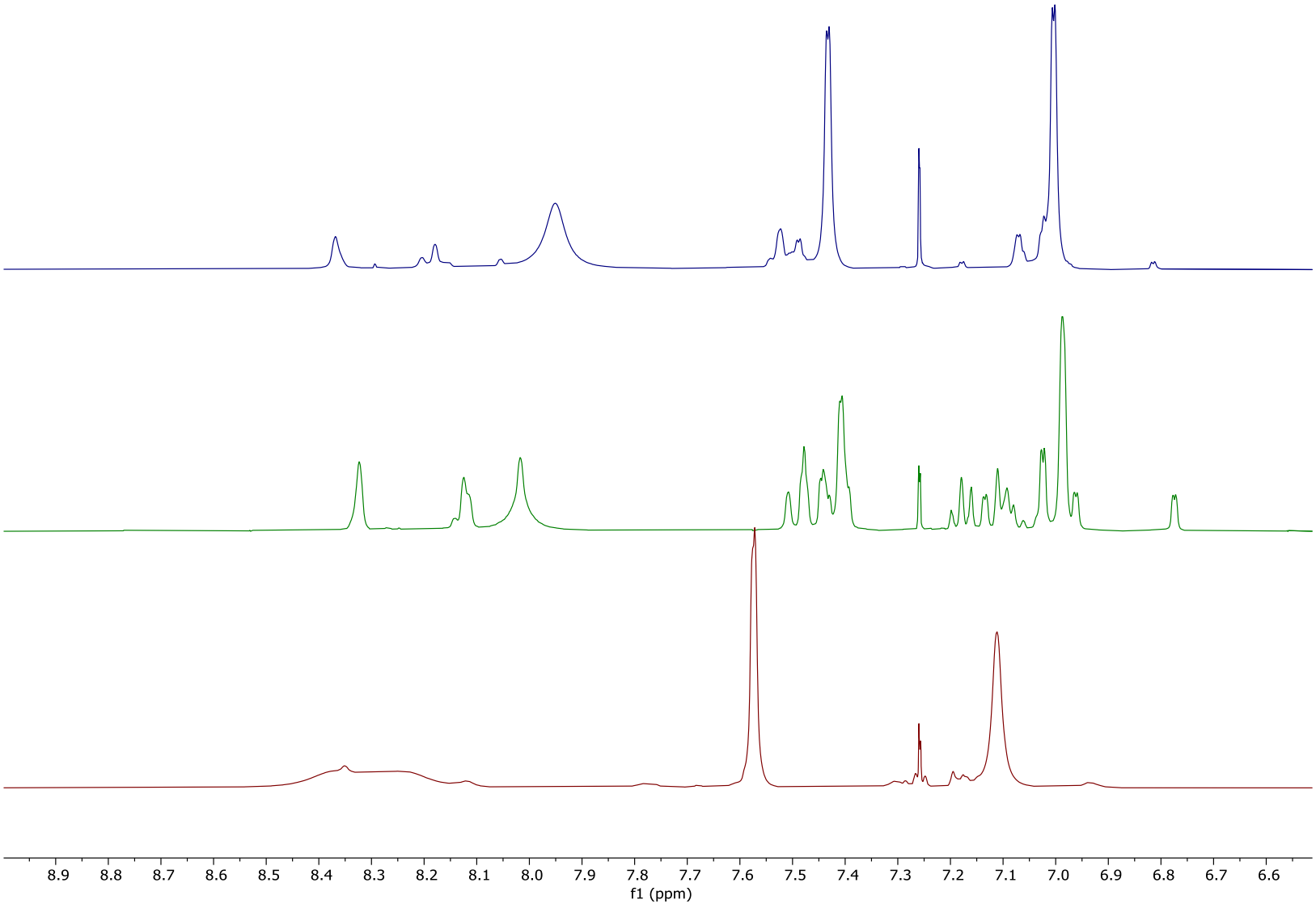

From bottom to top: (^{t}Bu-salen)AlCl; (^{t}Bu-salen)AlCl and excess 1,2-epoxyhexane; (^{t}Bu-salen)AlCl after evaporation of excess 1,2-epoxyhexane.

^{1}H NMR spectra of the addition of 1,2-epoxyhexane to (^{t}Bu-salen)AlCl in $CDCl_3$ (4.5–2.2 ppm)

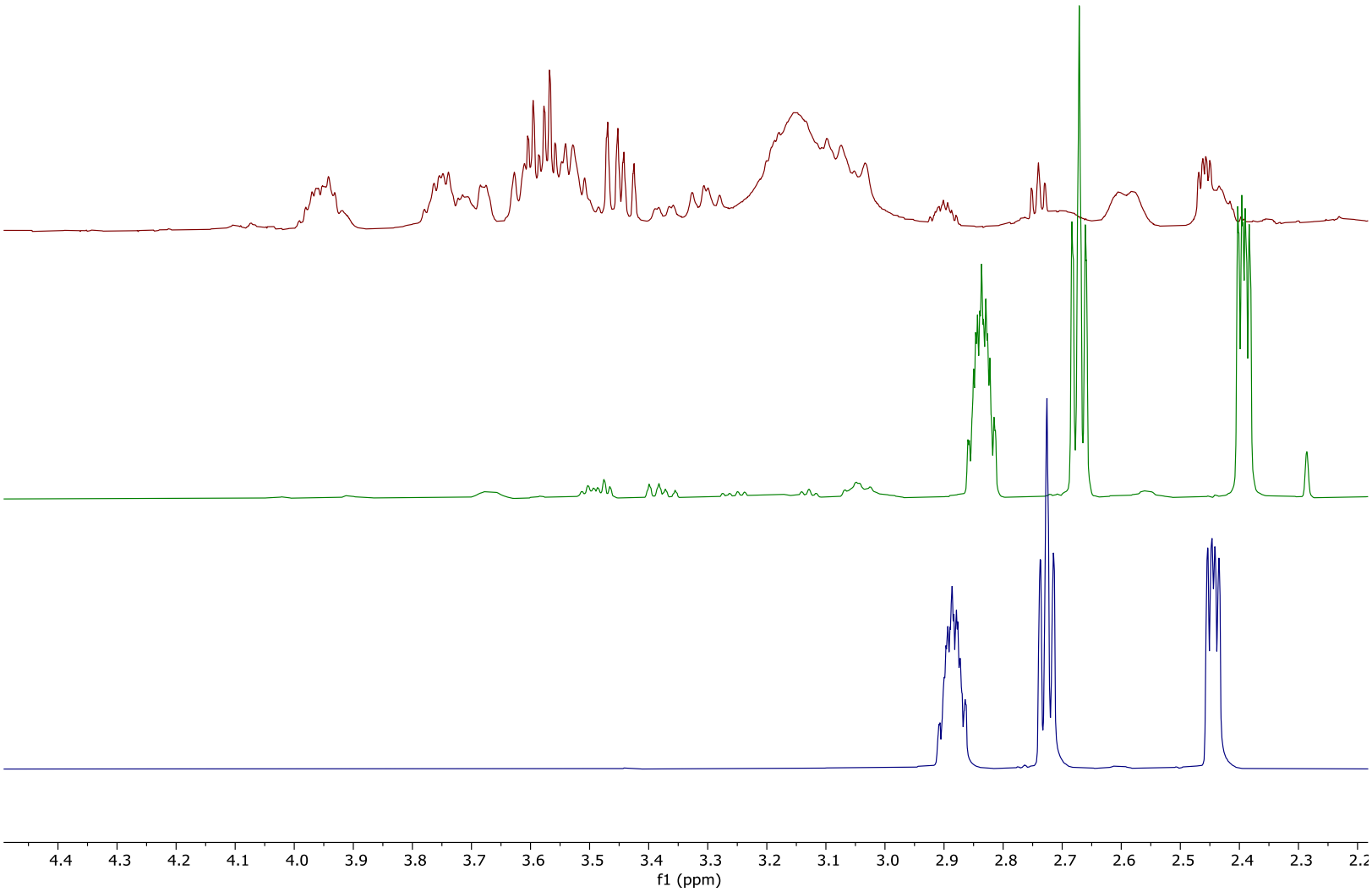

From bottom to top: 1,2-epoxyhexane; (^{t}Bu-salen)AlCl and excess 1,2-epoxyhexane; (^{t}Bu-salen)AlCl after evaporation of excess 1,2-epoxyhexane.

^{1}H NMR spectra of the addition of 1,2-epoxyhexane to complex **1**.TFA in $CDCl_3$ (full spectra)

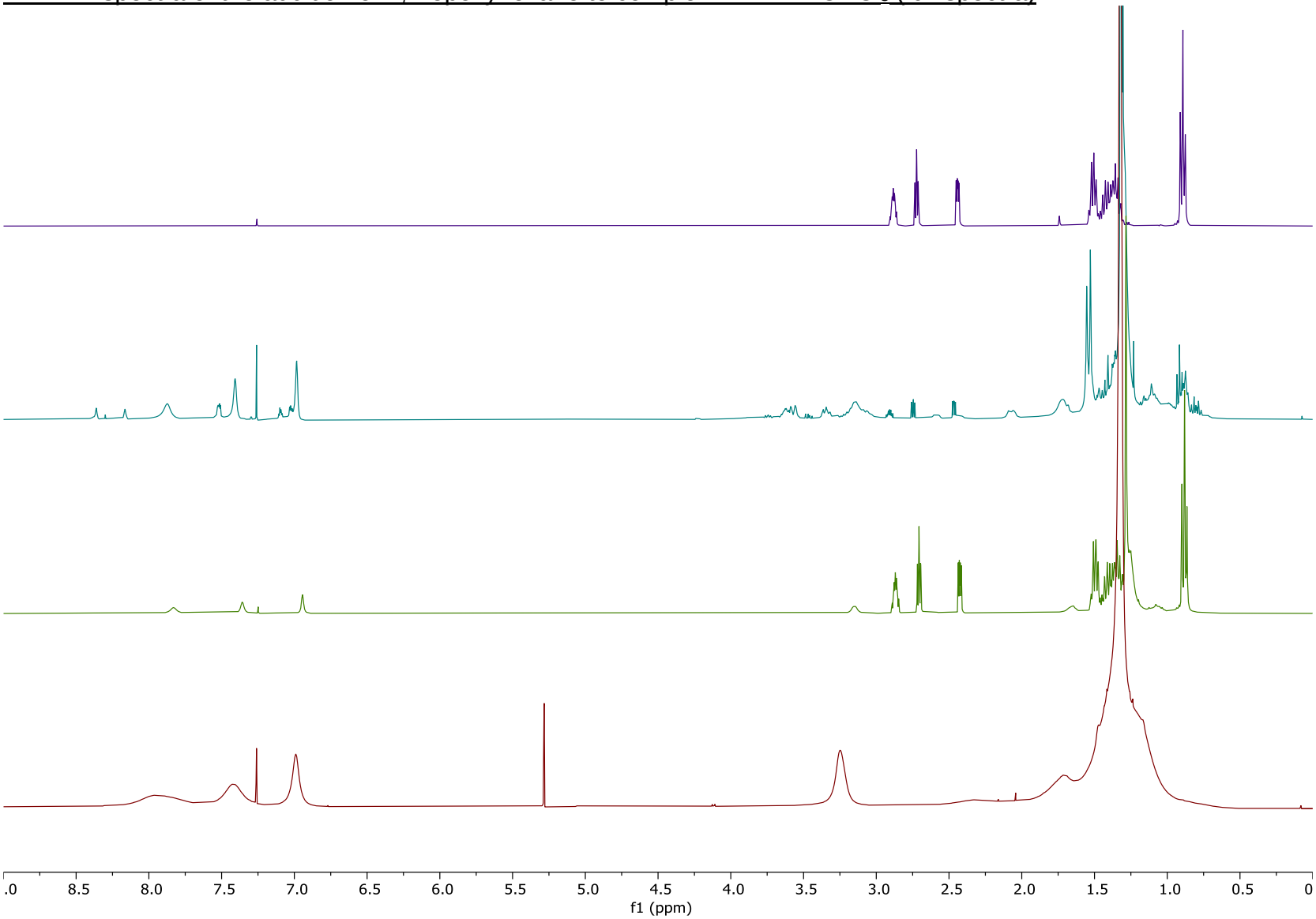

From bottom to top: complex **1.**TFA; complex **1.**TFA and excess 1,2-epoxyhexane; complex **1.**TFA after evaporation of excess 1,2-epoxyhexane; and 1,2-epoxyhexane.

^{1}H NMR spectra of the addition of 1,2-epoxyhexane to complex **1**.TFA in $CDCl_3$ (9.0–6.5 ppm)

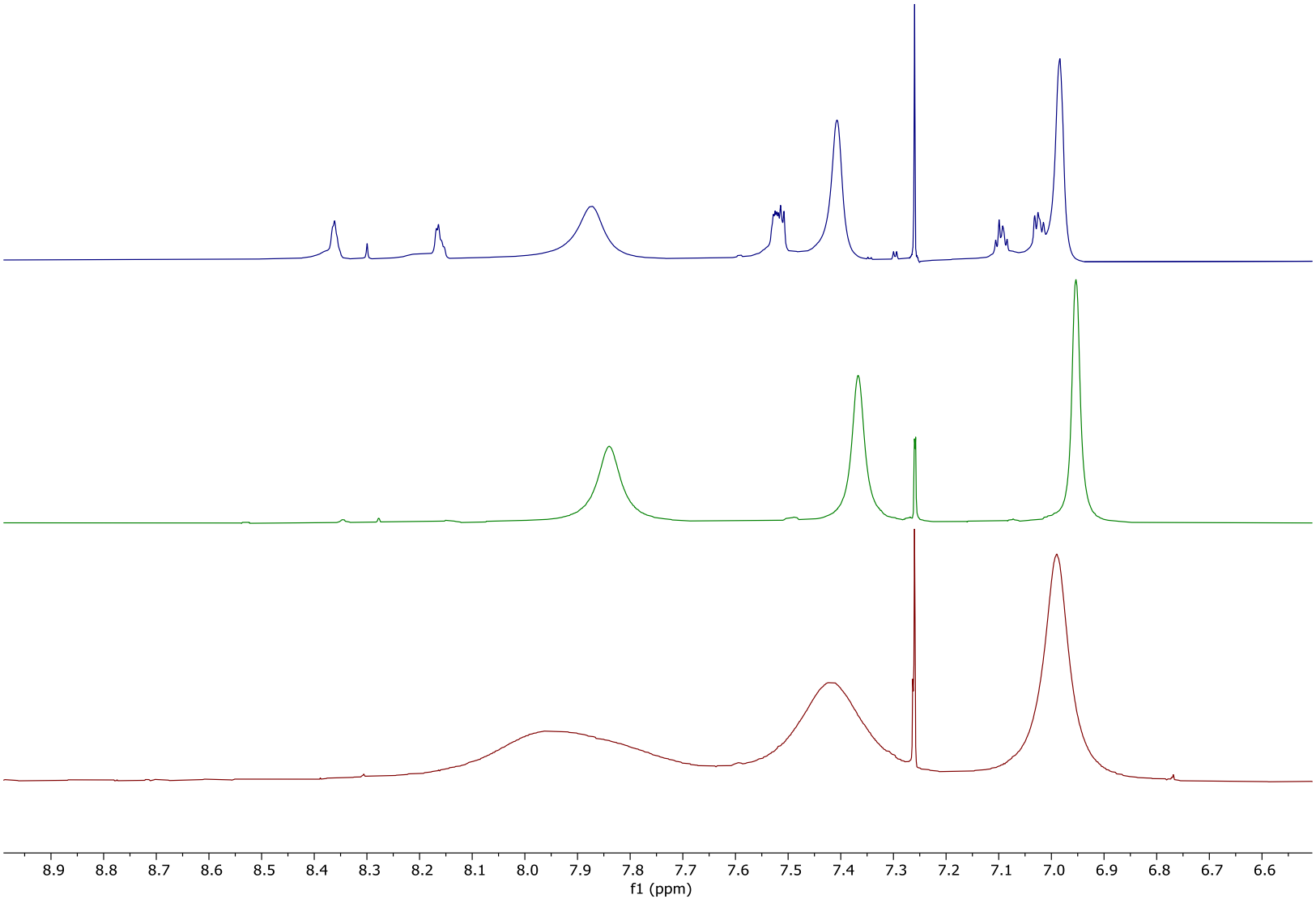

From bottom to top: complex **1.**TFA; complex **1.**TFA and excess 1,2-epoxyhexane; complex **1.**TFA after evaporation of excess 1,2-epoxyhexane.

^{1}H NMR spectra of the addition of 1,2-epoxyhexane to complex **1**.TFA in $CDCl_3$ (4.5–2.2 ppm)

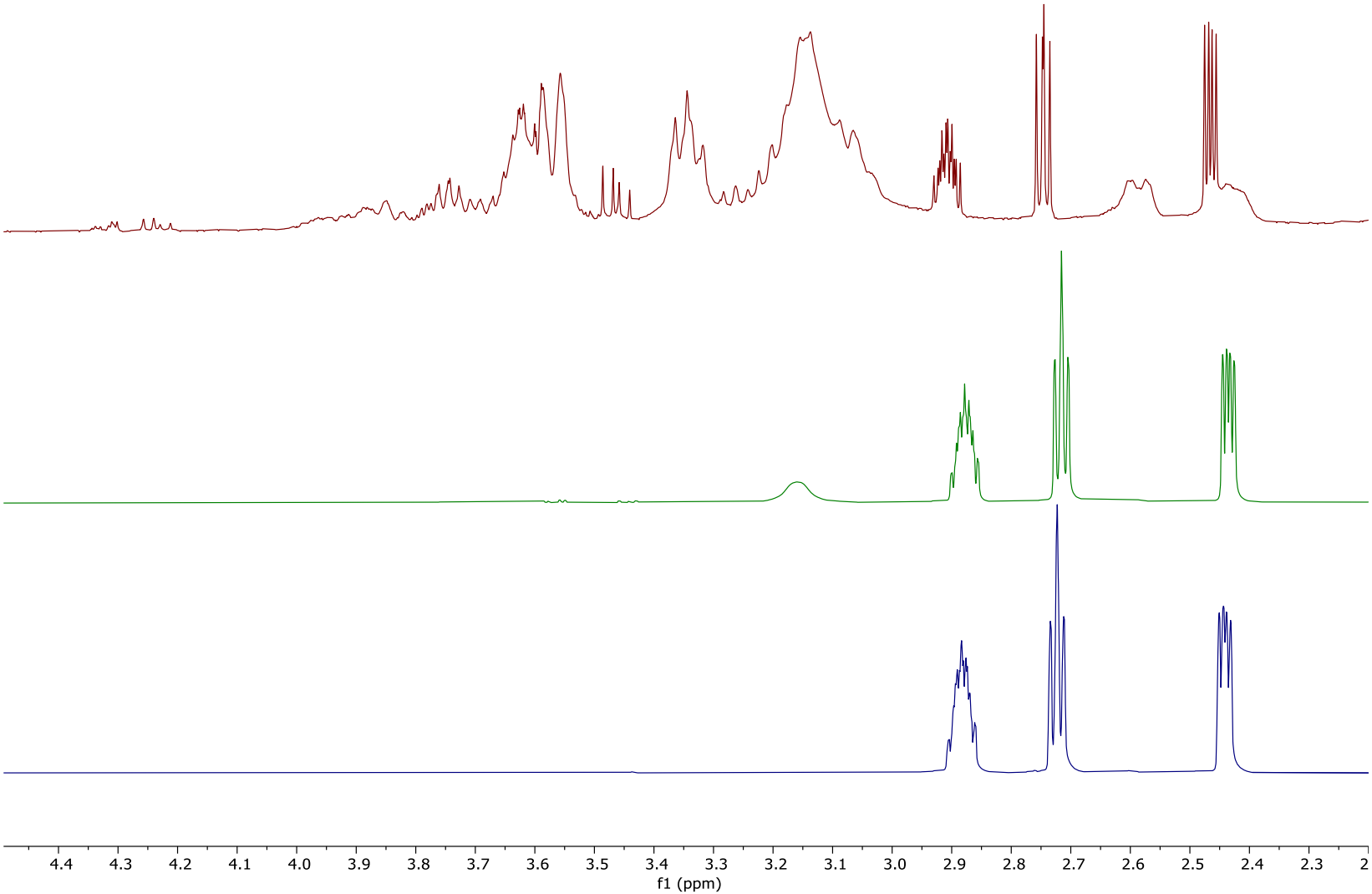

From bottom to top: 1,2-epoxyhexane; complex **1**.TFA and excess 1,2-epoxyhexane; complex **1**.TFA after evaporation of excess 1,2-epoxyhexane.

^{13}C NMR spectrum of the addition of 1,2-epoxyhexane to complex **1**.TFA in $CDCl_3$

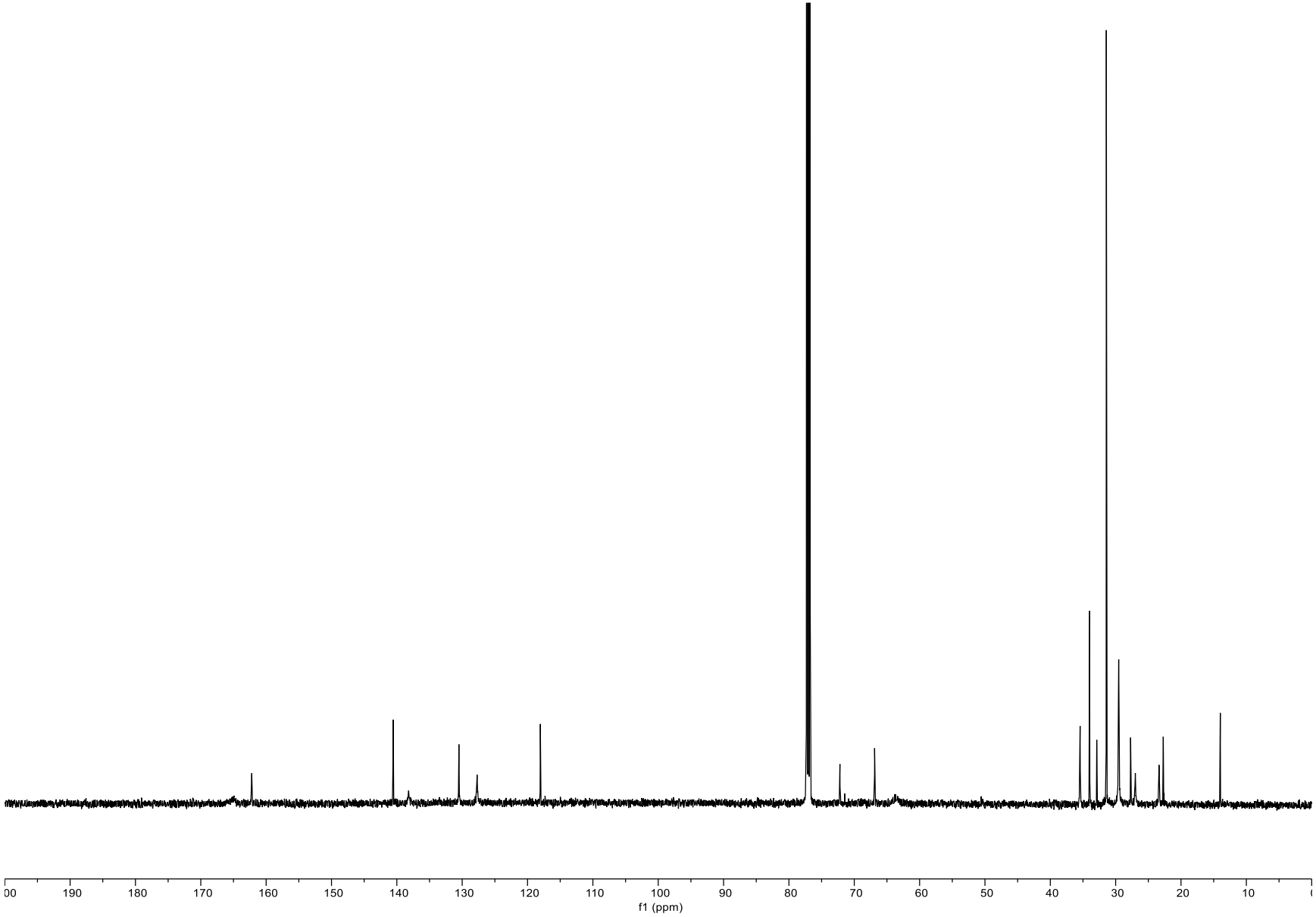

^{1}H NMR spectra of the addition of 1,2-epoxyhexane to complex **9** in $CDCl_3$ (full spectra)

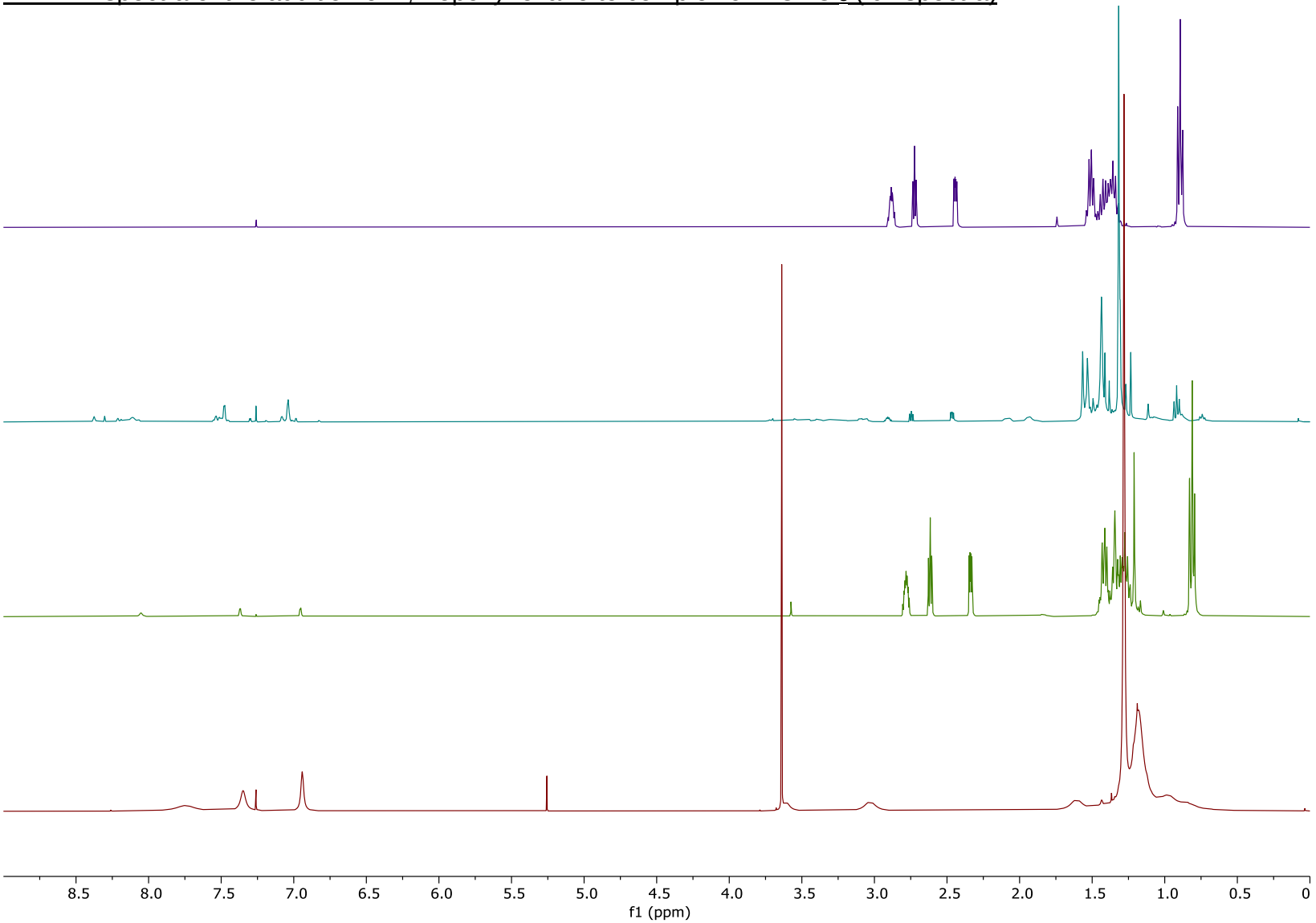

From bottom to top: complex **9**; complex **9** and excess 1,2-epoxyhexane; complex **9** after evaporation of excess 1,2-epoxyhexane; and 1,2-epoxyhexane.

^{1}H NMR spectra of the addition of 1,2-epoxyhexane to complex **9** in $CDCl_3$ (8.5–6.5 ppm)

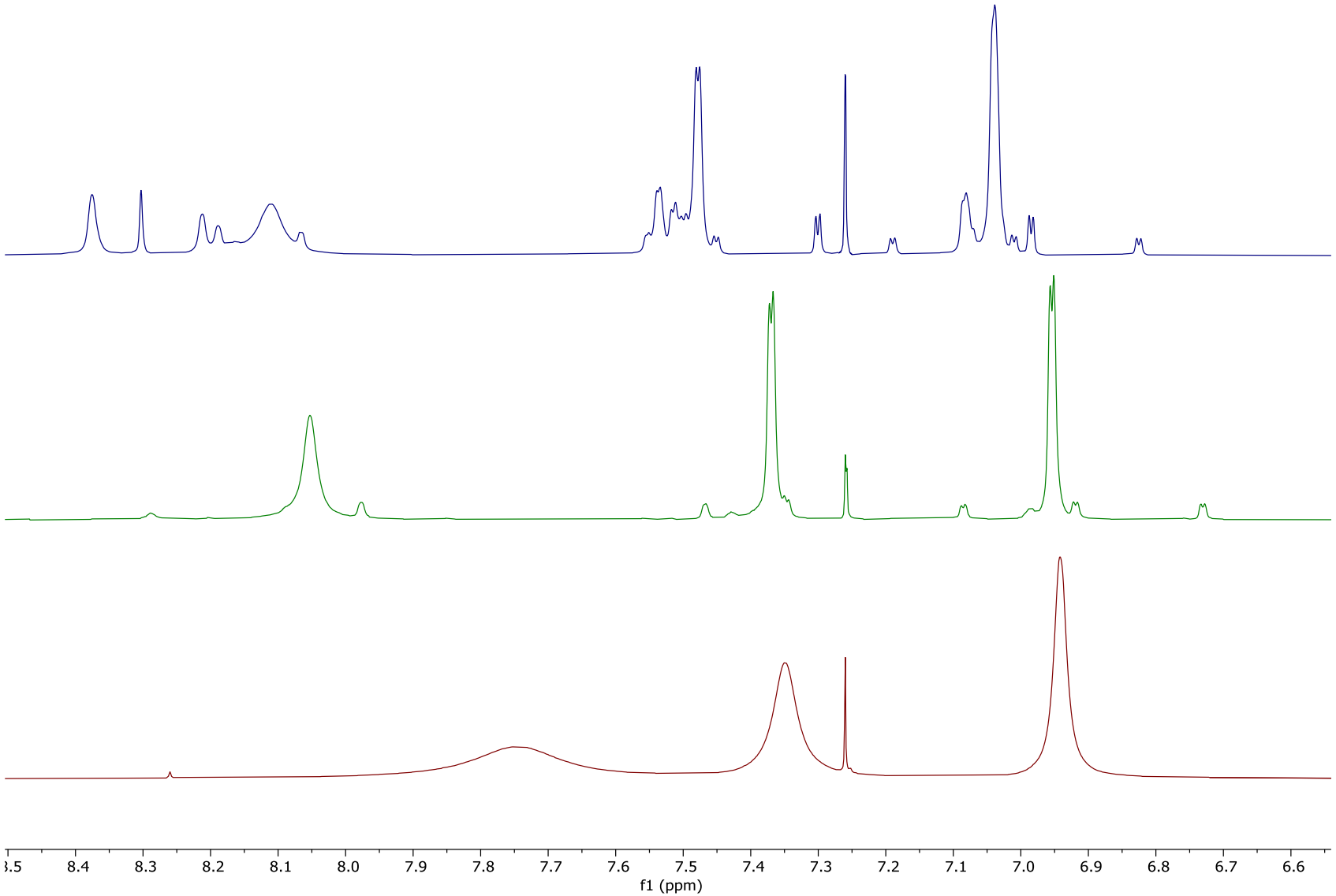

From bottom to top: complex **9**; complex **9** and excess 1,2-epoxyhexane; complex **9** after evaporation of excess 1,2-epoxyhexane.

^{1}H NMR spectra of the addition of 1,2-epoxyhexane to complex **9** in $CDCl_3$ (4.5–2.0 ppm)

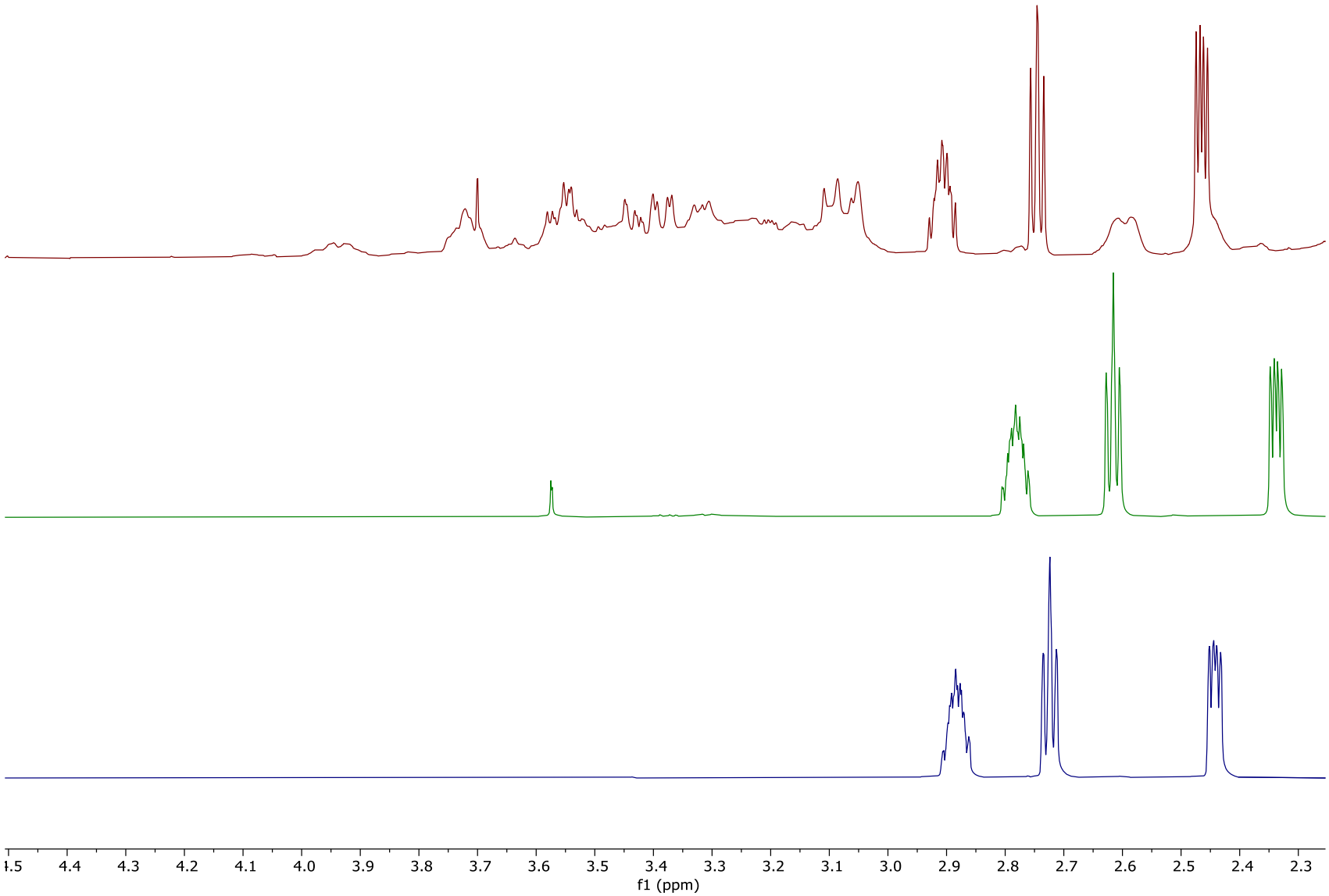

From bottom to top: 1,2-epoxyhexane; complex **9** and excess 1,2-epoxyhexane; complex **9** after evaporation of excess 1,2-epoxyhexane.

Line shape analysis

Methodology

Line shapes were modelled using WinDNMR-Pro.[1] Parameters from the actual spectrum recorded at the lowest temperature were used to establish the model, then the exchange rate constant was varied to give a simulation of the line shape that best matched the actual spectrum recorded at each temperature. Having determined the rate constant at each temperature, $\Delta G^{\ddagger}$ could be calculated at each temperature using equation 1.

1. $\Delta G^{\ddagger} = \frac{RT[\ln(k_B.h^{-1}.T)-\ln(k)]}{1000}$ kJ mol^{-1}

Where R = 8.3144 J mol^{-1} K^{-1}
k_B = 1.38 x 10^{-23} J K^{-1}
h = 6.63 x 10^{-34} J s^{-1}
T = temperature in K
k = the rate constant at temperature T in s^{-1}

$\Delta H^{\ddagger}$ and $\Delta S^{\ddagger}$ could then be obtained graphically using the form of the Eyring equation given in equation 2.

2. $\ln(k.T^{-1}) = \frac{-\Delta H^{\ddagger}}{RT} + \frac{\Delta S^{\ddagger}}{R} + \ln(k_B.h^{-1})$

In a plot of $\ln(k.T^{-1})$ versus T^{-1}, the gradient will be $(-\Delta H^{\ddagger}/R)$ and the intercept will be $[(\Delta S^{\ddagger}/R) + \ln(k_B.h^{-1})]$.

Hence $\Delta H^{\ddagger}$ can be obtained from equation 3.

3. $\Delta H^{\ddagger}$ = -gradient x R

And $\Delta S^{\ddagger}$ can be obtained from equation 4.

4. $\Delta S^{\ddagger}$ = R x [intercept - $\ln(k_B.h^{-1})$] = R x (intercept – 23.76)

1.TFA

The parameters used were:

Peak (as labelled in Figure 8)	Frequency (Hz)	Half width (Hz)	% intensity
a: set 1	770.0	17	16.0
c: set 2	702.0	8	34.6
d: set 2	669.0	7	32.8
b: set 1	567.0	16	16.6

The two sets of *tert*-butyl signals were simulated separately, each as a two spin uncoupled system. The actual peak shapes at each temperature were then best simulated by simulations with the following rate constants for the exchange process and this allowed $\Delta G^{\ddagger}$ at each temperature to be calculated using equation 1. The average value of these 24 calculations of $\Delta G^{\ddagger}$ is 56.9 kJ mol^{-1} and all the values are within +/- 1.3 kJ mol^{-1} of this average.

	set 1		set 2	
Temperature (K)	k (s^{-1})	$\Delta G^{\ddagger}$ (kJ mol^{-1})	k (s^{-1})	$\Delta G^{\ddagger}$ (kJ mol^{-1})
233	1.5	55.8	0.5	57.93
243	5	55.9	2	57.70
253	15	55.9	6	57.85
263	45	55.8	17	57.94
273	120	55.8	49	57.83
283	280	55.9	129	57.76
293	757	55.6	300	57.82
298	1000	55.9	450	57.85
303	1500	55.8	650	57.93
313	3000	56.0	1400	57.93
323	6000	56.0	3000	57.82
328	9000	55.8	4300	57.78

The simulated spectra (all with the same vertical and horizontal scales) are given below:

<u>k = 1.5 s^{-1} (simulating the set 1 spectrum recorded at 233 K)</u>

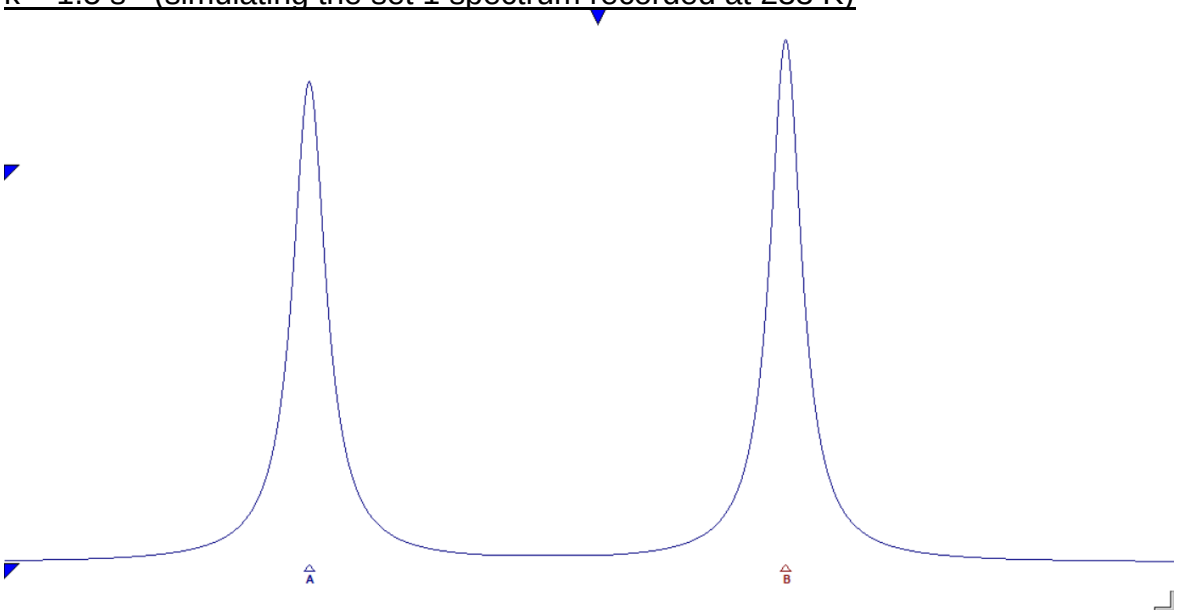

k = 0.5 s^{-1} (simulating the set 2 spectrum recorded at 233 K)

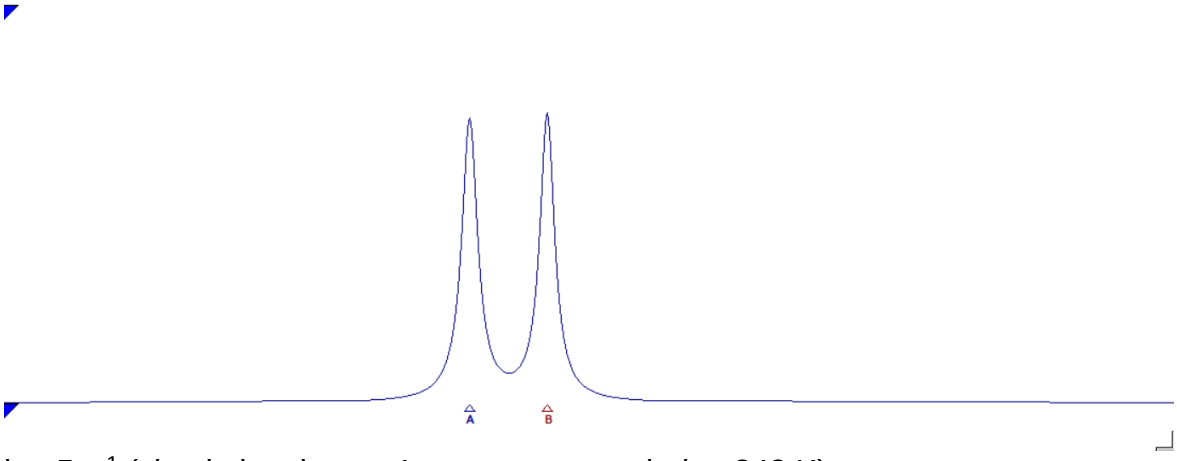

k = 5 s^{-1} (simulating the set 1 spectrum recorded at 243 K)

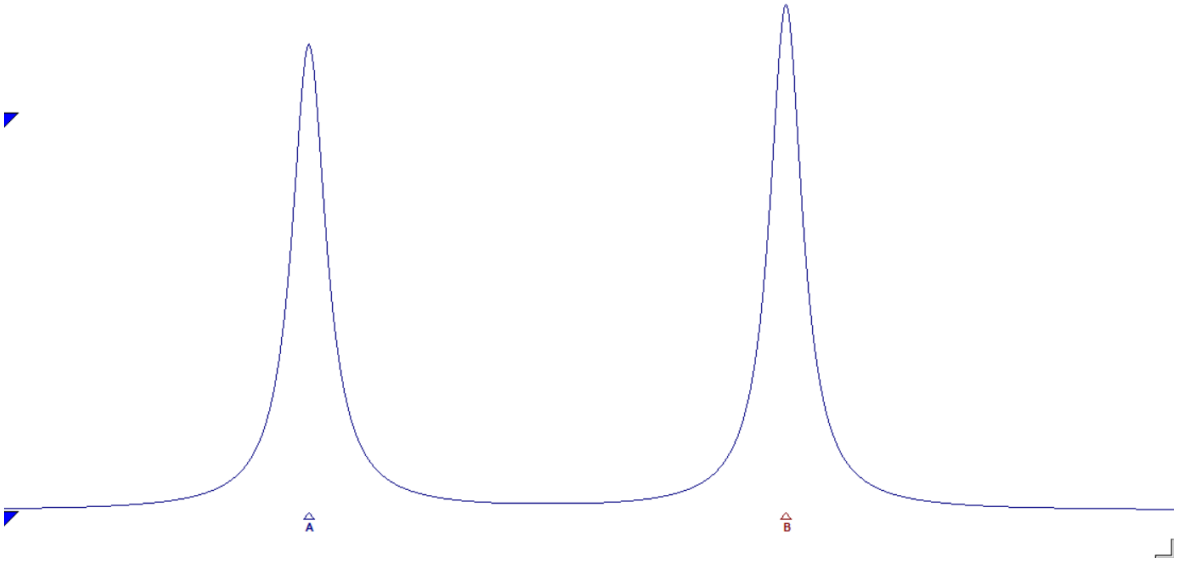

k = 2 s^{-1} (simulating the set 2 spectrum recorded at 243 K)

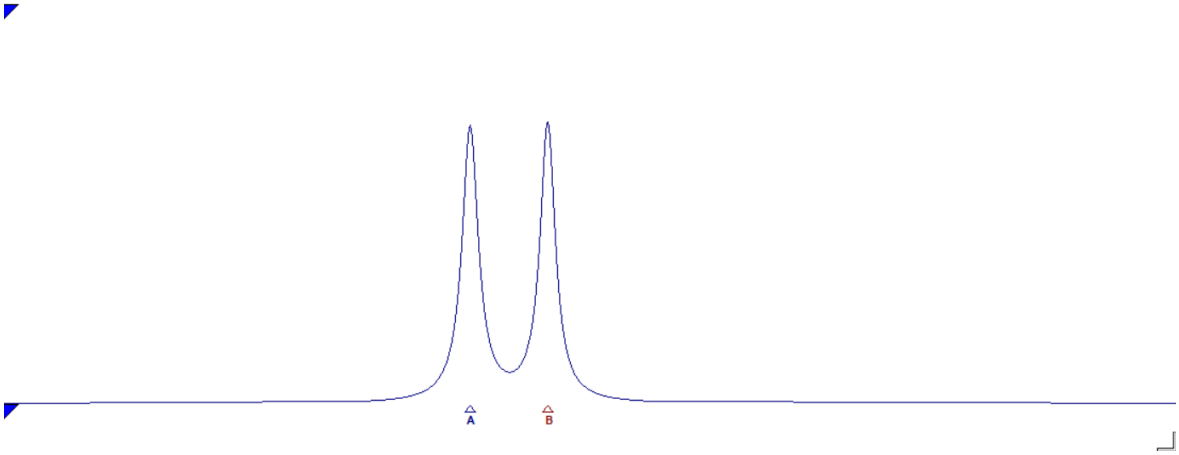

k = 15 s^{-1} (simulating the set 1 spectrum recorded at 253 K)

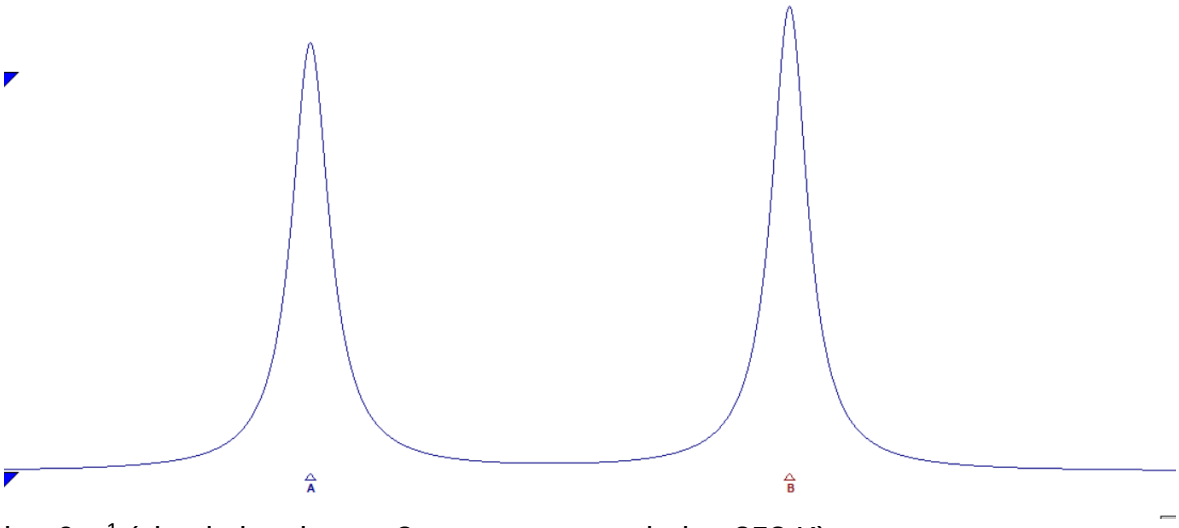

k = 6 s^{-1} (simulating the set 2 spectrum recorded at 253 K)

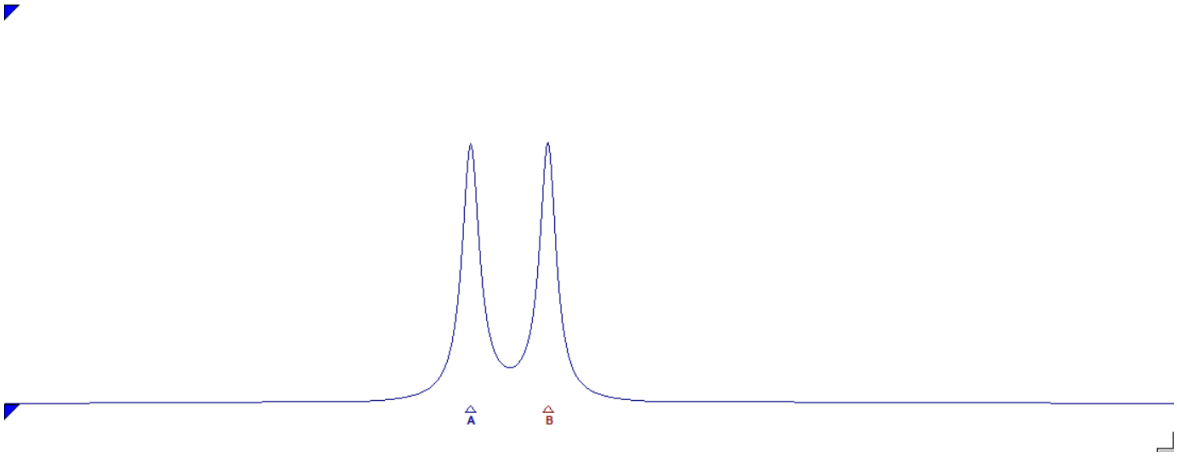

k = 45 s^{-1} (simulating the set 1 spectrum recorded at 263 K)

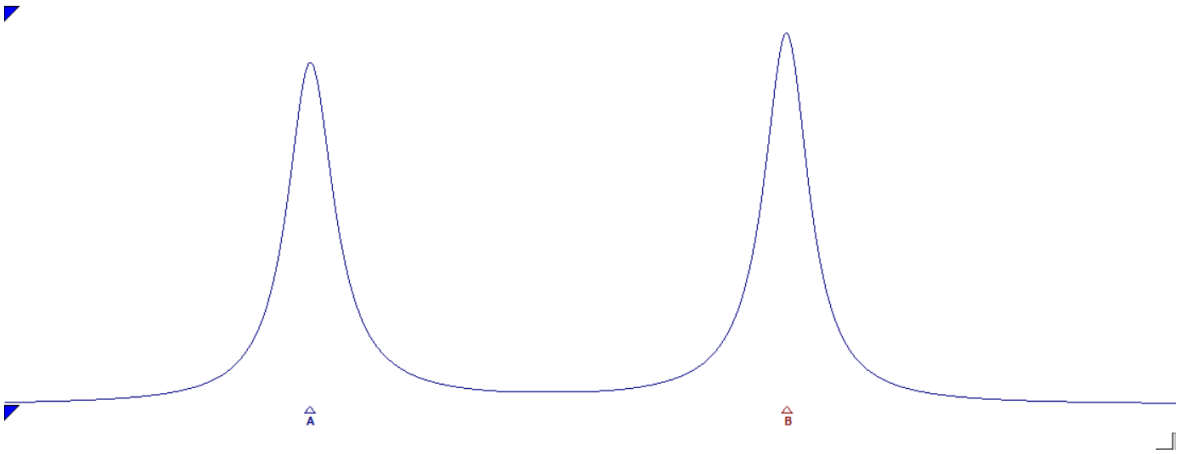

k = 17 s^{-1} (simulating the set 2 spectrum recorded at 263 K)

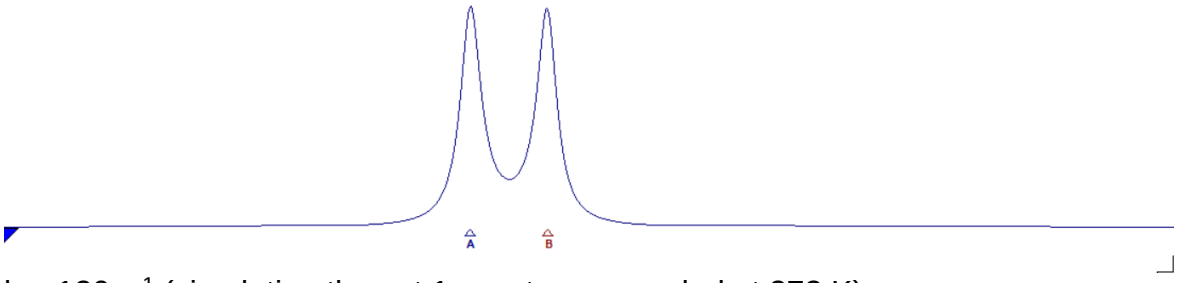

k = 120 s^{-1} (simulating the set 1 spectrum recorded at 273 K)

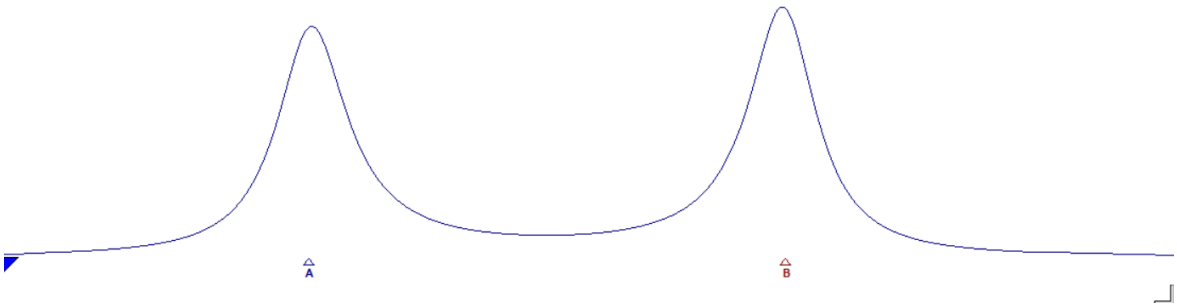

k = 49 s^{-1} (simulating the set 2 spectrum recorded at 273 K)

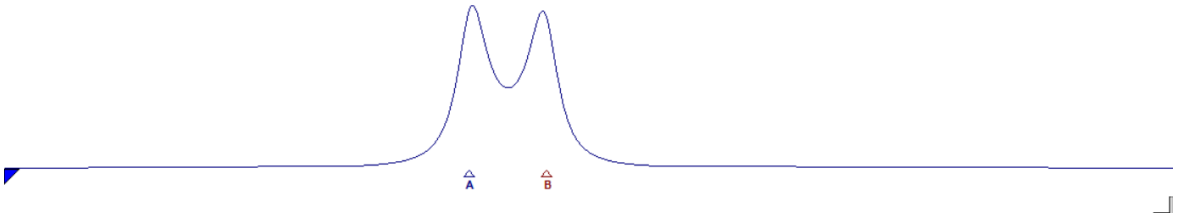

k = 280 s^{-1} (simulating the set 1 spectrum recorded at 283 K)

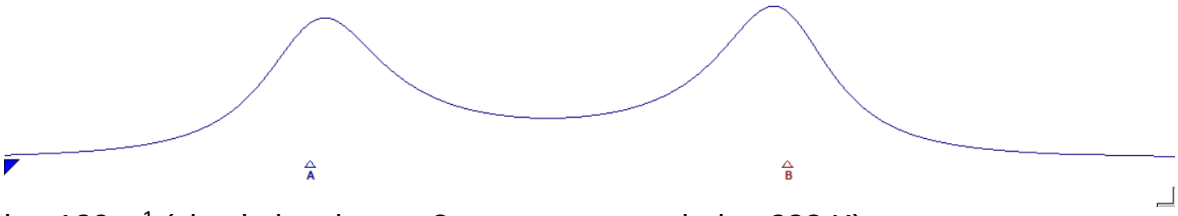

k = 129 s^{-1} (simulating the set 2 spectrum recorded at 283 K)

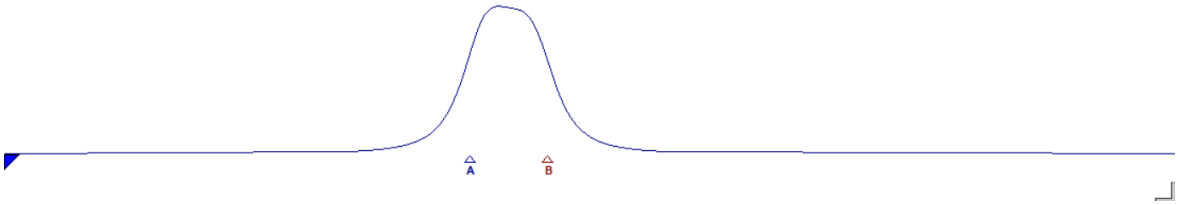

k = 757 s^{-1} (simulating the set 1 spectrum recorded at 293 K)

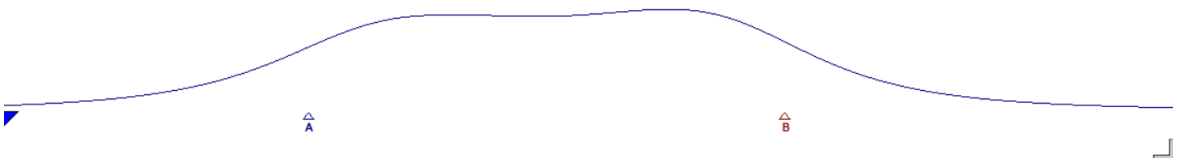

k = 300 s^{-1} (simulating the set 2 spectrum recorded at 293 K)

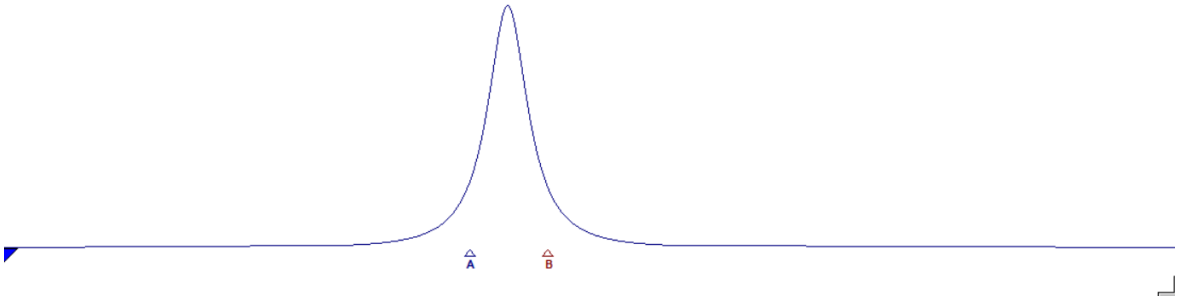

k = 1000 s^{-1} (simulating the set 1 spectrum recorded at 298 K)

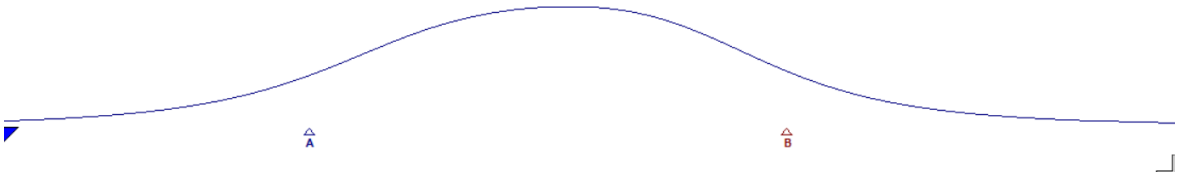

k = 450 s^{-1} (simulating the set 2 spectrum recorded at 298 K)

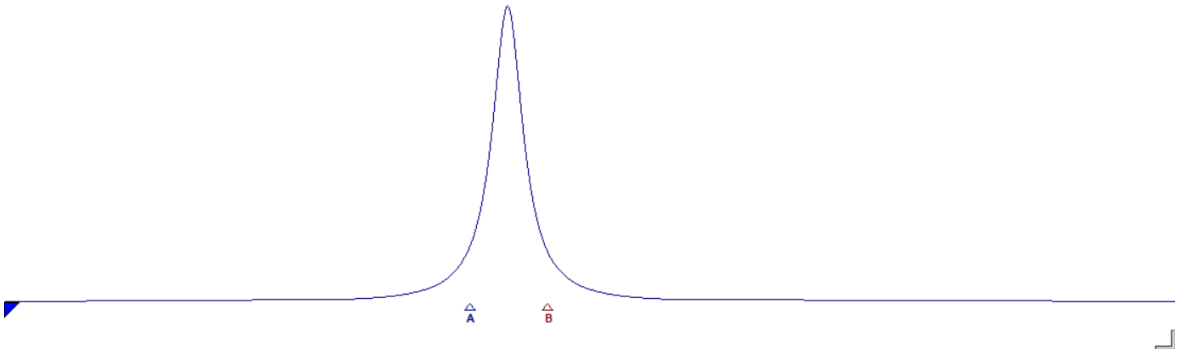

k = 1500 s^{-1} (simulating the set 1 spectrum recorded at 303 K)

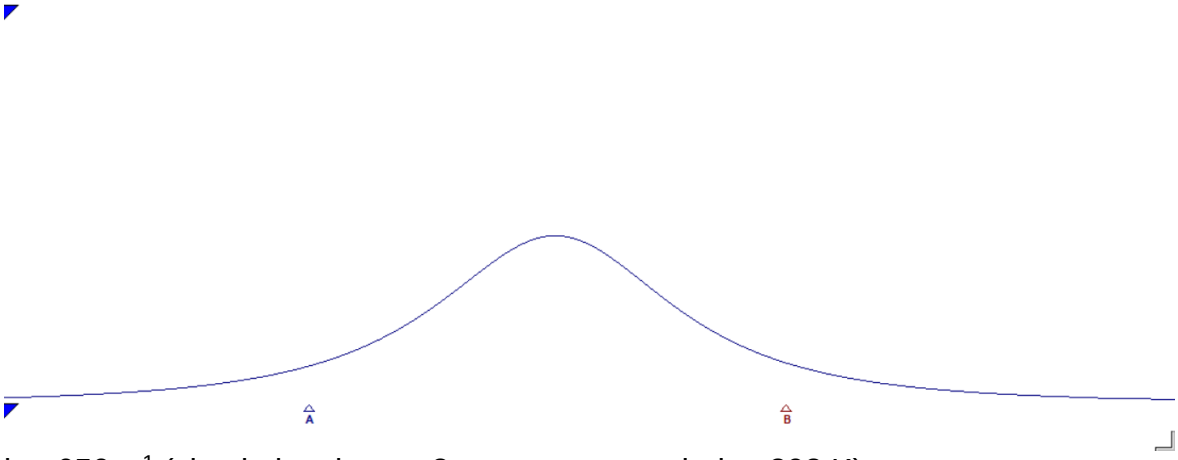

k = 650 s^{-1} (simulating the set 2 spectrum recorded at 303 K)

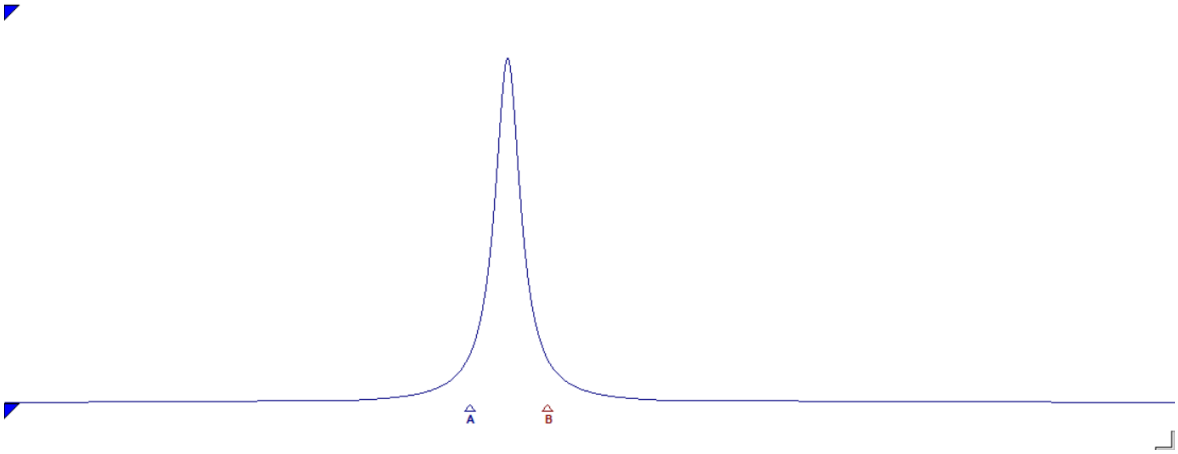

k = 3000 s^{-1} (simulating the set 1 spectrum recorded at 313 K)

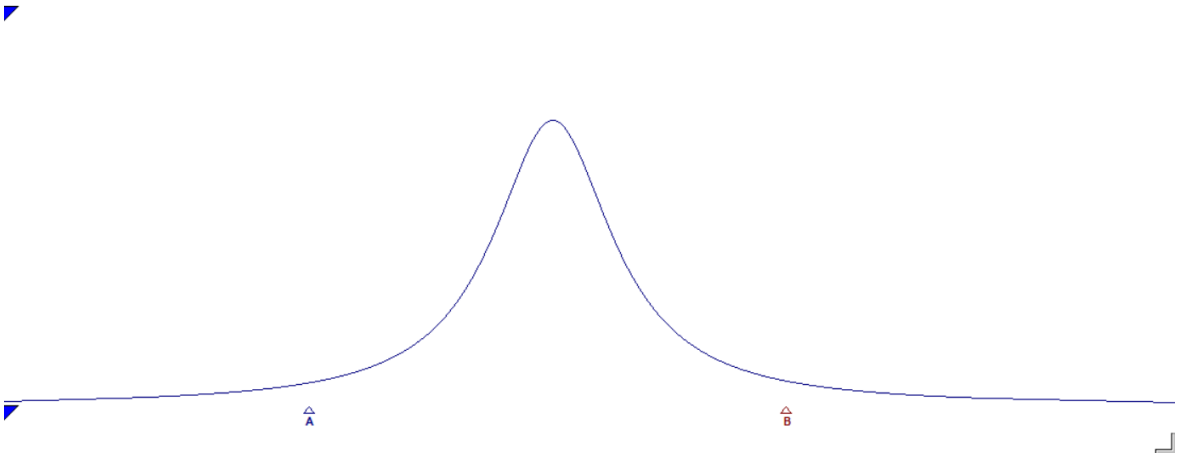

k = 1400 s^{-1} (simulating the set 2 spectrum recorded at 313 K)

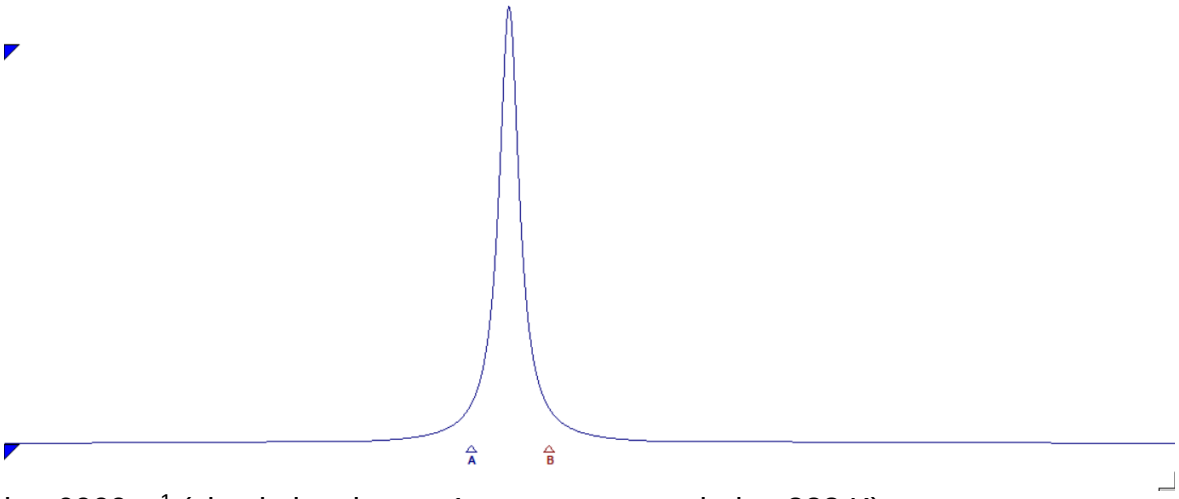

k = 6000 s^{-1} (simulating the set 1 spectrum recorded at 323 K)

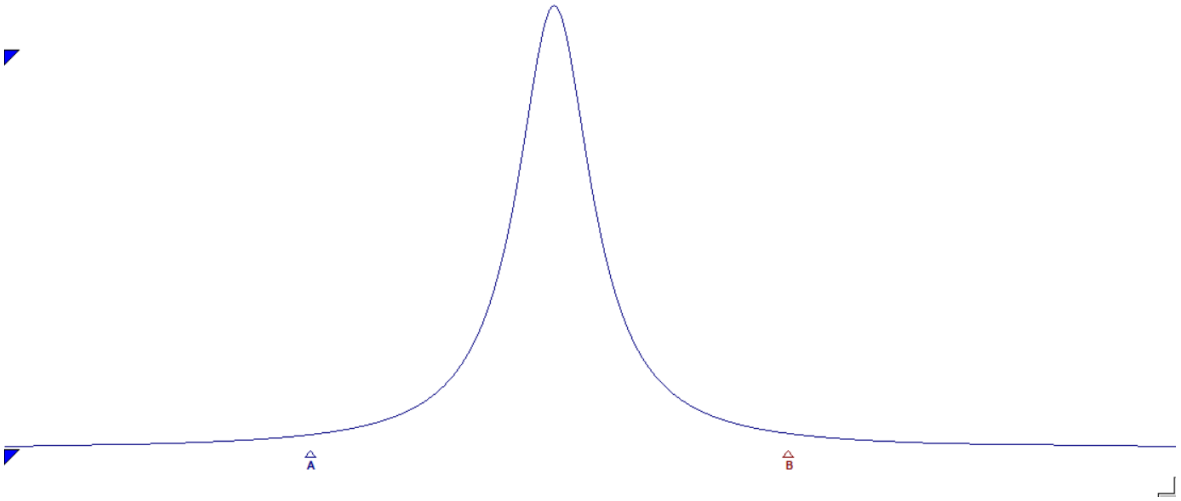

k = 3000 s^{-1} (simulating the set 2 spectrum recorded at 323 K)

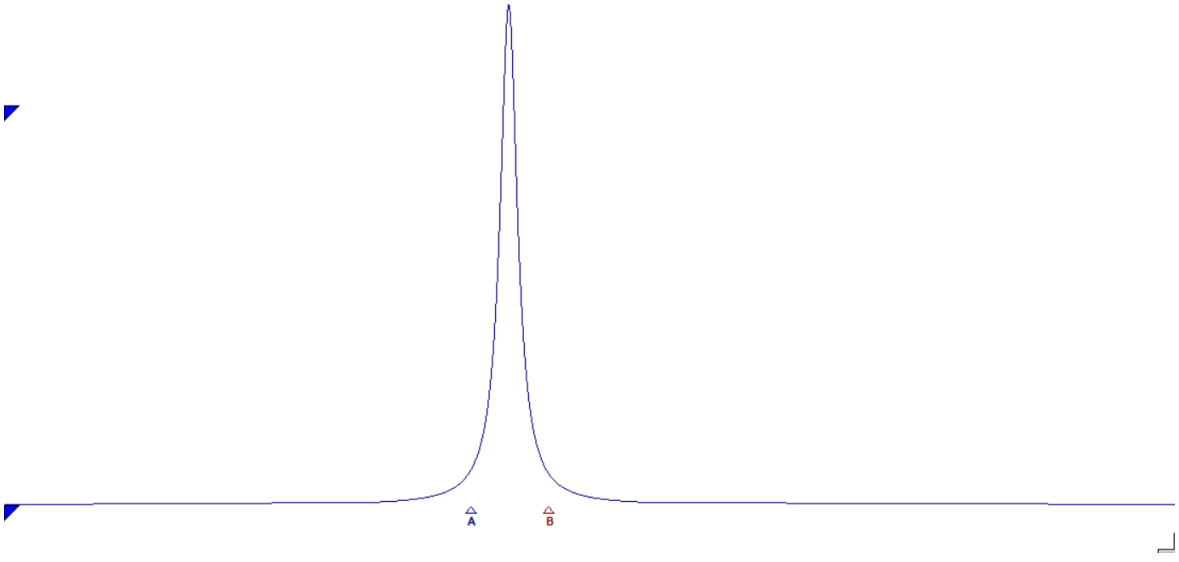

k = 9000 s^{-1} (simulating the set 1 spectrum recorded at 328 K)

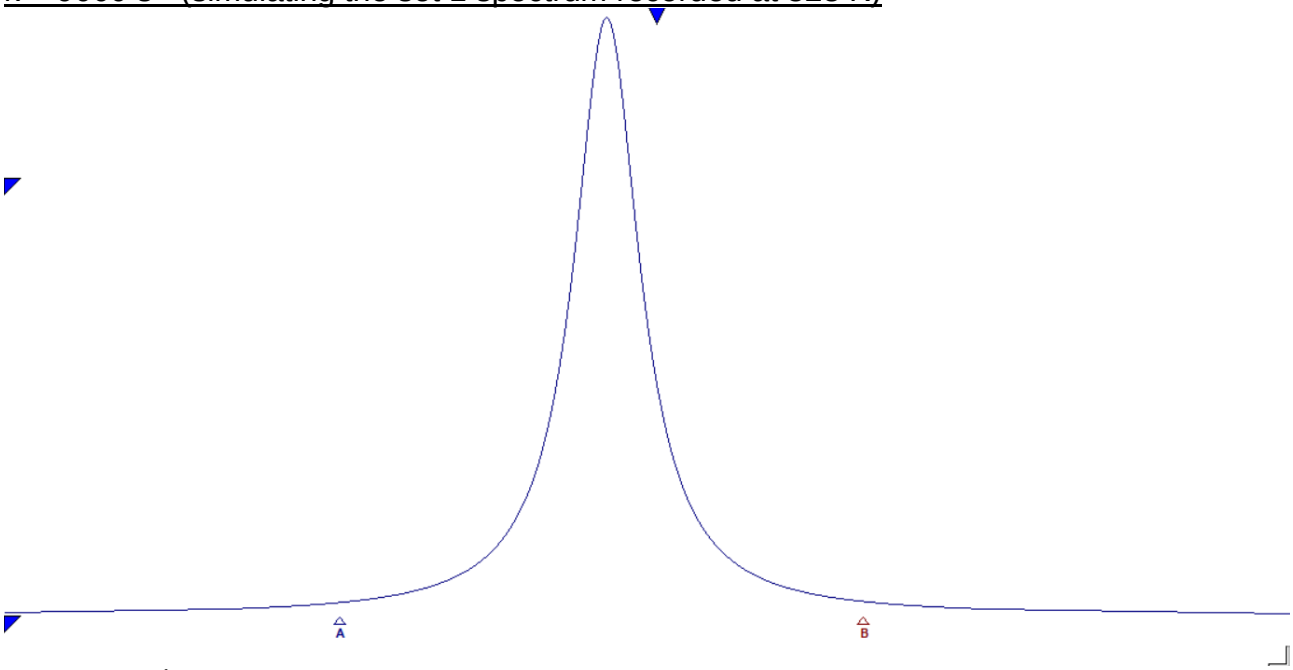

k = 4300 s^{-1} (simulating the set 2 spectrum recorded at 328 K)

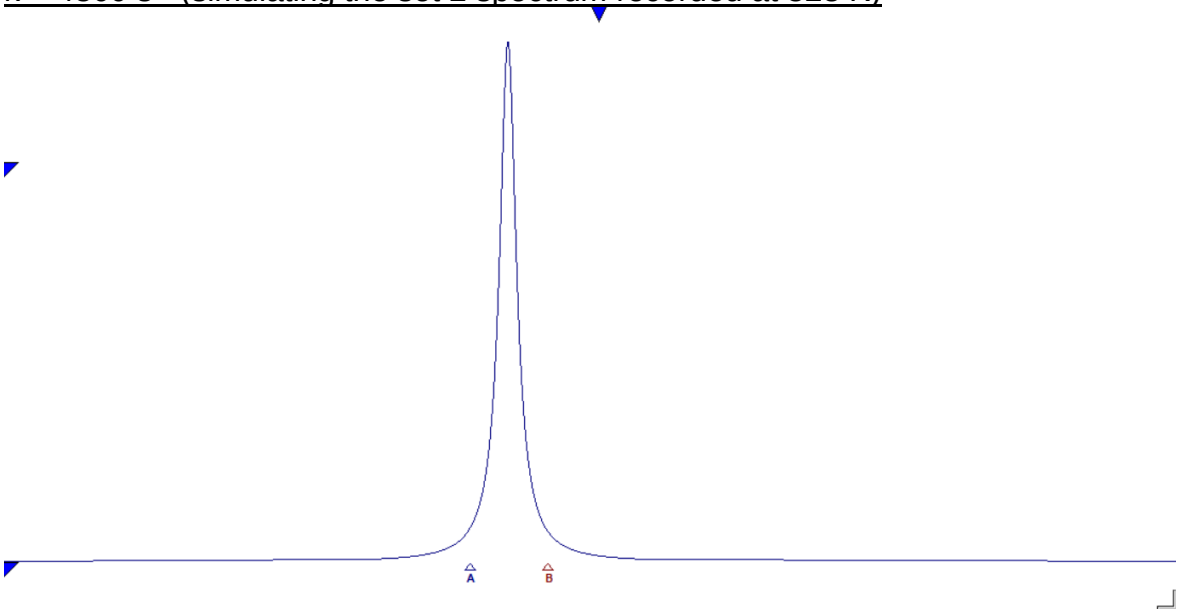

Plots of $\ln(k.T^{-1})$ versus T^{-1} based on these simulated rate constants are given below and application of equations 3 and 4 allowed $\Delta H^{\ddagger}$ and $\Delta S^{\ddagger}$ to be determined as 59.0 +/- 3.2 kJ mol^{-1} and 0.0 +/- 0.1 J $mol^{-1}K^{-1}$.

Plot based on set 1

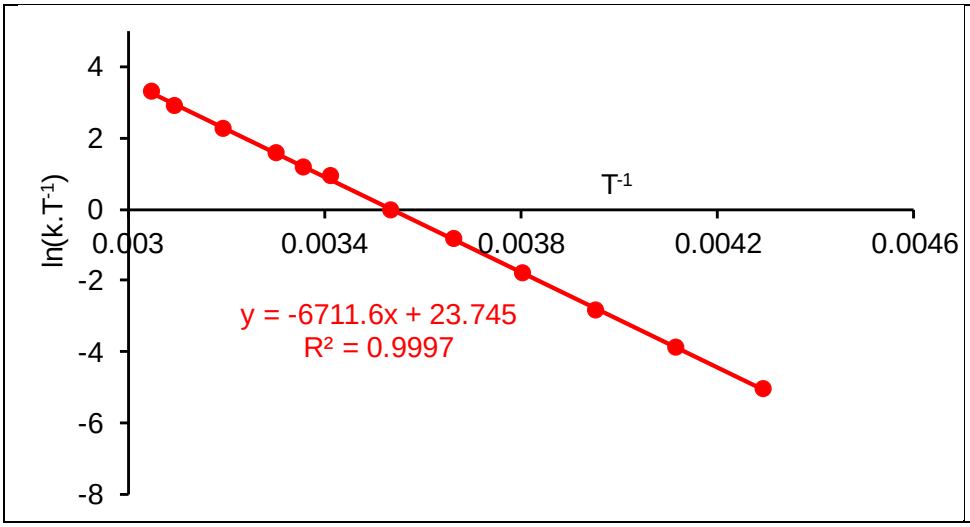

$\Delta H^{\ddagger}$ = 55.8 kJ mol^{-1}
$\Delta S^{\ddagger}$ = -0.1 J $mol^{-1}K^{-1}$

Plot based on set 2

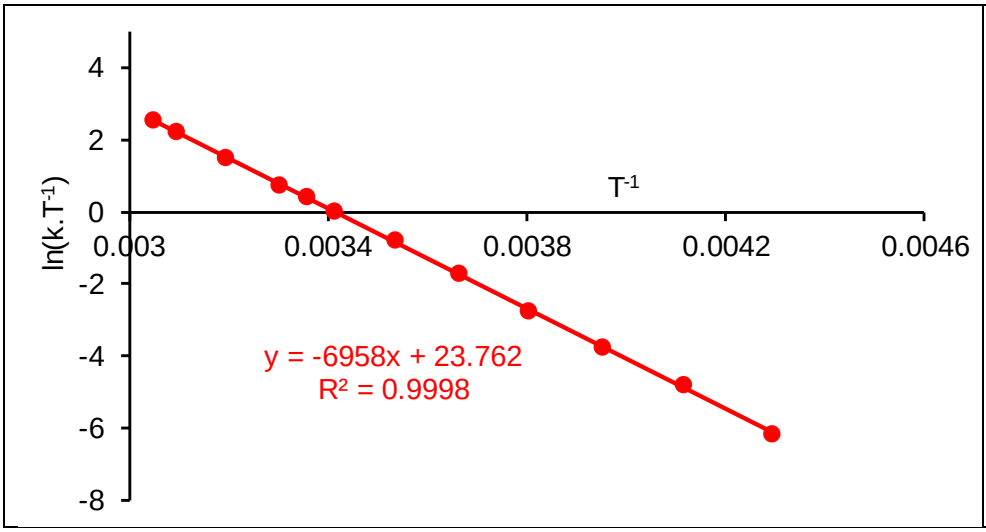

$\Delta H^{\ddagger}$ = 57.9 kJ mol^{-1}
$\Delta S^{\ddagger}$ = 0.0 J $mol^{-1}K^{-1}$

Compound 8

The parameters used were:

Peak (as labelled in the VT spectra in the ESI)	Frequency (Hz)	Half width (Hz)	% intensity
a: imine	4270.4	10.1	50.0
b: imine	4174.2	8.8	50.0
c: aromatic set 1	3814.7	9.1	50.0
d: aromatic set 1	3803.4	9.1	50.0
e: aromatic set 2	3636.1	8.9	50.0
f: aromatic set 2	3586.2	8.9	50.0

The imines, aromatic set 1 and aromatic set 2 were simulated separately, each as a two spin uncoupled system. The actual peak line shapes at each temperature were then best simulated by simulations with the following rate constants for the exchange process and this allowed $\Delta G^{\ddagger}$ at each temperature to be calculated using equation 1. The average value of these 30 calculations of $\Delta G^{\ddagger}$ is 49.0 kJ mol^{-1} and all the values are within +/- 1.0 kJ mol^{-1} of this average.

	imines		aromatic set 1		aromatic set 2	
Temperature (K)	k (s^{-1})	$\Delta G^{\ddagger}$ (kJ mol^{-1})	k (s^{-1})	$\Delta G^{\ddagger}$ (kJ mol^{-1})	k (s^{-1})	$\Delta G^{\ddagger}$ (kJ mol^{-1})
218	5	49.9	10	48.7	10	48.7
223	10	49.8	20	48.5	20	48.5
233	40	49.4	50	49.0	60	48.7
243	120	49.4	170	48.7	190	48.5
253	327	49.4	500	48.6	500	48.6
263	650	50.0	1300	48.5	1200	48.6
273	1600	49.9	3000	48.5	3000	48.5
283	3500	50.0	6000	48.7	6000	48.7
293	7500	50.0	14000	48.5	14000	48.5
298	11000	49.9	19000	48.6	19000	48.6

The simulated spectra (all with the same vertical and horizontal scales) are given below:

<u>k = 5 s^{-1} (simulating the imine spectrum recorded at 218 K)</u>

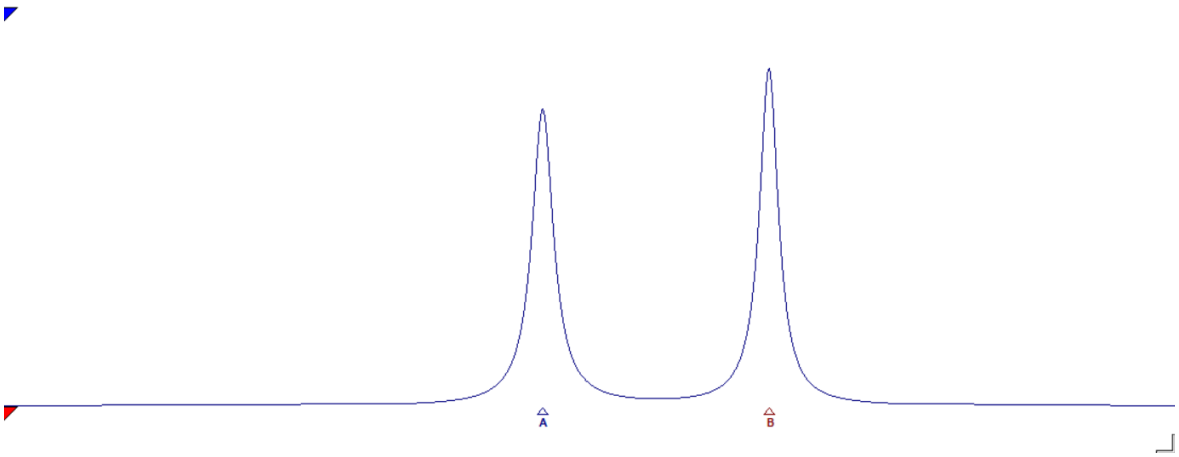

k = 10 s^{-1} (simulating the aromatic set 1 spectrum recorded at 218 K)

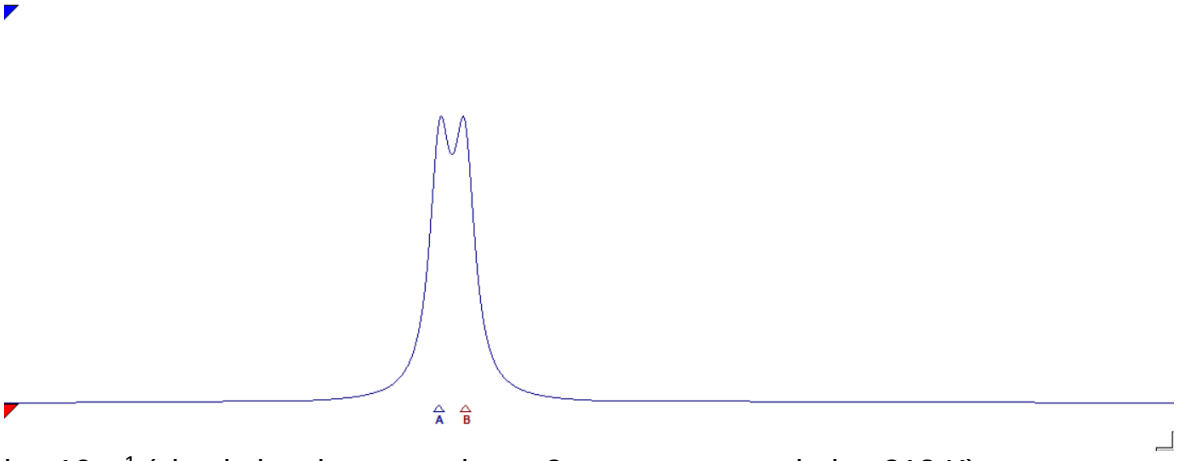

k = 10 s^{-1} (simulating the aromatic set 2 spectrum recorded at 218 K)

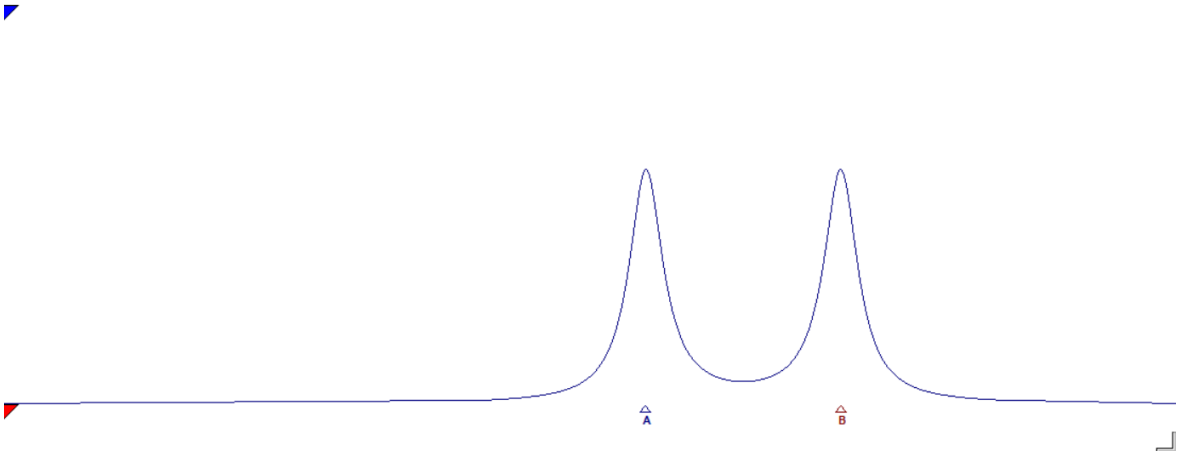

k = 10 s^{-1} (simulating the imine spectrum recorded at 223 K)

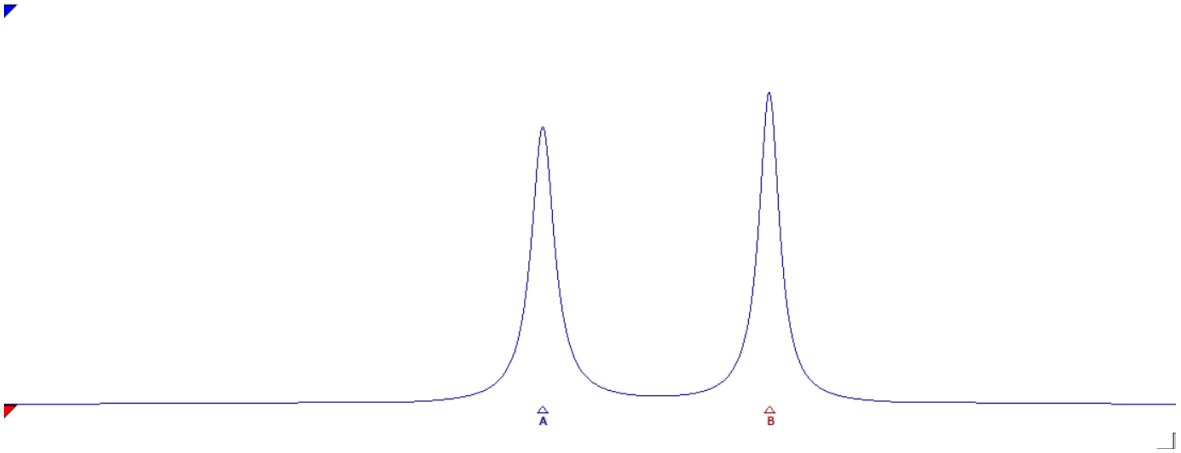

k = 20 s^{-1} (simulating the aromatic set 1 spectrum recorded at 223 K)

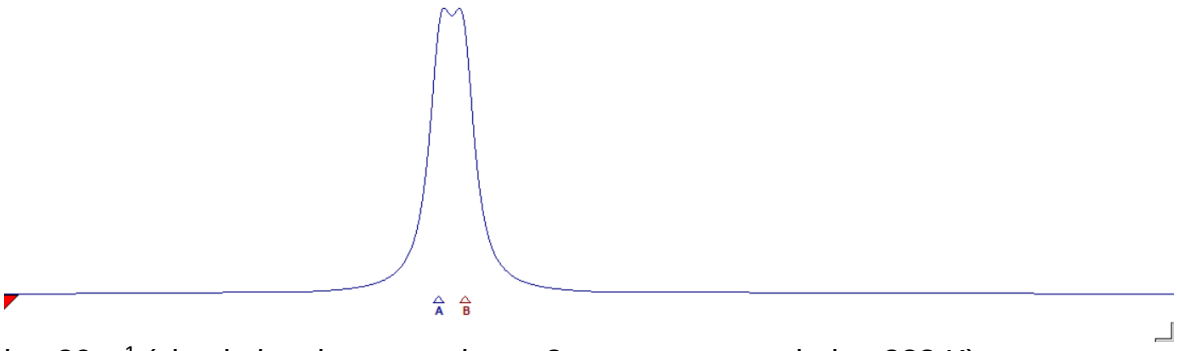

k = 20 s^{-1} (simulating the aromatic set 2 spectrum recorded at 223 K)

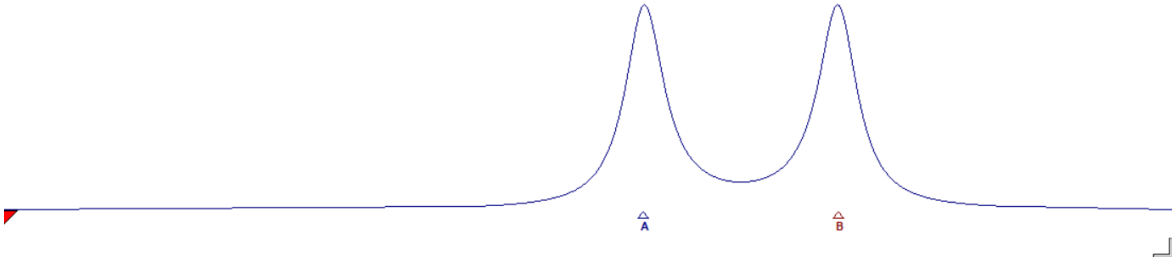

k = 40 s^{-1} (simulating the imine spectrum recorded at 233 K)

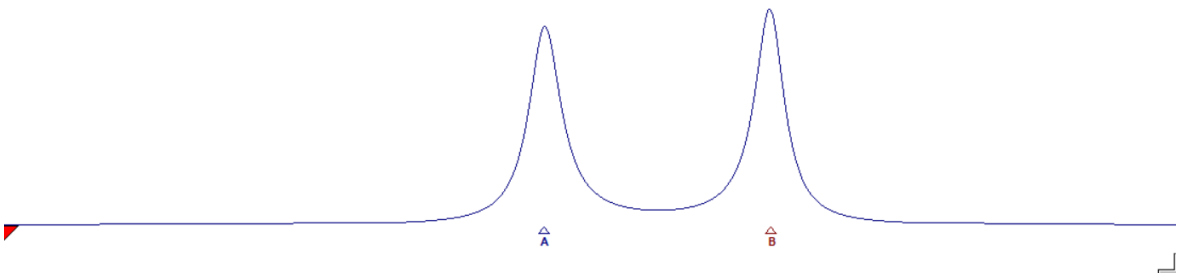

k = 50 s^{-1} (simulating the aromatic set 1 spectrum recorded at 233 K)

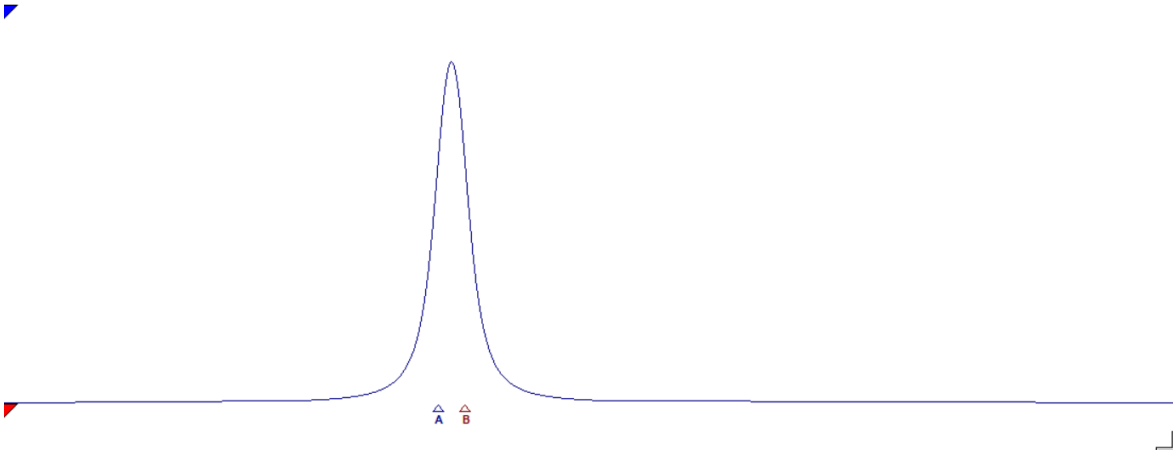

k = 60 s^{-1} (simulating the aromatic set 2 spectrum recorded at 233 K)

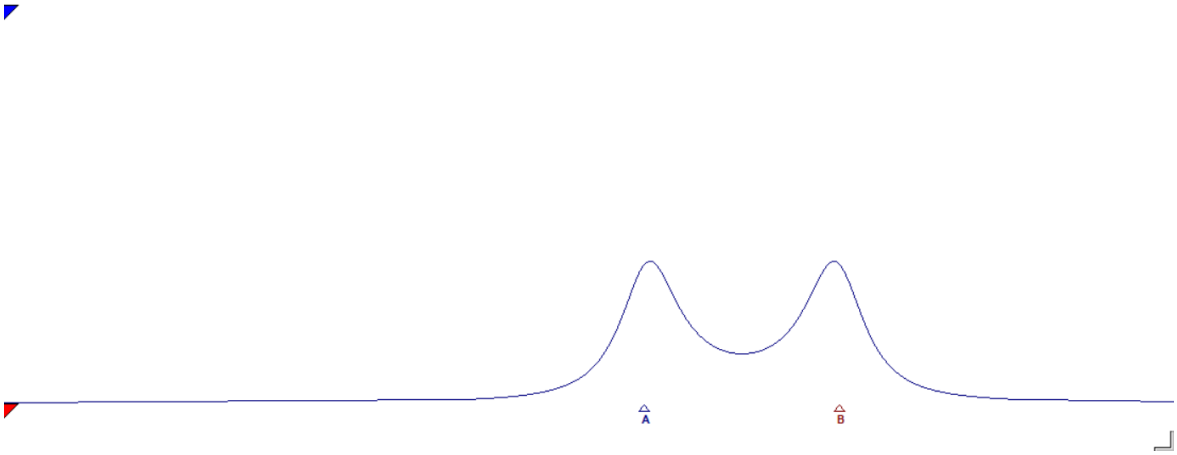

k = 120 s^{-1} (simulating the imine spectrum recorded at 243 K)

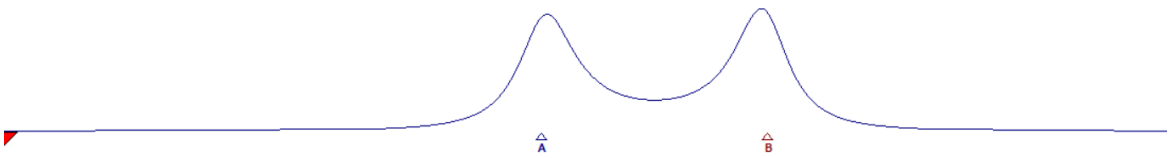

k = 170 s^{-1} (simulating the aromatic set 1 spectrum recorded at 243 K)

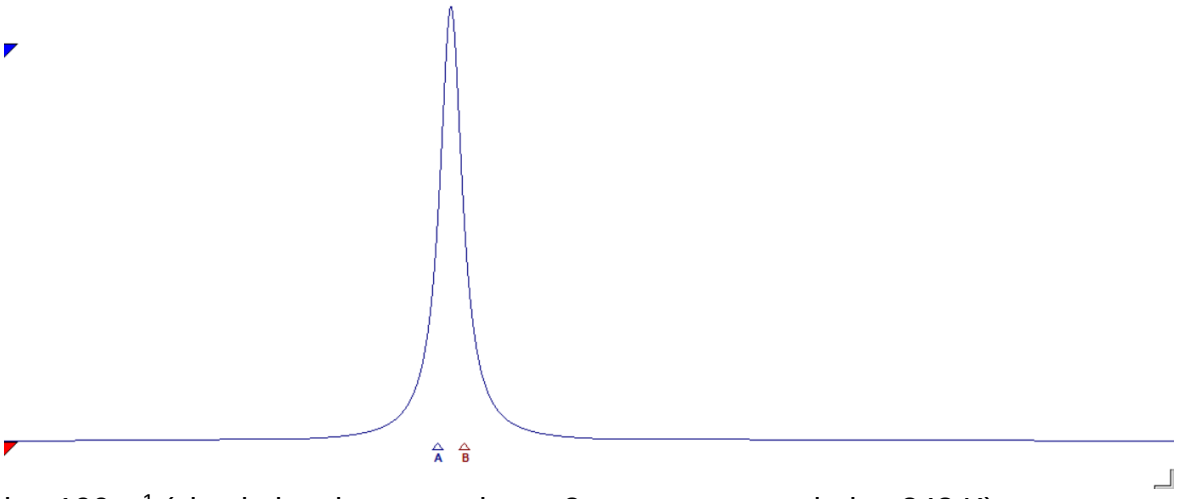

k = 190 s^{-1} (simulating the aromatic set 2 spectrum recorded at 243 K)

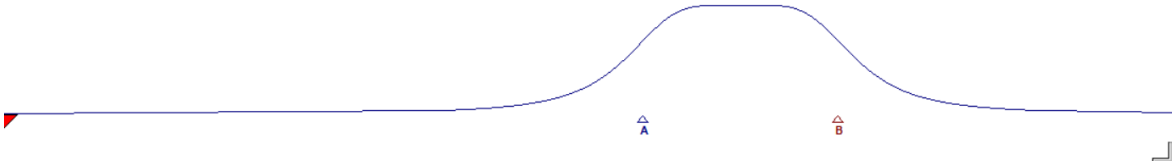

k = 327 s^{-1} (simulating the imine spectrum recorded at 253 K)

k = 500 s^{-1} (simulating the aromatic set 1 spectrum recorded at 253 K)

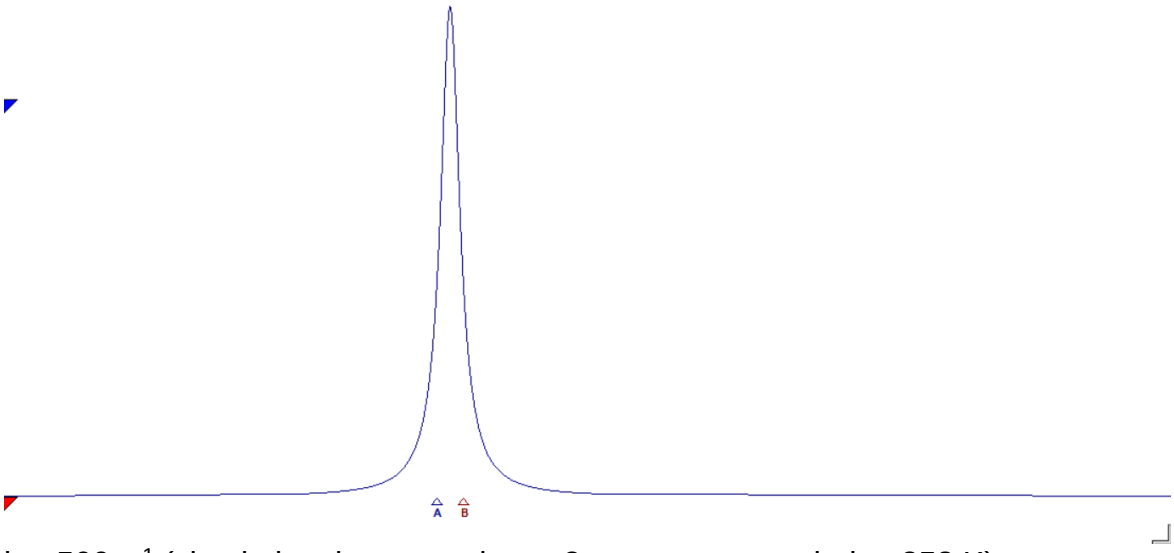

k = 500 s^{-1} (simulating the aromatic set 2 spectrum recorded at 253 K)

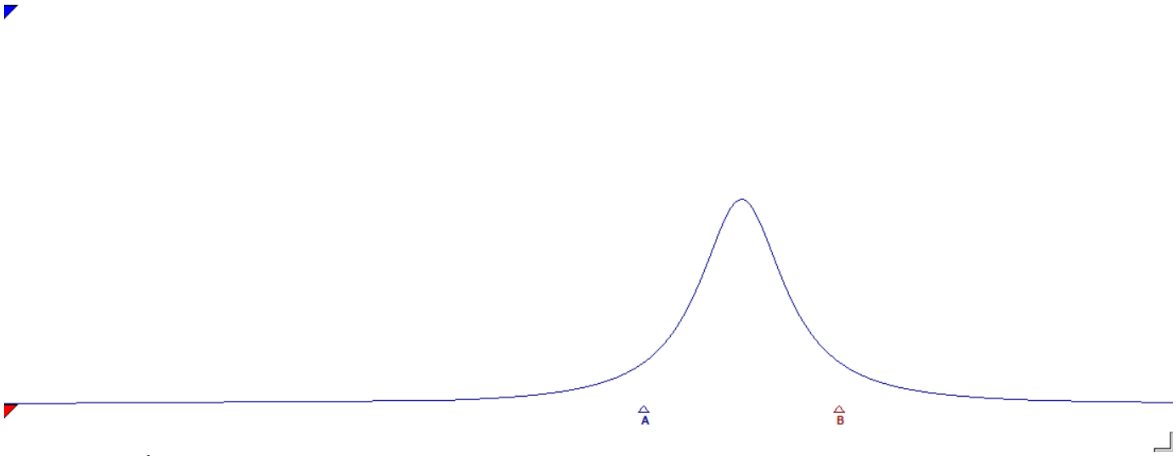

k = 650 s^{-1} (simulating the imine spectrum recorded at 263 K)

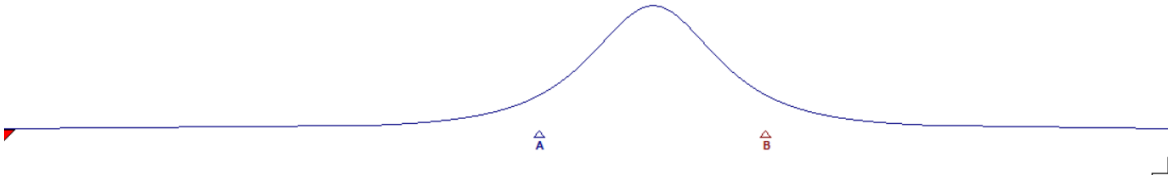

k = 1300 s^{-1} (simulating the aromatic set 1 spectrum recorded at 263 K)

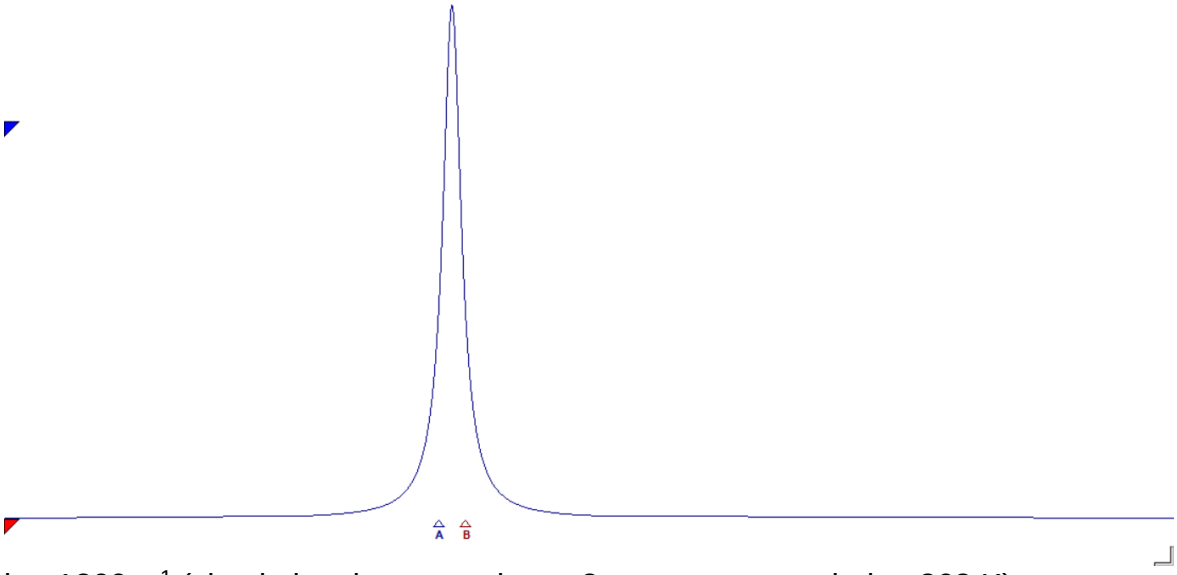

k = 1200 s^{-1} (simulating the aromatic set 2 spectrum recorded at 263 K)

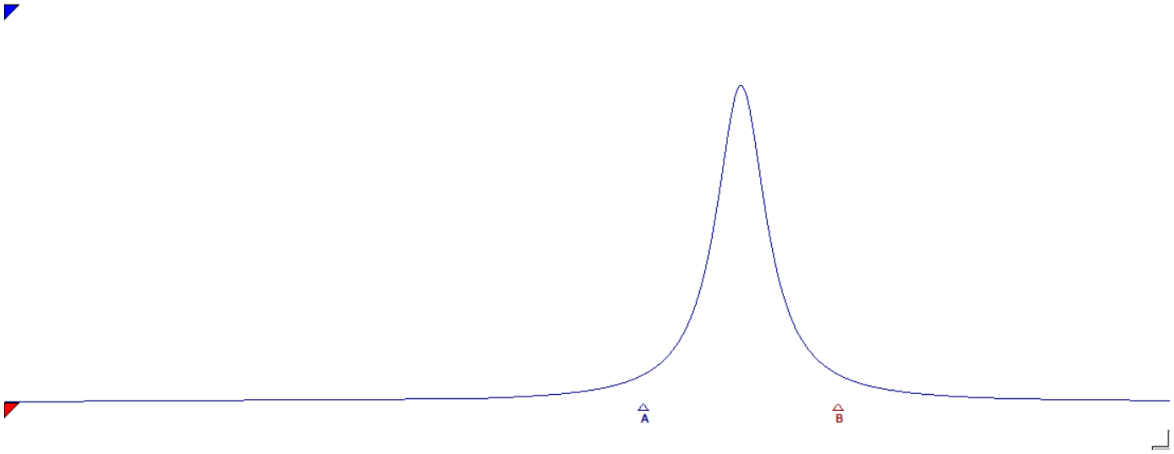

k = 1600 s^{-1} (simulating the imine spectrum recorded at 273 K)

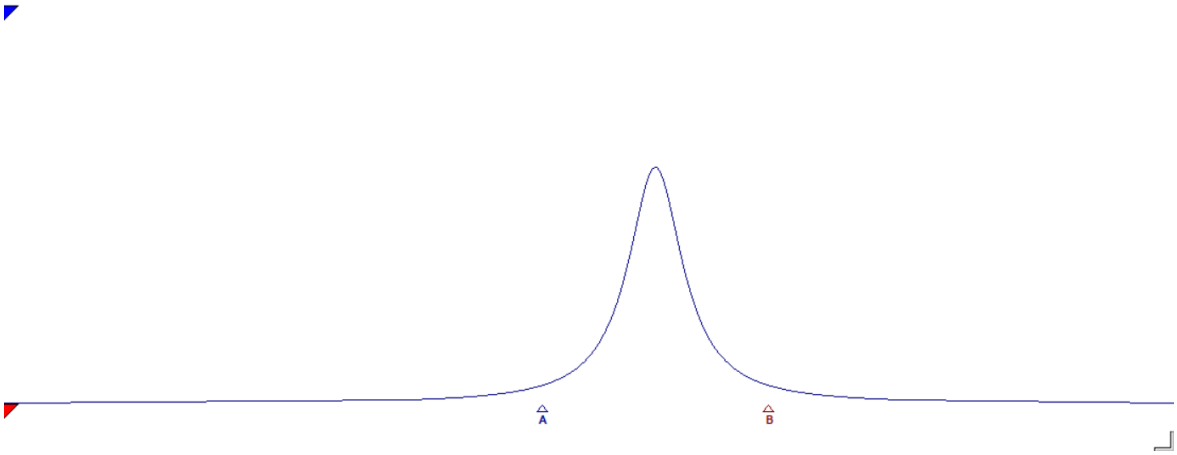

k = 3000 s^{-1} (simulating the aromatic set 1 spectrum recorded at 273 K)

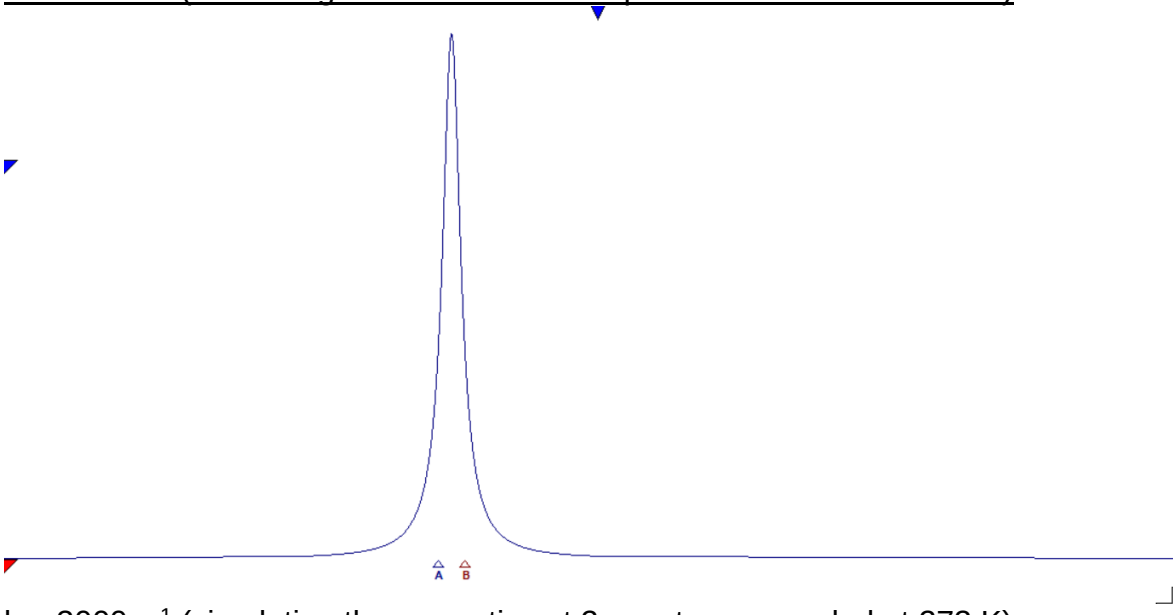

k = 3000 s^{-1} (simulating the aromatic set 2 spectrum recorded at 273 K)

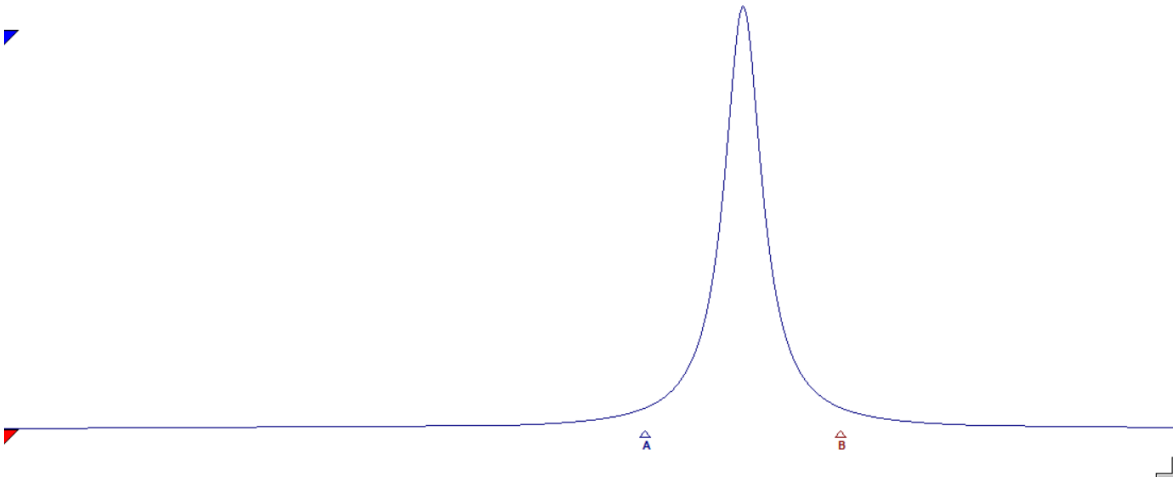

k = 3500 s^{-1} (simulating the imine spectrum recorded at 283 K)

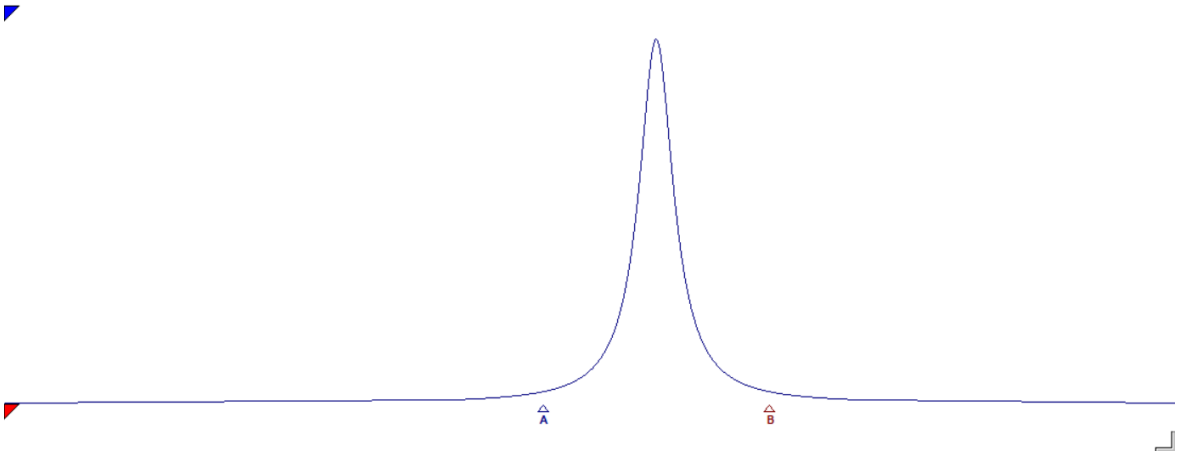

k = 6000 s^{-1} (simulating the aromatic set 1 spectrum recorded at 283 K)

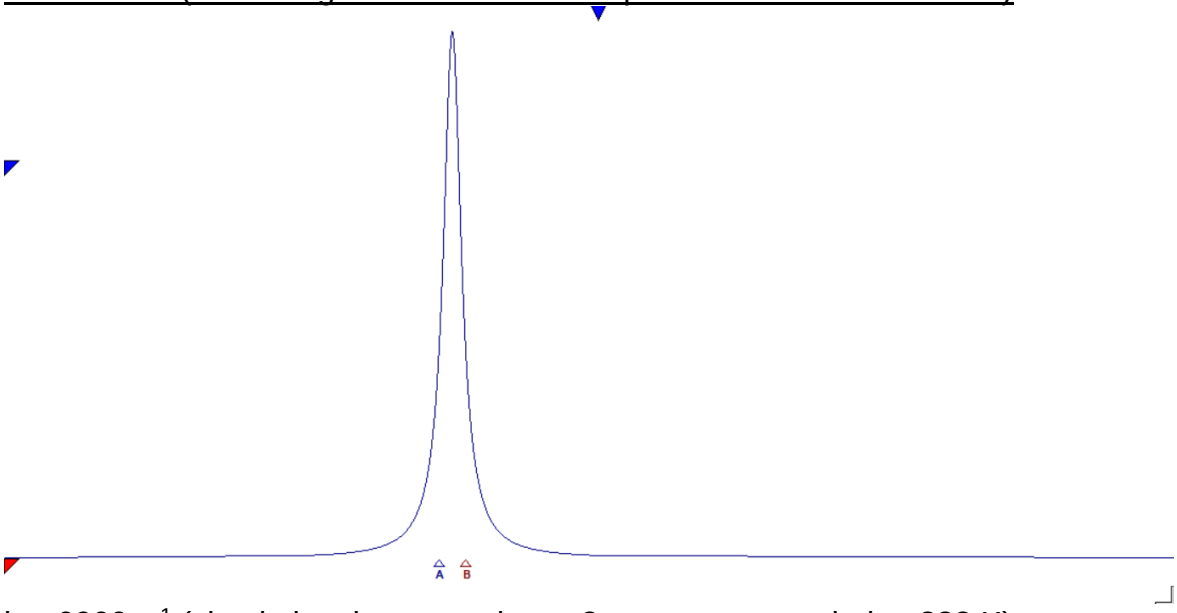

k = 6000 s^{-1} (simulating the aromatic set 2 spectrum recorded at 283 K)

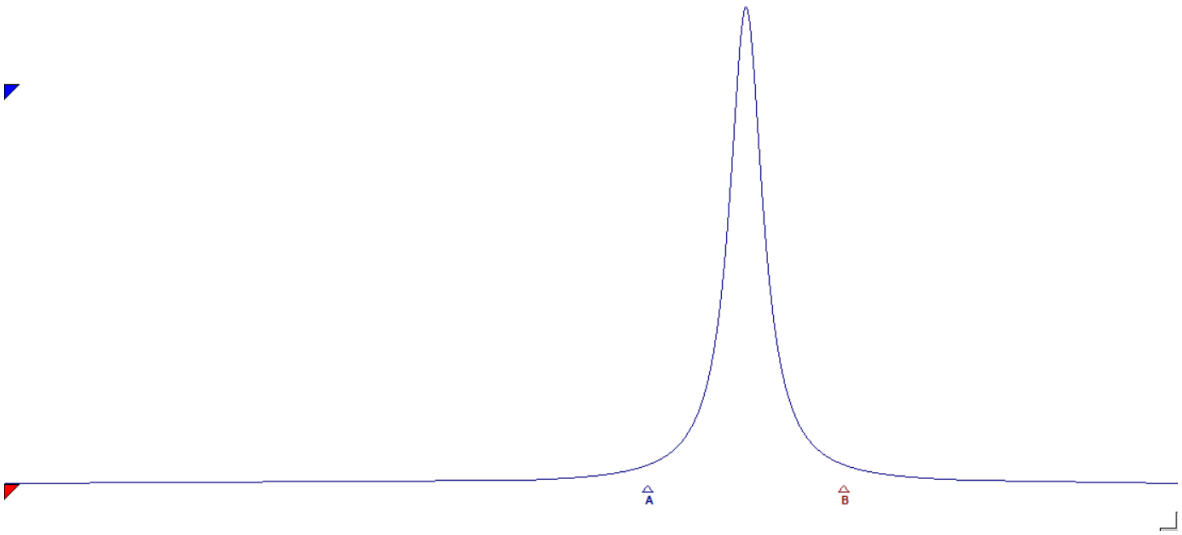

k = 7500 s^{-1} (simulating the imine spectrum recorded at 293 K)

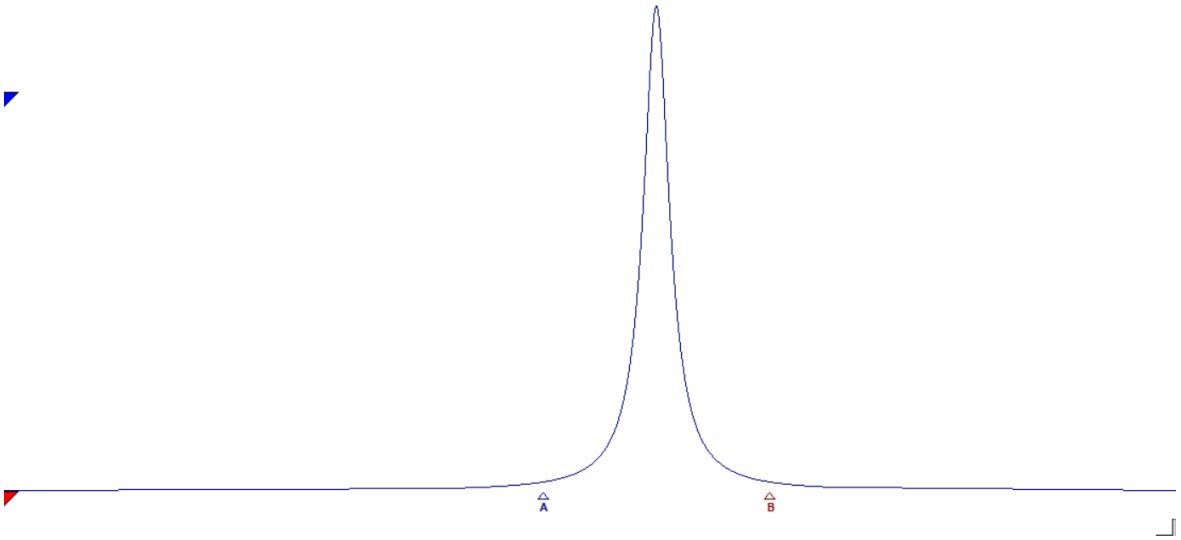

k = 14000 s^{-1} (simulating the aromatic set 1 spectrum recorded at 293 K)

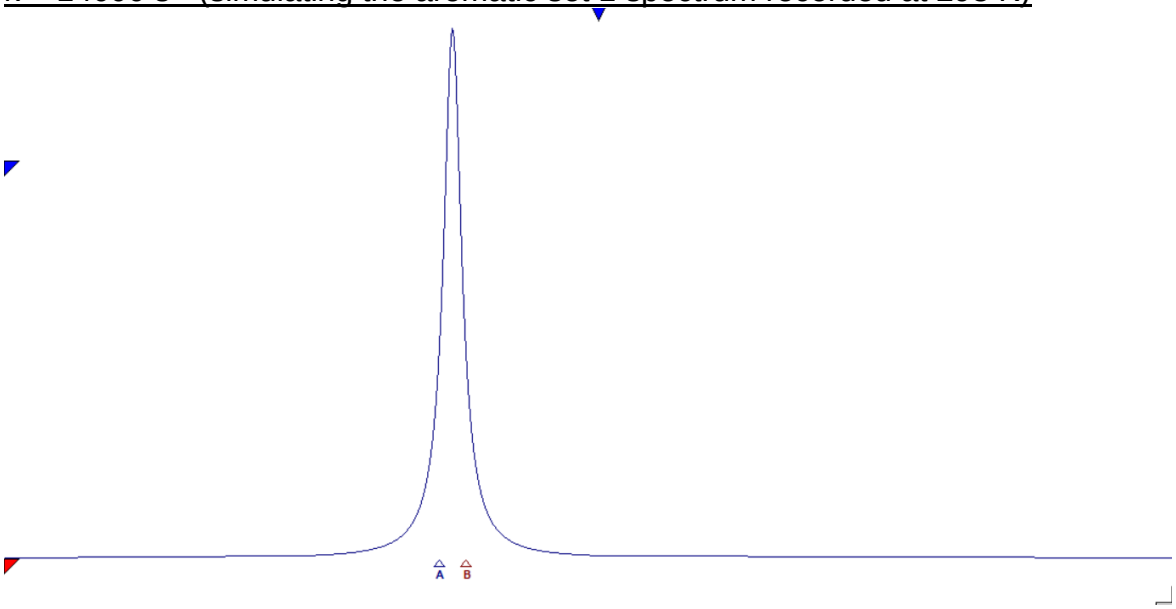

k = 14000 s^{-1} (simulating the aromatic set 2 spectrum recorded at 293 K)

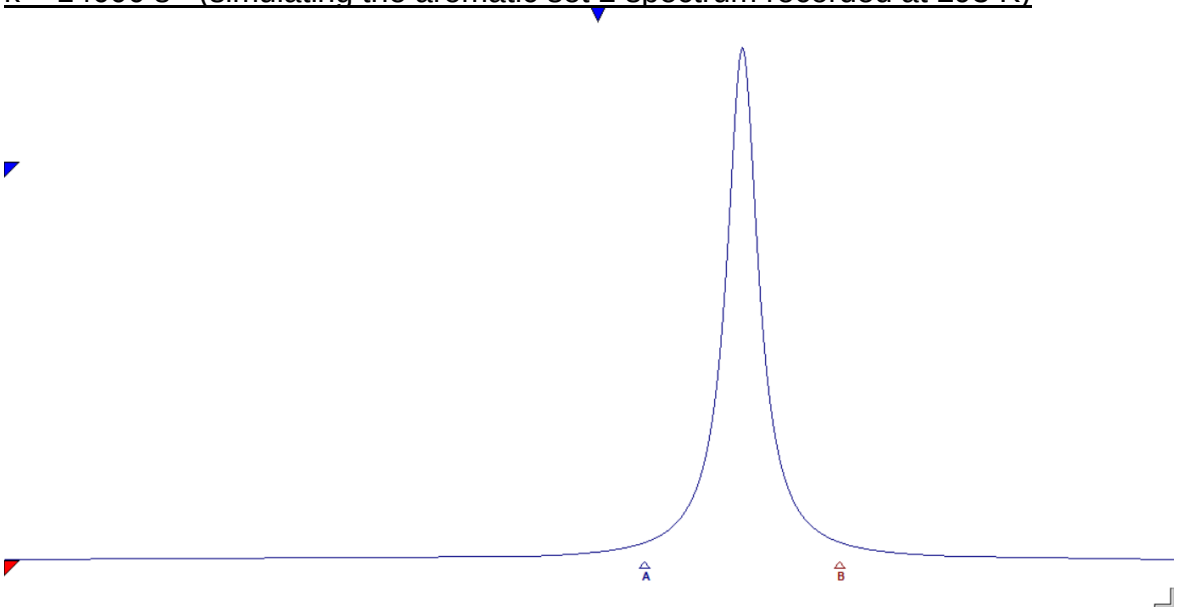

k = 11000 s^{-1} (simulating the imine spectrum recorded at 298 K)

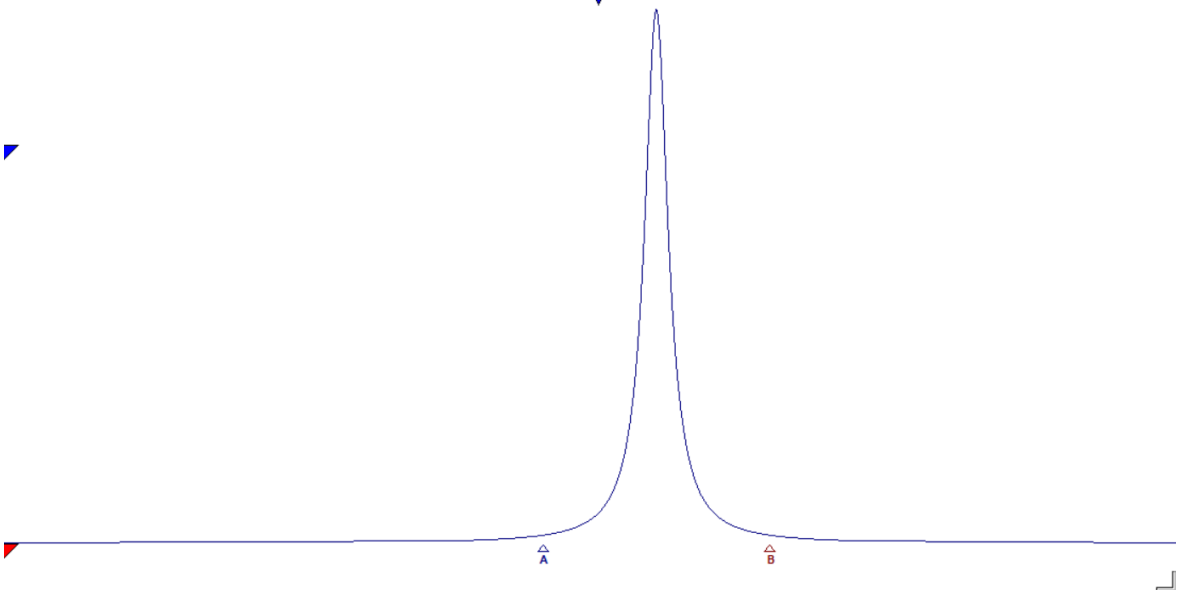

k = 19000 s^{-1} (simulating the aromatic set 1 spectrum recorded at 298 K)

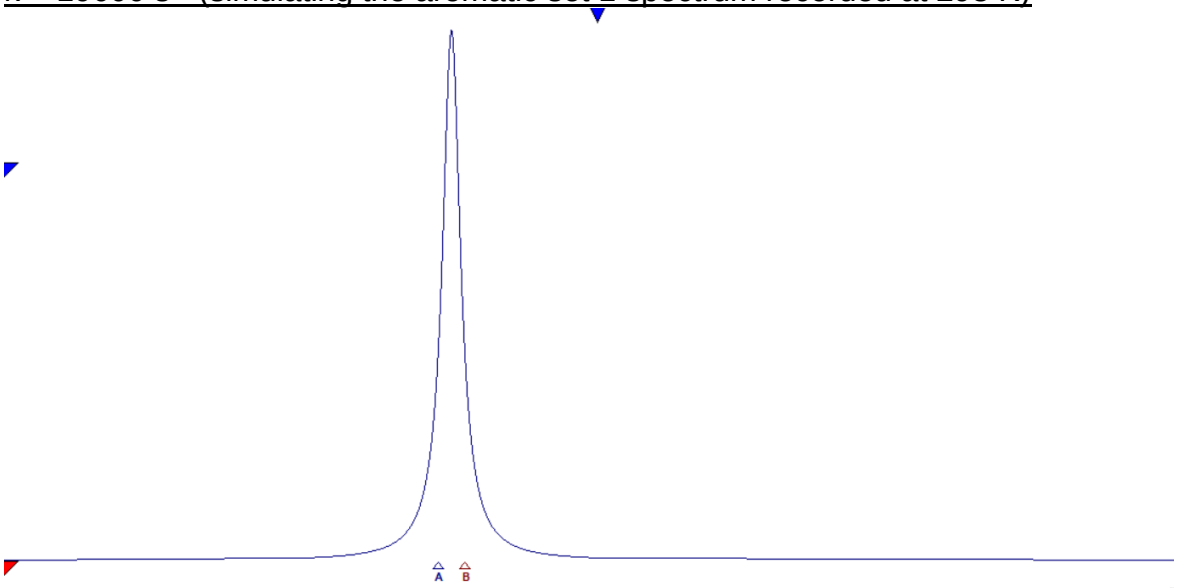

k = 19000 s^{-1} (simulating the aromatic set 2 spectrum recorded at 298 K)

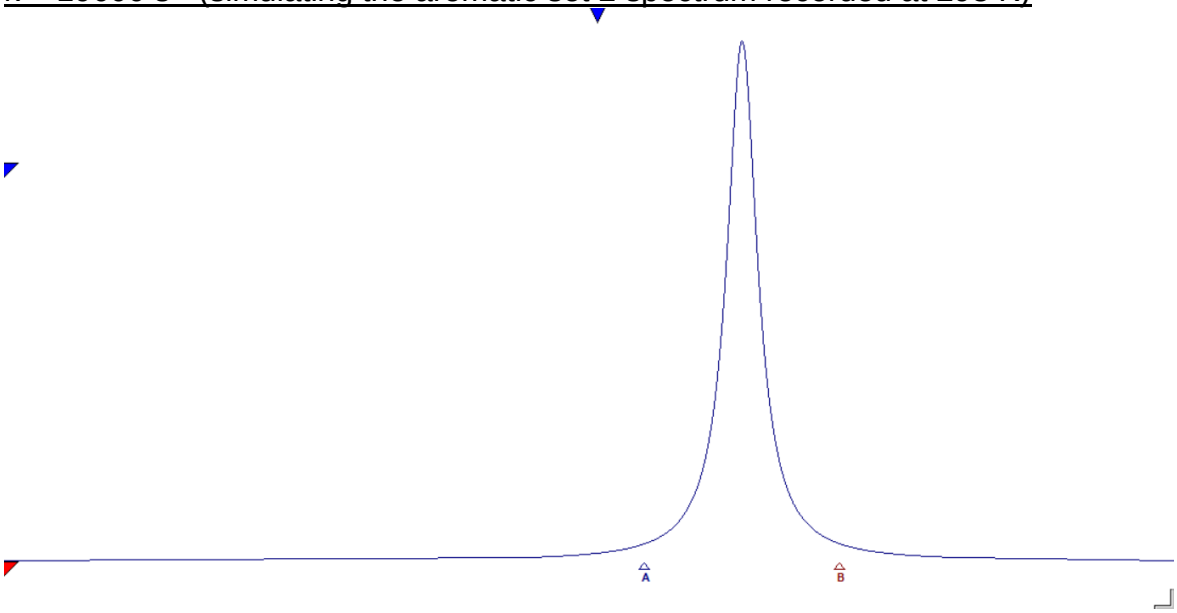

Plots of $\ln(k.T^{-1})$ versus T^{-1} based on these simulated rate constants are given below and application of equations 3 and 4 allowed $\Delta H^{\ddagger}$ and $\Delta S^{\ddagger}$ to be determined as 48.9 +/- 0.3 kJ mol^{-1} and -0.2 +/- 3.2 J $mol^{-1}K^{-1}$.

Plot based on imines

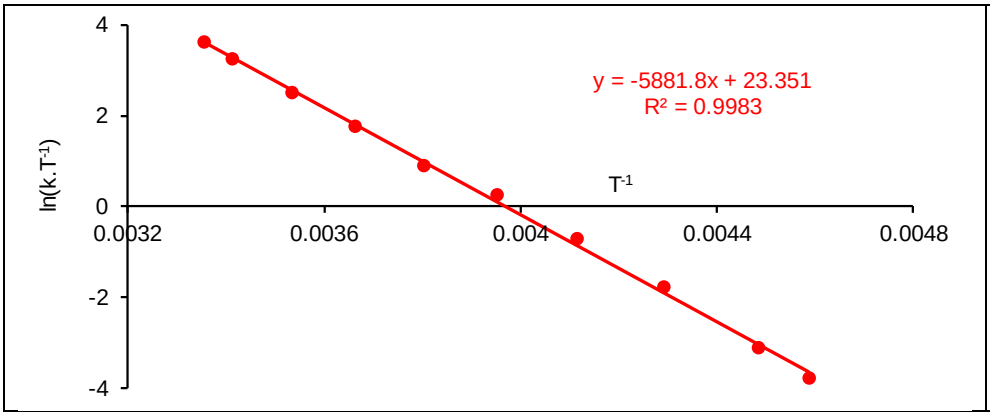

$\Delta H^{\ddagger}$ = 48.9 kJ mol^{-1}
$\Delta S^{\ddagger}$ = -3.4 J $mol^{-1}K^{-1}$

Plot based on aromatic set 1

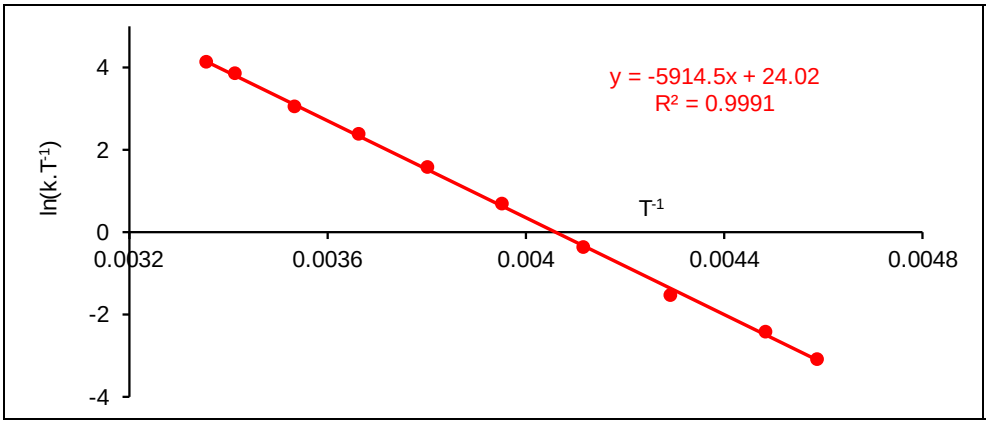

$\Delta H^{\ddagger}$ = 49.2 kJ mol^{-1}
$\Delta S^{\ddagger}$ = 2.2 J $mol^{-1}K^{-1}$

Plot based on aromatic set 2

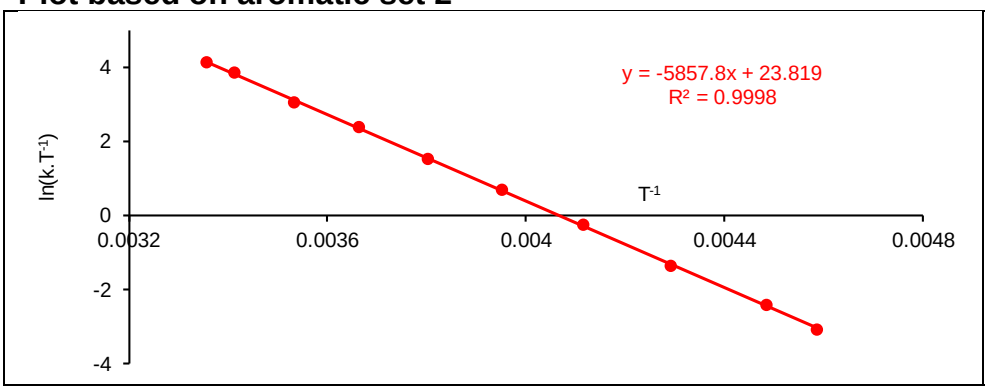

$\Delta H^{\ddagger}$ = 48.7 kJ mol^{-1}
$\Delta S^{\ddagger}$ = 0.5 J $mol^{-1}K^{-1}$

1:2.5 mixture of 10 and 11

The parameters used were:

Peak (as labelled in Figure 11)	Frequency (Hz)	Half width (Hz)	% intensity
a	759.45	2.97	23.0
b	750.64	2.97	21.4
c	709.22	2.97	29.3
e	661.1	2.97	23.5
f	644.3	2.97	23.1
g	635.1	2.97	18.7
h	614.1	2.97	34.7
d	481.32	2.97	26.3

The actual peak line shapes at each temperature were then best simulated by simulations with the following rate constants for the exchange process. Peaks a-d and e-h were simulated separately. This allowed $\Delta G^{\ddagger}$ at each temperature to be calculated using equation 1. The values for $\Delta G^{\ddagger}$ obtained using both data sets were then averaged. For this system, the average $\Delta G^{\ddagger}$ values increases steadily from 51.8 kJ mol^{-1} at 218 K to 68.6 kJ mol^{-1} at 328 K.

	Analysis of peaks a–d		Analysis of peaks e–h		
Temperature (K)	k (s^{-1})	$\Delta G^{\ddagger}$ (kJ mol^{-1})	k (s^{-1})	$\Delta G^{\ddagger}$ (kJ mol^{-1})	$\Delta G^{\ddagger}_{avg}$ (kJ mol^{-1})
218	3.2	50.7	1	52.8	51.8
223	4	51.5	1.4	53.5	52.5
233	6.8	52.9	2.8	54.6	53.8
243	8.8	54.7	4.4	56.1	55.4
253	13	56.2	6	57.9	57.1
263	18	57.8	9.1	59.3	58.6
273	25	59.4	12.2	61.0	60.2
283	34.3	60.9	15.9	62.7	61.8
293	40.1	62.7	18.5	64.6	63.7
298	48.1	63.4	25.7	64.9	64.2
303	55.4	64.1	29.3	65.7	64.9
313	77.4	65.5	41	67.1	66.3
323	104.4	66.8	52.6	68.7	67.8
328	117.4	67.6	58.8	69.5	68.6

The simulated spectra (all with the same vertical and horizontal scales) are given below:

Peaks a-d: k = 3.2 s^{-1} (simulating the spectrum recorded at 218 K)

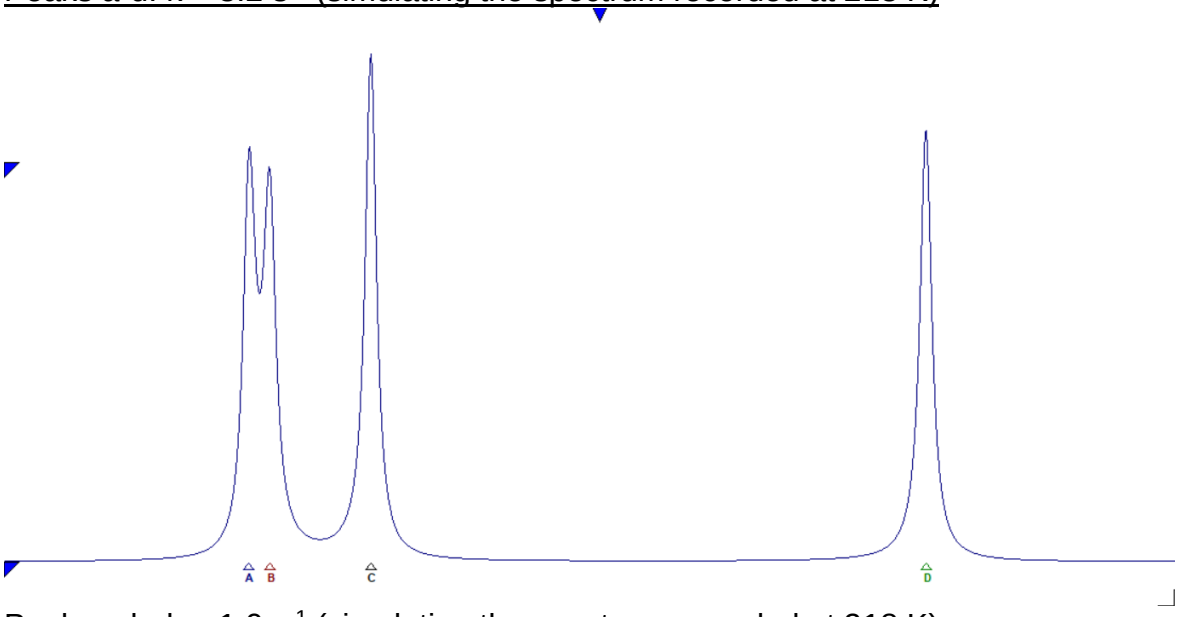

Peaks e-h: k = 1.0 s^{-1} (simulating the spectrum recorded at 218 K)

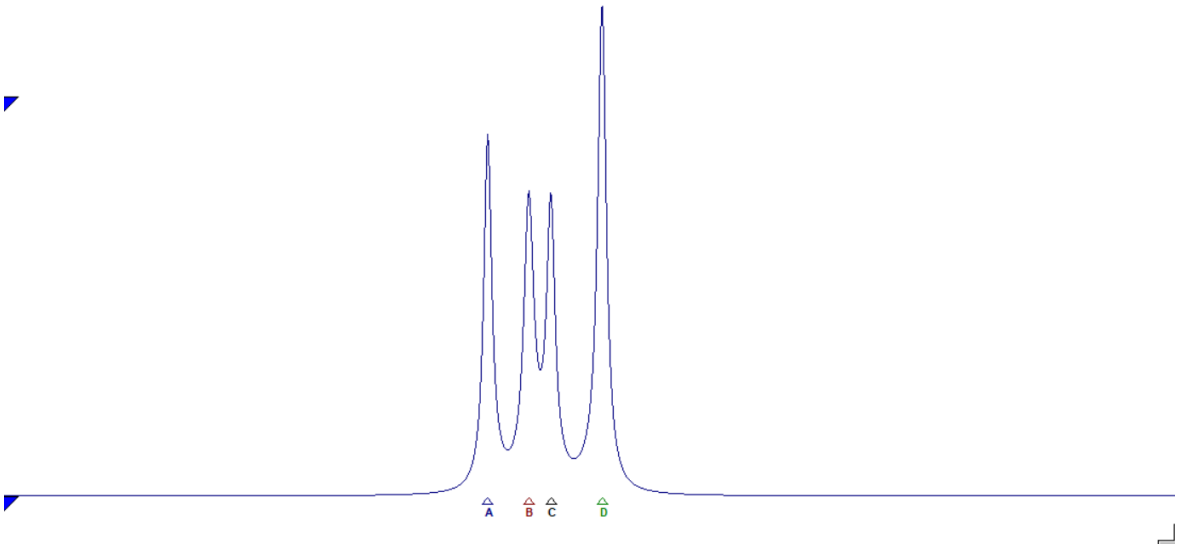

Peaks a-d: k = 4.0 s^{-1} (simulating the spectrum recorded at 223 K)

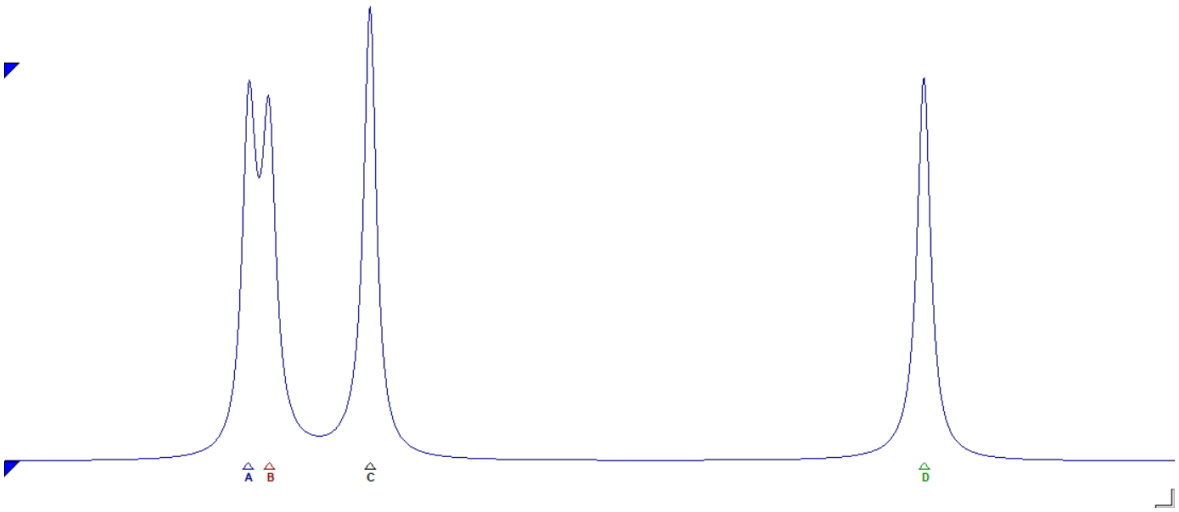

Peaks e-h: k = 1.4 s^{-1} (simulating the spectrum recorded at 223 K)

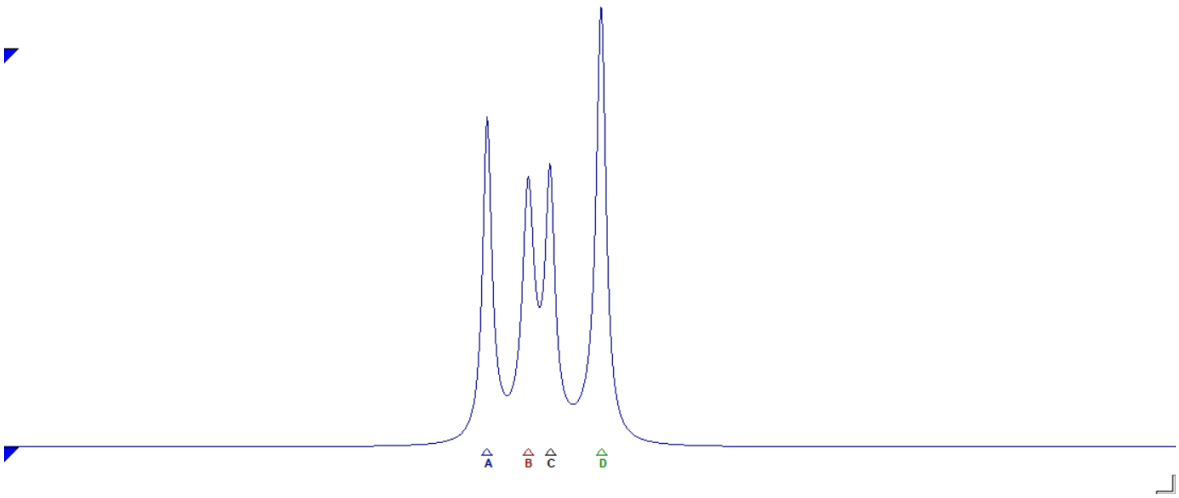

Peaks a-d: k = 6.8 s^{-1} (simulating the spectrum recorded at 233 K)

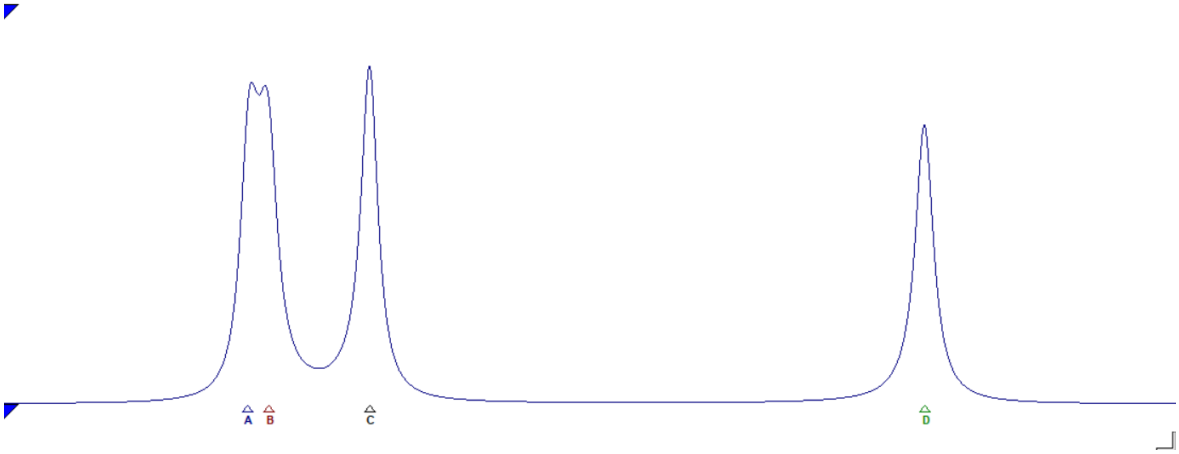

Peaks e-h: k = 2.8 s^{-1} (simulating the spectrum recorded at 233 K)

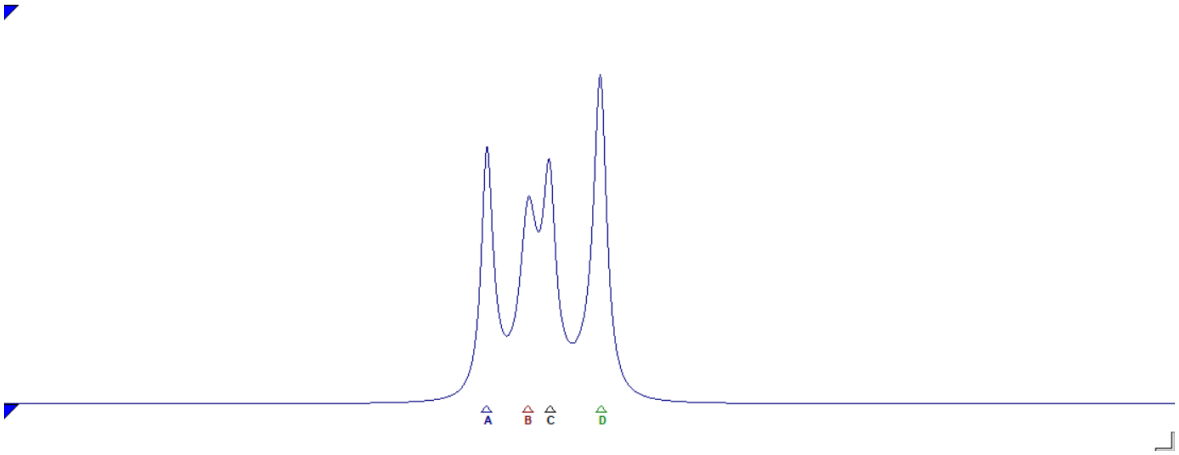

Peaks a-d: k = 8.8 s^{-1} (simulating the spectrum recorded at 243 K)

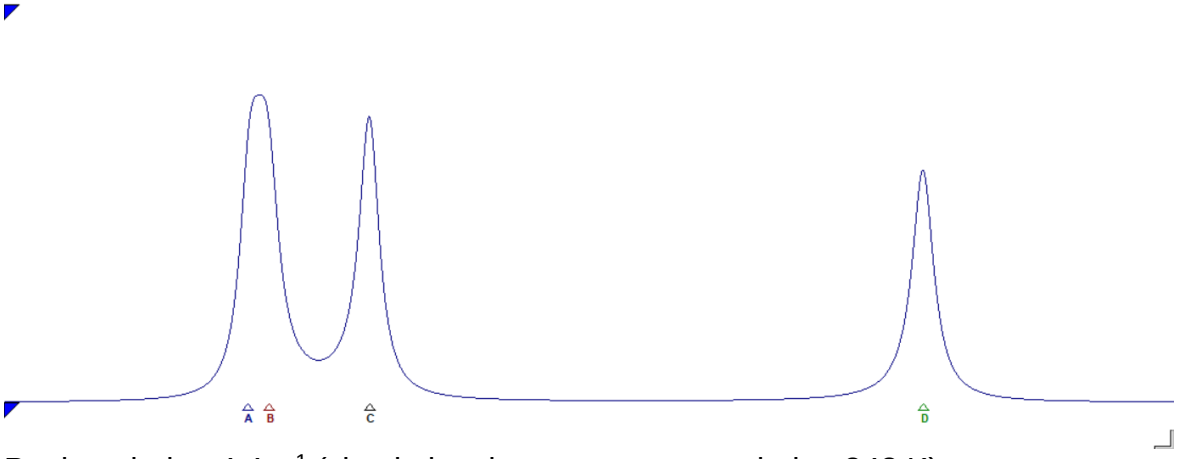

Peaks e-h: k = 4.4 s^{-1} (simulating the spectrum recorded at 243 K)

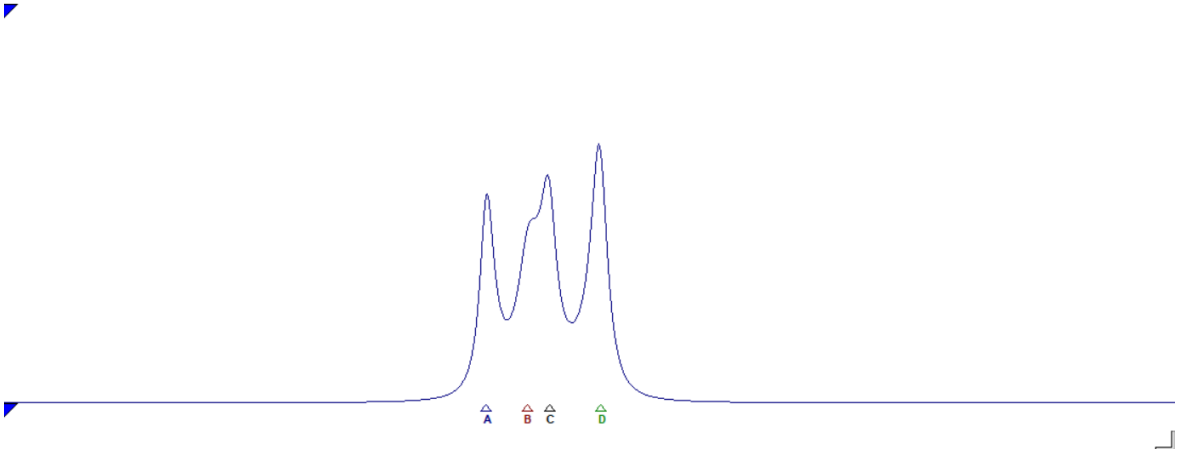

Peaks a-d: k = 13.0 s^{-1} (simulating the spectrum recorded at 253 K)

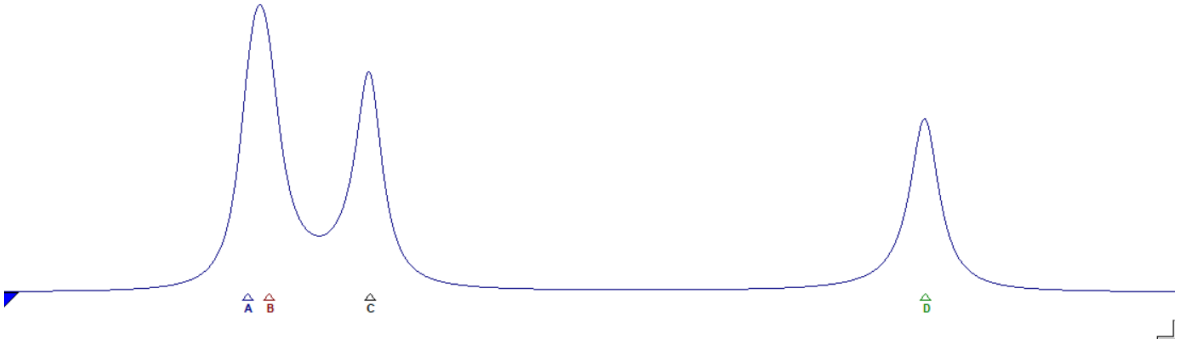

Peaks e-h: k = 6.0 s^{-1} (simulating the spectrum recorded at 253 K)

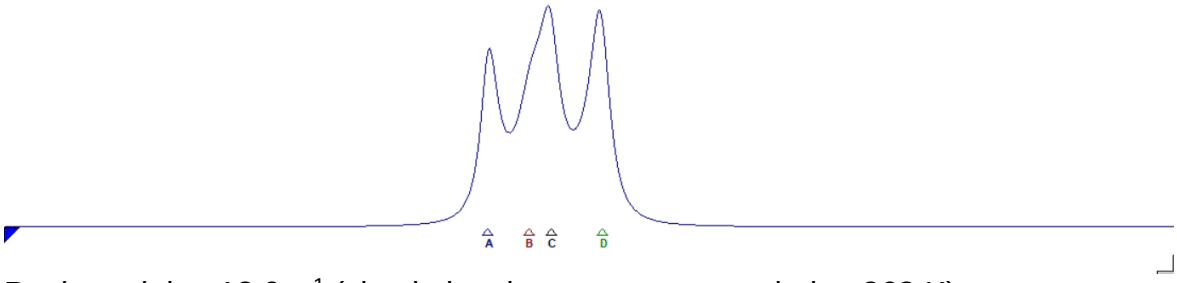

Peaks a-d: k = 18.0 s^{-1} (simulating the spectrum recorded at 263 K)

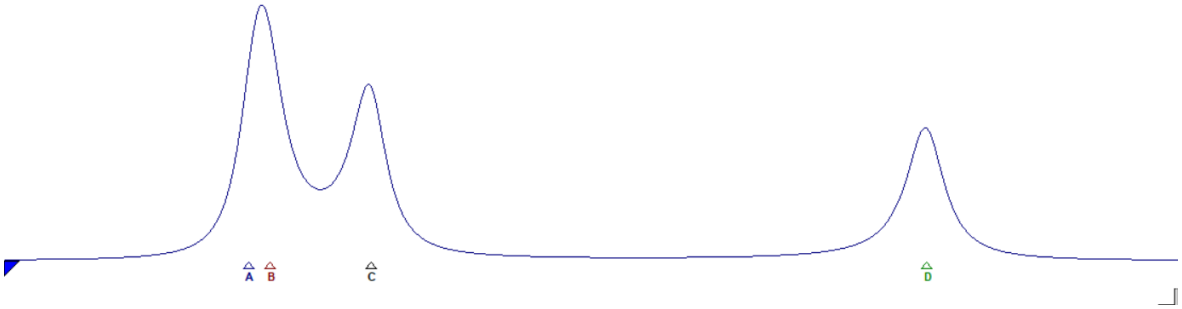

Peaks e-h: k = 9.1 s^{-1} (simulating the spectrum recorded at 263 K)

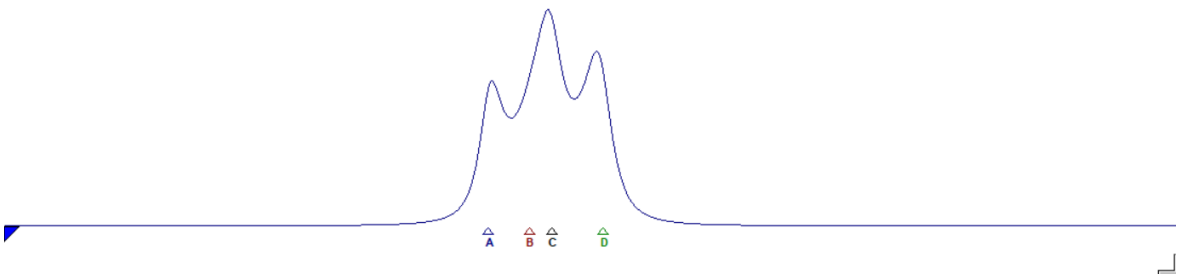

Peaks a-d: k = 25.0 s^{-1} (simulating the spectrum recorded at 273 K)

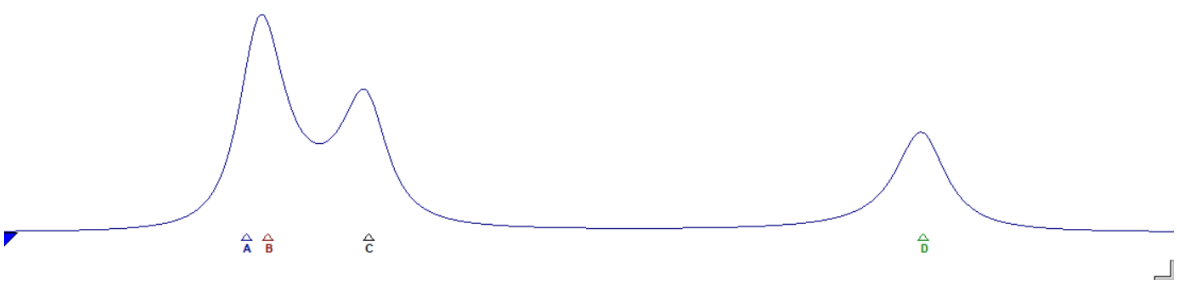

Peaks e-h: k = 12.2 s^{-1} (simulating the spectrum recorded at 273 K)

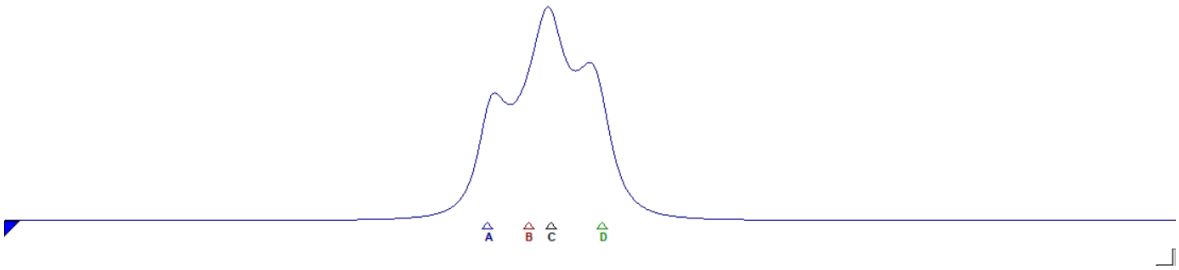

Peaks a-d: k = 34.3 s^{-1} (simulating the spectrum recorded at 283 K)

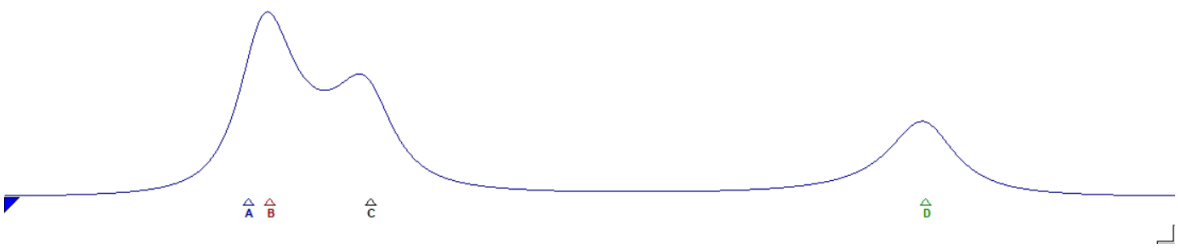

Peaks e-h: k = 15.9 s^{-1} (simulating the spectrum recorded at 283 K)

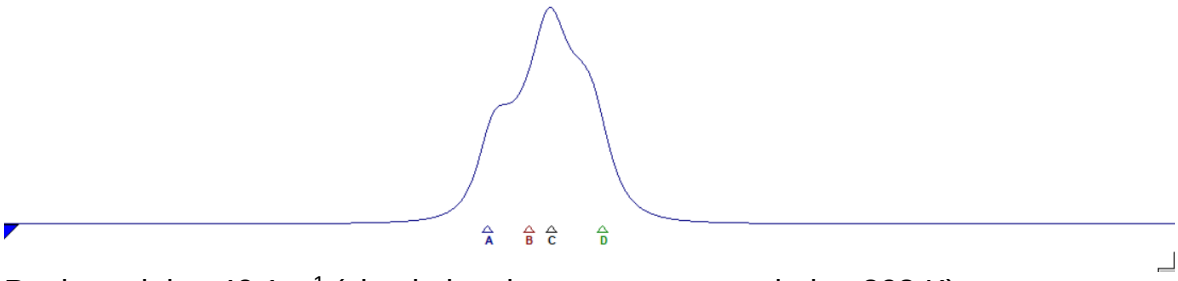

Peaks a-d: k = 40.1 s^{-1} (simulating the spectrum recorded at 293 K)

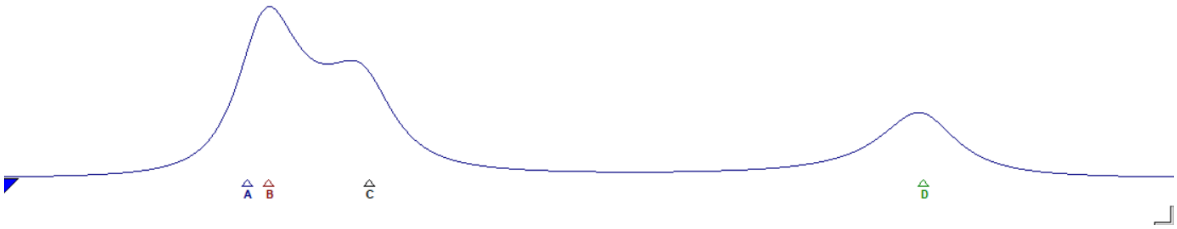

Peaks e-h: k = 18.5 s^{-1} (simulating the spectrum recorded at 293 K)

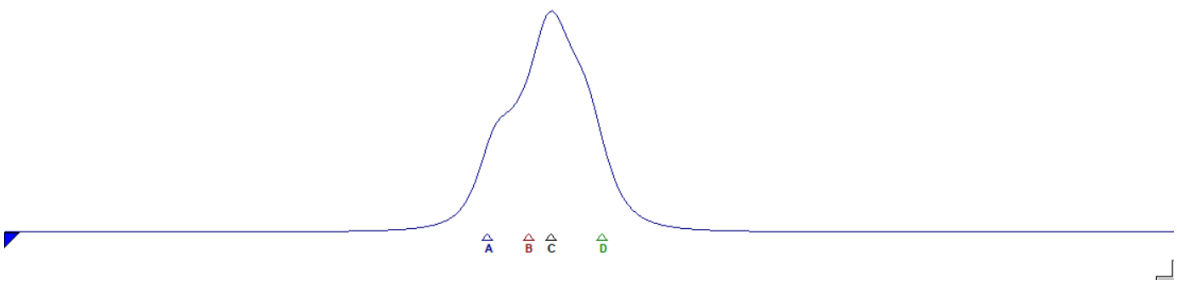

Peaks a-d: k = 48.1 s^{-1} (simulating the spectrum recorded at 298 K)

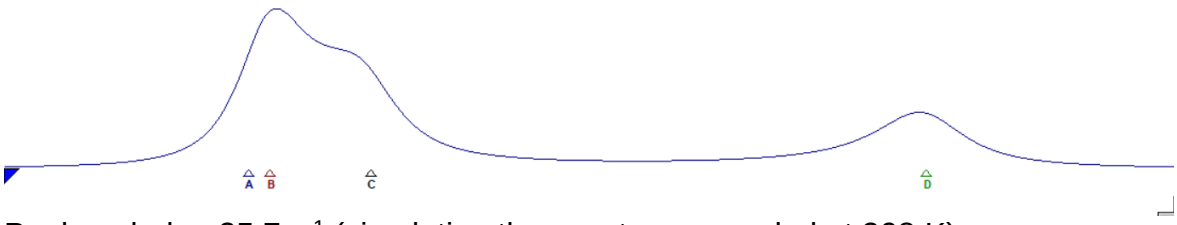

Peaks e-h: k = 25.7 s^{-1} (simulating the spectrum recorded at 298 K)

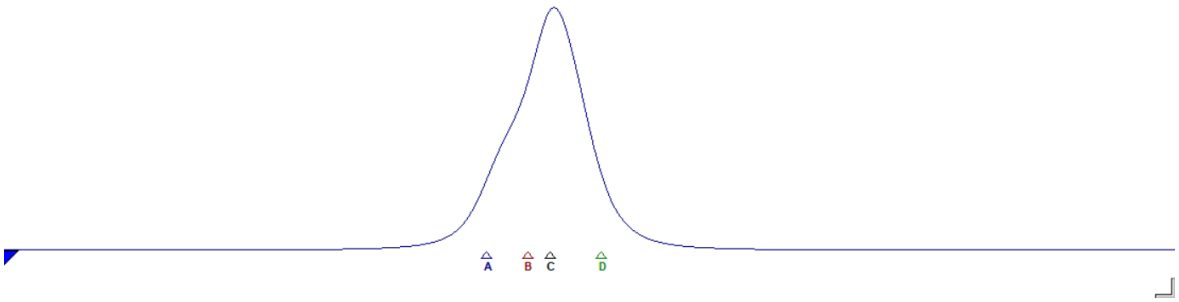

Peaks a-d: k = 55.4 s^{-1} (simulating the spectrum recorded at 303 K)

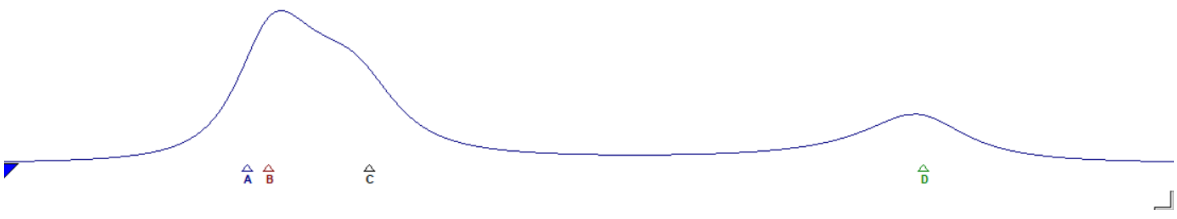

Peaks e-h: k = 29.3 s^{-1} (simulating the spectrum recorded at 303 K)

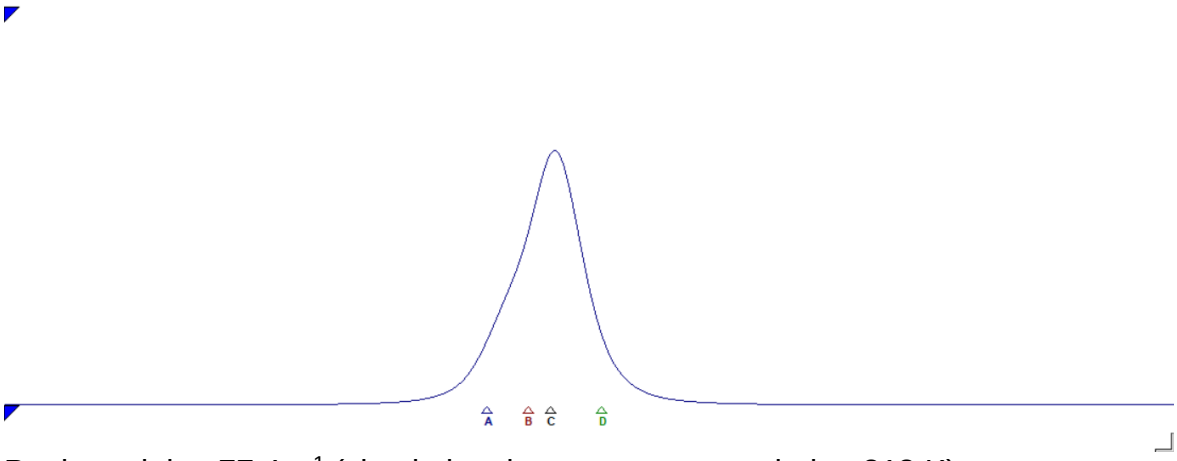

Peaks a-d: k = 77.4 s^{-1} (simulating the spectrum recorded at 313 K)

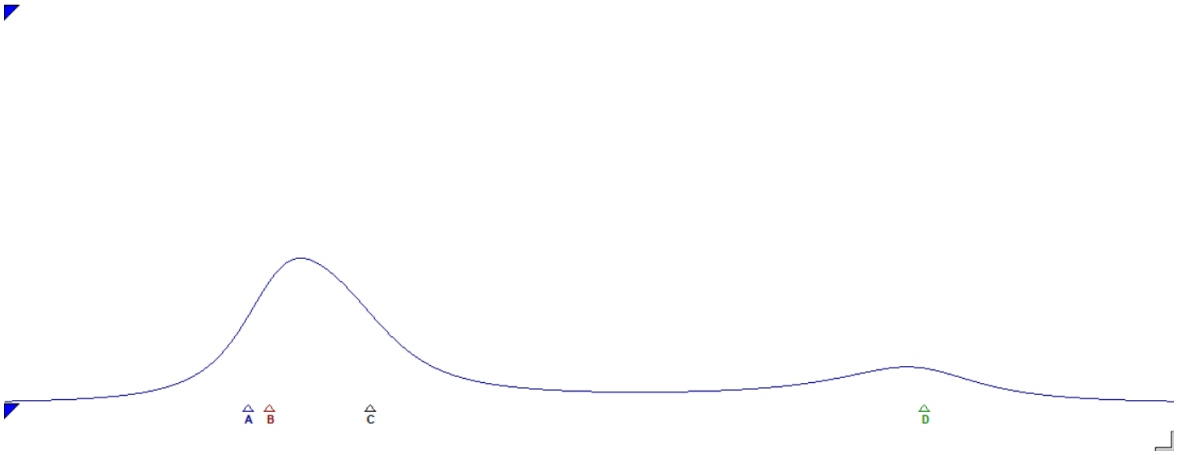

Peaks e-h: k = 41.0 s^{-1} (simulating the spectrum recorded at 313 K)

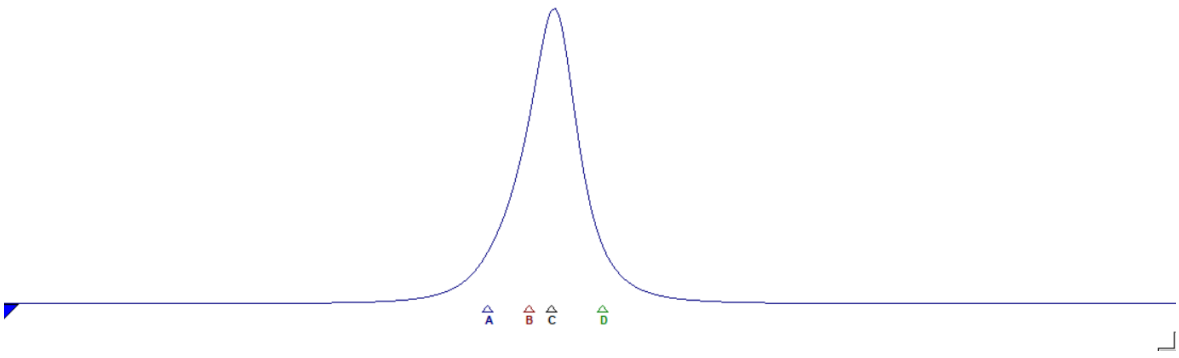

Peaks a-d: k = 104.4 s^{-1} (simulating the spectrum recorded at 323 K)

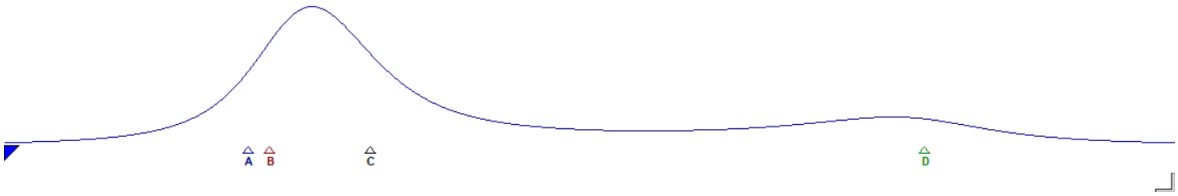

Peaks e-h: k = 52.6 s^{-1} (simulating the spectrum recorded at 323 K)

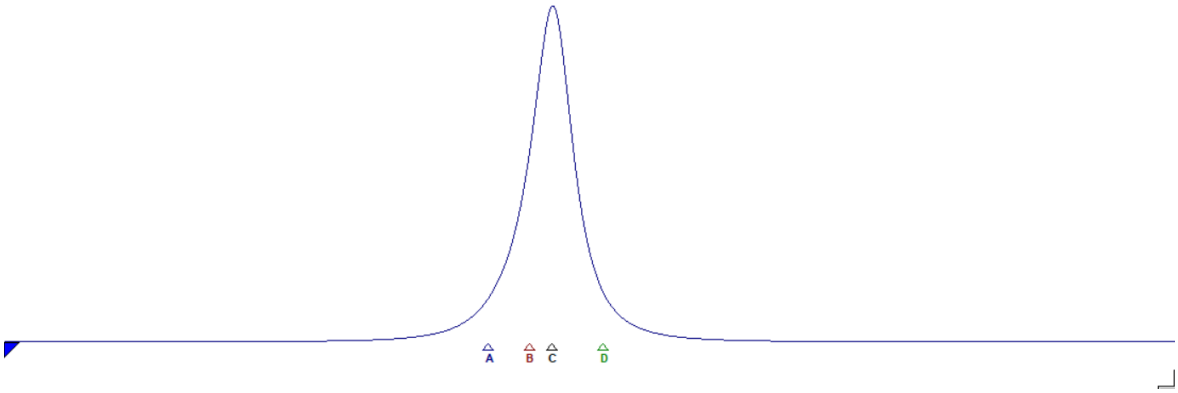

Peaks a-d: k = 117.4 s^{-1} (simulating the spectrum recorded at 328 K)

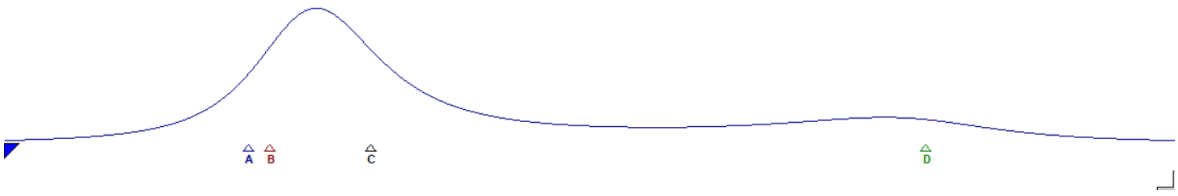

Peaks e-h: k = 58.8 s^{-1} (simulating the spectrum recorded at 328 K)

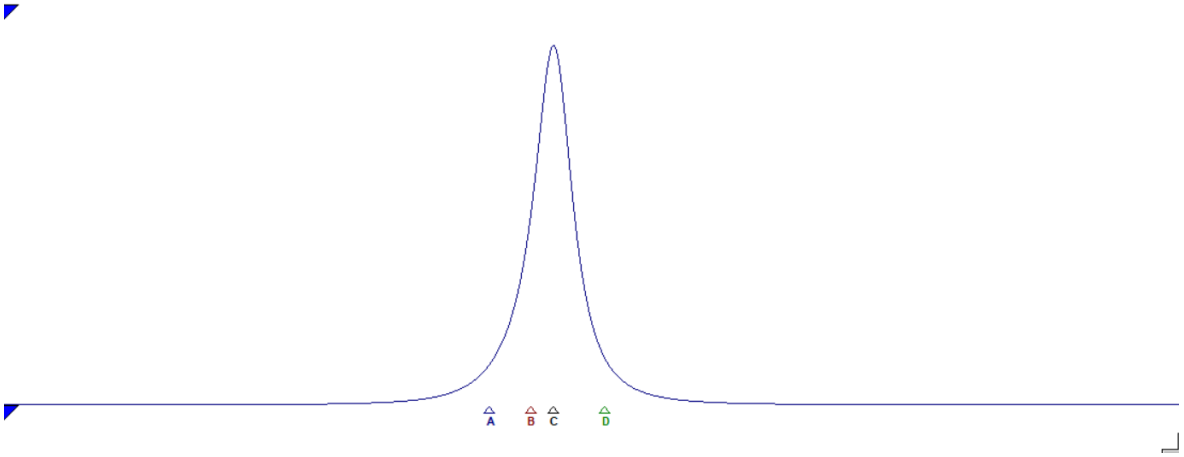

Plots of $\ln(k.T^{-1})$ versus T^{-1} based on these simulated rate constants are given below and application of equations 3 and 4 allowed $\Delta H^{\ddagger}$ and $\Delta S^{\ddagger}$ to be determined as 17.9 +/- 0.3 kJ mol^{-1} and -155 +/- 1 J $mol^{-1}K^{-1}$.

Plot based on peaks a–d

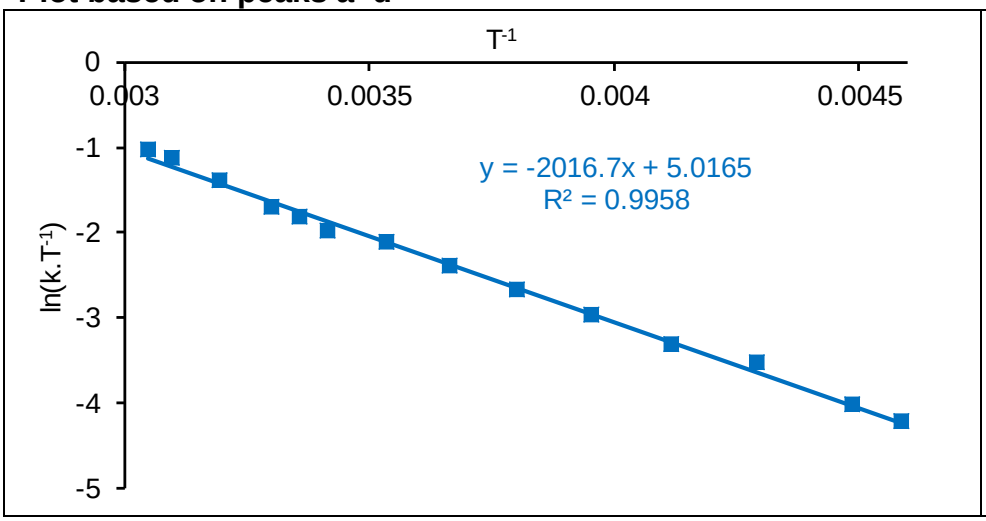

$\Delta H^{\ddagger}$ = 16.8 kJ mol^{-1}
$\Delta S^{\ddagger}$ = -156 J $mol^{-1}K^{-1}$

Plot based on peaks e–h

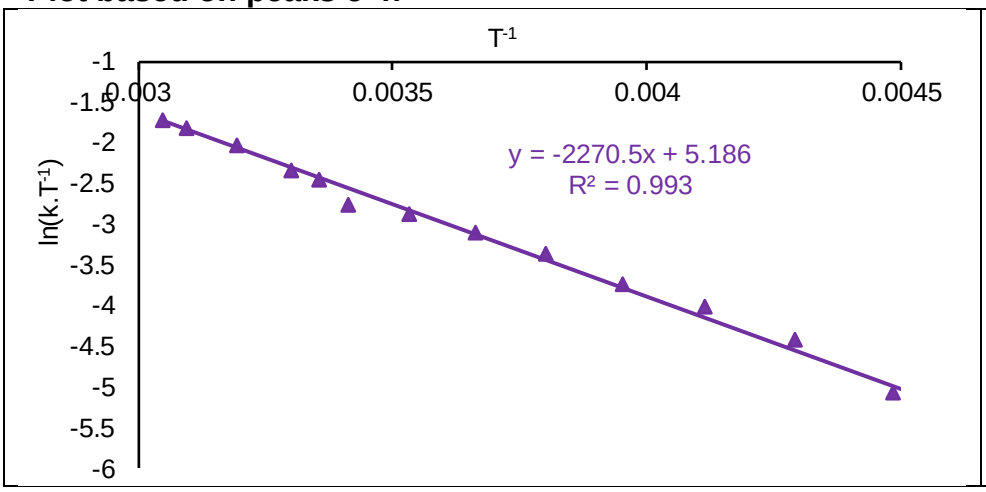

$\Delta H^{\ddagger}$ = 18.9 kJ mol^{-1}
$\Delta S^{\ddagger}$ = -154 J $mol^{-1}K^{-1}$

NMR spectra of styrene carbonate

^{1}H NMR spectrum of reaction mixture

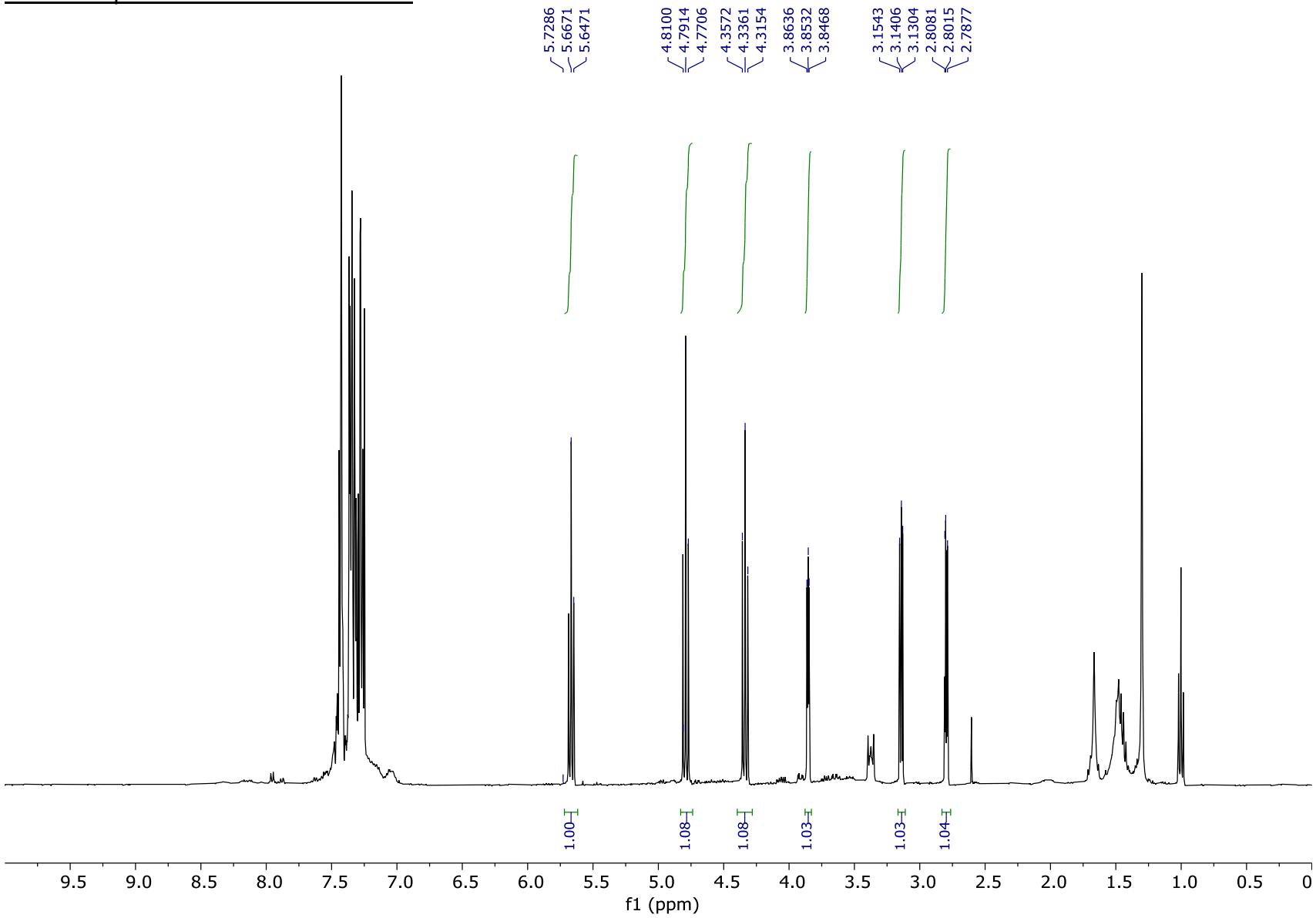

Peaks at 5.7, 4.8 and 4.3 ppm corrspond to styrene carbonate.

Peaks at 3.9, 3.1 and 2.8 ppm corrspond to styrene oxide.

The peaks at 3.3 and 1.5-0.8 ppm correspond to tetrabutyl ammonium bromide.

^{1}H NMR spectrum of purified styrene carbonate

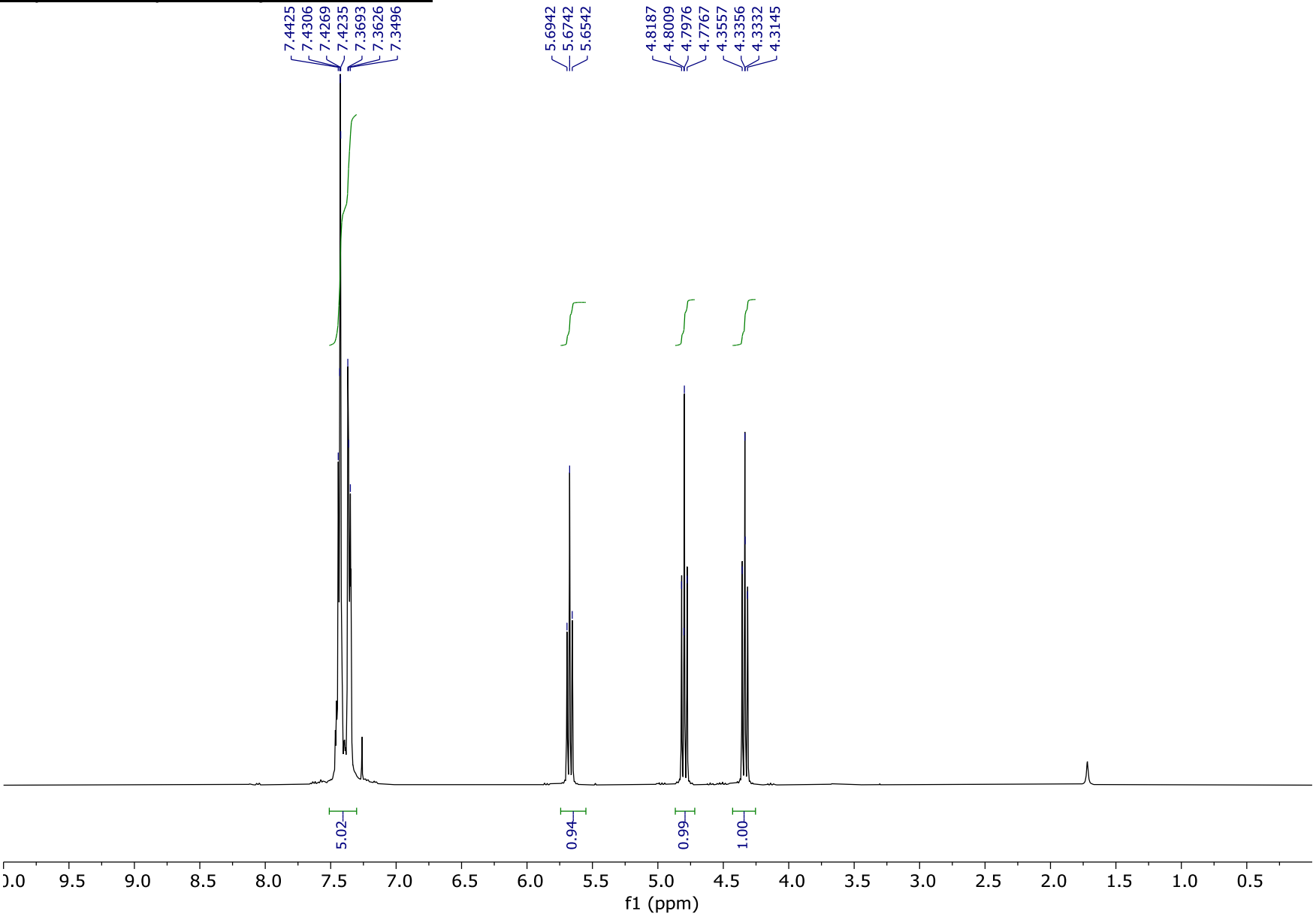

^{13}C NMR spectrum of purified styrene carbonate

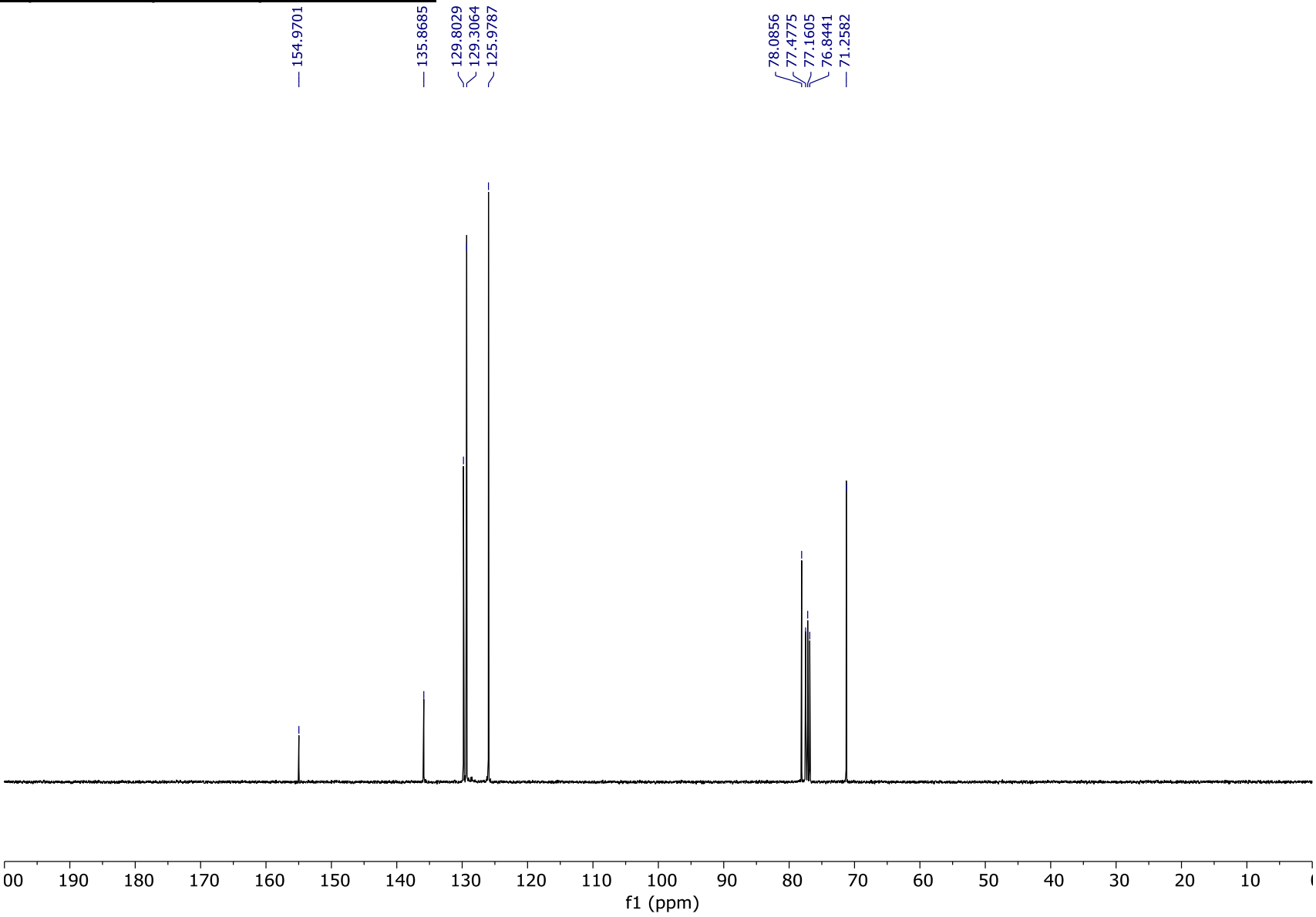

Reference

1. WinDNMR-Pro was downloaded from: https://www.chem.wisc.edu/areas/reich/plt/windnmr.htm (accessed 7th January 2020).